DISTRIBUTION OF THE EPITHELIAL RESTS OF MALASSEZ AND THEIR RELATIONSHIP TO BLOOD VESSELS OF THE PERIODONTAL LIGAMENT DURING RAT TOOTH DEVELOPMENT

By

Petrina Sai Peng Kat
B.D.S., B.Sc. Dent (Honours) (Adelaide)

A Research Report presented to the Faculty of Health Sciences, The University of Adelaide in fulfillment of the requirements for the degree of Master of Dental Surgery (Orthodontics)

February 2001

SIGNED STATEMENT

This report contains no material which has been accepted for the award of any other degree or diploma in any other university or tertiary institution and, to the best of my knowledge and belief, it contains no material previously published or written by another person, except where due reference has been made in the text.

I give my consent to this copy of my thesis, when deposited in the University Library, being available for loan and photocopying.

Petrina Kat

ACKNOWLEDGEMENTS

I would like to thank the following people for their contribution in one way or another to this research report:

Professor Wayne Sampson, Begg Chair of Orthodontics, University of Adelaide, my research supervisor, for his wisdom and guidance through all the stages of this study including the proof reading of this report

Associate Professor David Wilson and Senior Lecturer Dr Ole Wiebkin, additional research supervisors, for their invaluable insight and advice throughout this project.

Dr Robert Moore, for generously allowing the Bone Labaratory in the Institute of Medical and Veterinary Science to be used during the initial phases of immunohistochemical staining.

Mr Jim Manavis from the Institute of Medical and Veterinary Science, for his enthusiasm and help in the development of the immunohistochemical protocol utilised in this study.

Ms Sandie Powell and Mrs Margaret Leppard, for the technical assistance provided during the laboratory phases of the project.

Professor Grant Townsend, for assistance in the statistical analysis of the data in this project.

Dr Daniel de Angelis and Dr Richard Salmon, for assistance in the preparation of the rat tissues utilised in the preliminary and final study and for making the last three years more enjoyable. I could not have asked for two better people to do this course with.

My family (Ma, Pa, Jason, Basil and Benen), for encouraging me to always aim high (I wouldn't be where I am today without you) and for supporting me throughout all my academic (and not so academic) endeavors.

Darren di Iulio, for proof reading my first draft, for his continuous support, encouragement and enthusiasm throughout the duration of this course.

The Australian Society of Orthodontists Foundation for Research and Education, for their generous support of this research project.

To Ma and Pa

If I have seen further it is by standing on the shoulders of giants.
Isaac Newton (1642-1727)
British scientist

Where observation is concerned, chance favours only the prepared mind.
Louis Pasteur (1822-1895)
French scientist

CATALOGUE OF ABBREVIATIONS

ABC	Avidin-biotin-peroxidase complex system
DAB	Diaminobenzidine Tetrahydrochloride
EGF	Epidermal growth factor
ERM	Epithelial rests of Malassez
FGF	Fibroblast growth factor
HERS	Hertwig's epithelial root sheath
HRP	Horseradish peroxidase
IL	Interleukin
PDGF	Platelet derived growth factor
PDL	Periodontal ligament
RECA	Rat endothelial cell antigen
RER	Rough endoplasmic reticulum
TGF	Transforming growth factor
TNF	Tumour necrosis factor
UEA	*Ulex europaeus* I agglutinin
vWF	Von Willebrand factor
$\bar{x}$	Mean
SD	Standard deviation

CONTENTS

LIST OF FIGURES

TABLES

1 ABSTRACT

The epithelial rests of Malassez (ERM) are a network of cells which are remnants of Hertwig's epithelial root sheath (HERS). They were originally thought to be functionless. However, they are now believed to not only play a role in dental cyst formation but may also protect against root resorption. This has yet to be confirmed.

The aim of this study was to adopt a double immunohistochemical staining technique to study the distribution of ERM and blood vessels in the periodontal ligament (PDL) of the first molar root in developing rat teeth.

Four Sprague-Dawley rats were sacrificed at each time period of two days, one, two, four and six weeks respectively. Their maxillae were dissected out, processed and embedded in paraffin blocks. They were then sectioned longitudinally and transversely. The sections were stained with a double immunohistochemical technique which utilised AE1-AE3 (at a concentration of 1:2000) and Factor VIII (at a concentration of 1:10 000) to enable simultaneous labelling of ERM and blood vessels within the same tissue section.

Counts for ERM (which were divided into individual "cells" and "clusters", according to their presentation) and blood vessels were only obtained for the mesiobuccal roots of three, four and six-week-old rats.

This study noted that all ERM cells and clusters were found in the tooth third of the PDL. With increasing age, ERM cells and clusters increased in number especially in the cervical third of the mesiobuccal root. The largest number of cells and clusters was noted on the distal surface of the root in all age groups. Cell and cluster numbers across the root surfaces increased from three to four weeks, but decreased from four to six weeks.

The greatest number of blood vessels was noted in the bone-side third of the PDL. The distal surface had the highest proportion of vessels, and the palatal surface the least. Vessel numbers in all surface quadrants did not increase much from three to four weeks, but there was a general increase from four to six weeks of age.

The distribution of the ERM and blood vessels could be attributed to tooth eruption, root development, periodontal inflammation and/or possibly root resorption.

Nevertheless, the low number of animals in this experiment prevented statistically significant results to be obtained. Further work is required to confirm the findings of this study.

2 AIMS

The aims of this research project are as follows:

1. To evaluate the development and distribution of epithelial rests of Malassez in the periodontal ligament, around and along the length of the mesiobuccal root of the first maxillary molar in the rat.

2. To evaluate the development and distribution of blood vessels in the periodontal ligament, around and along the length of the mesiobuccal root of the first maxillary molar in the rat.

3. To investigate the relationship between the epithelial rests of Malassez and blood vessels in the mesiobuccal root of the first molar in the rat.

4. To adapt suitable immunohistochemical techniques for simultaneous demonstration of ERM and PDL blood vessels.

3 LITERATURE REVIEW

3.1 Embryology of Human Tooth Development

In the human, after thirty seven days of embryonic development, a continuous band of thickened epithelium forms around the mouth in the upper and lower developing jaws from the fusion of thickened epithelial plates. This is referred to as the primary epithelial band. It gives rise to the vestibular lamina (which eventually develops into the vestibule between the cheek and tooth bearing areas) and the dental lamina which gives rise to the primary and secondary dentition [1].

The epithelial band eventually grows into the ectomesenchyme of the jaw and forms the epithelial bud. Cellular density starts to increase and the epithelial in-growth begins to resemble a cap, and subsequently a bell. These stages are termed the "cap stage" and "bell stage" respectively. This structure eventually forms the dental organ (which eventually forms the enamel of the tooth). The ectomesenchymal cells on which the dental organ is sitting become highly condensed and form the dental papilla (which eventually forms the dentine and pulp). A line of condensed ectomesenchyme limits the dental papilla and encapsulates the dental organ. This structure is called the dental follicle (which gives rise to the periodontal and tooth supporting tissues). The dental organ, dental papilla and the dental follicle together make up the tooth germ [1].

The entire deciduous dentition is initiated between the sixth and eighth week of embryonic development, the successive permanent teeth between the twentieth week in utero to the tenth month after birth, and the first and second permanent molars around the twentieth week in utero (third molars start forming around the fifth year of life) [2]. During this period, the respective tooth germs continue to grow and the epithelial cells within the dental organ differentiate into different components. The cells in the centre of the organ become star-shaped and are thus termed the stellate reticulum. The cells at the periphery assume a cuboidal shape and form the external, or outer dental epithelium whilst the cells immediately adjacent to the dental papilla which are short and columnar - shaped form the internal, or inner, dental epithelium [1].

The cells within the dental papilla divide and differentiate into odontoblasts (that is, the dentine-forming cells). These cells progressively mature to form the tubular structure that makes up dentine. After the first layer of dentine is formed, the cells of the internal dental epithelium differentiate into ameloblasts and produce an organic matrix against the newly formed dentine surface that becomes partially mineralised. This matrix eventually forms enamel. This process continues until the crown of the tooth is formed [1].

3.2 Tooth Root Development

Root formation proper begins just prior to eruption. By this time, ameloblastic activity is essentially complete, such that the crown of the tooth is covered by reduced enamel epithelium (which consists of a layer of ameloblasts and remnants of the remaining layers of the dental organ) and the cervical margin of the enamel organ is located at the future cementoenamel junction [2].

The periodontal ligament (PDL) develops just after tooth root formation begins [3]. As described earlier, the periodontal tissues are derived from the dental follicle (alternatively termed the dental sac). There is some debate as to the precise origin of the dental follicle cells. It is traditionally believed that these cells are derived from mesoderm near the site of the developing tooth [4]. However, Freeman [3] believes that they originate, at least in part, from neural crest cells that have migrated to the region of the developing jaws.

3.3 Rat Tooth Development

Rat teeth develop in a similar manner to human teeth, although at a more accelerated rate. Molar development will be concentrated on in this section, as these are the teeth that will be used in this investigation. The first molar is the largest of the three molars in each quadrant. It begins formation on the twenty-first day *in utero*. The second and third molars begin their formation on the second and fourteenth day respectively. Proliferation of the formative organs and histodifferentiation of the formative cells proceed in a similar manner to human tissues [4]. A summary of the development of rat teeth is depicted in Table 1.

Age	Developmental stage	
	Incisors	First molar
13 – 14 days in utero	Dental lamina formation	Dental lamina formation
18 – 19 days in utero	Bud stage	Bud stage
20 – 21 days in utero	Bell stage	Bell stage
11 days	First appearance in oral cavity. Continuous crown development.	Crown development complete
14 – 16 days	Incisors in functional occlusion	Bifurcation of roots
19 days		First appearance in oral cavity.
25 days		Molars in functional occlusion

Table 1

Rat Tooth Development Timing and Stages

This table shows the timing and stages of development of rat incisors and first molar teeth.

(Adapted from Schour and Massler. The teeth. **In** Farris and Griffith Ed. "The Rat in Laboratory Investigation". New York: Hafner Publishing Co, 1971. Pp104-165)

Root formation commences at the age of ten days after birth [5,6]. Unlike human teeth, the rat maxillary first molar has five roots. Also, rats do not have a set of deciduous teeth. They only possess one set of teeth that remain throughout their life. With functional attrition, the rat molars undergo continuous eruption throughout life, which is compensated for by the formation of secondary cementum. The formation of this cementum commences at the age of twenty days [5].

3.4 Hertwig's Epithelial Root Sheath (HERS)

By the time root formation commences, enamel and dentine formation of the crown have reached the cervical loop, an area where the internal and external dental epithelium become contiguous. The cells of the cervical loop proliferate and form a double layer of cells known as Hertwig's epithelial root sheath (HERS) [1, 7-10]. It consists of 2 parts: Firstly, the root sheath that grows around the dental papilla, between the papilla and dental follicle and encloses all but the basal portion of the papilla. Secondly, the rim of the sheath, known as the epithelial diaphragm that encloses the primary apical foramen [1]. It is shaped like a solid disc with a central circular hole. Root elongation occurs progressively as a result of cell proliferation taking place at the innermost tip of the diaphragm, with newly formed epithelial cells passing outwards to take their place in the vertical portion [2]. However, whether this proliferation takes place coronal to the root diaphragm or within the diaphragm has not yet been determined [11].

The role of HERS in the induction of root dentinogenesis was first proposed by von Brunn in 1889 (in Thomas and Kollar 1989 [12]). It is now generally agreed that the cells of HERS induce adjacent dental papilla cells to differentiate into odontoblasts and commence formation of root dentine [4, 13, 14]. Diamond and Applebaum [8] noted that this process did not commence until the completion of enamel matrix formation in the crown of the human tooth. Thomas and Kollar [12] noted that HERS can only induce dentine formation in dental papilla cells that had previously been induced by inner enamel epithelium. Dental papilla from younger embryos are not primed for differentiation and no dentine formation can occur in dental sac tissue. Thus, HERS can induce dentine formation only in older, committed dental papilla [12]. Through a series of cell-to-cell interactions, the odontoblasts deposit and mineralise dentine matrix [15, 16]. However, the

exact process by which this occurs is still not completely understood [17]. Furthermore, there is some variation in this process between species [15].

Various investigators [5, 14, 17, 18] also contend that the HERS plays a role in the formation of cementum, although not all are in agreement [19]. Owens [18] noted a thin layer of unmineralised "surface dentinal matrix" during early root development of the rat molar. He suggested that this was in actual fact an initial layer of acellular cementum which was secreted by HERS cells, thus confirming a secretory function by the HERS cells. Alatli et al [5], Hammarström [20] and Lindskog [21-23] were in agreement, proposing that dentine mineralisation induced the inner layer of HERS to secrete enamel-related proteins as an initial step in the formation of this layer of acellular cementum, which was defined as "intermediate cementum".

The intermediate cementum becomes mineralised with further root development, separating root dentine from cementum. In fully mineralised teeth, it becomes hypercalcified and persists as a specific layer of hard tissue separate from the dental cementum throughout life [21]. Harrison and Roda [24] suggested some potential functions for this structure in developing and adult teeth. Firstly, it is a precursor to cementogenesis in root development. Secondly, it acts as a barrier between cementum and dentine (thus, acting as a barricade to the external passage of medicaments placed in the root canal during endodontic therapy). Thirdly, it is also a precursor for cementogenesis in wound healing.

The mechanisms involved in the formation of cellular cementum are still unclear [20]. Lester [15] and Owens [14] proposed that the inner layer of HERS exerts an inductive influence on the adjacent cells of the dental follicle. This led Hammarström [20] to postulate that it may be possible that these cells differentiate into cells forming the matrix for cellular cementum in the same way that cells in the dental papilla differentiate into odontoblasts.

Ten Cate [19] noted that the epithelial sheath is also responsible in determining the size, shape and number of tooth roots, thereby playing a role in determining the amount of tissue available for tooth support. He argues, however, that the layer of "acellular cementum" secreted by HERS is not cementum but a variant of dentine sealing off the peripheral extent of the dentinal tubules. He classified it as the hyaline layer of Hopewell-Smith. This is in agreement with Owens' [25] earliest observations.

Some work has been done on the histology of HERS in human tissue [8, 26, 27]. However, most of the literature on the histologic appearance of HERS has been performed on other mammalian tissue, such as the rat [5, 18, 28], mouse [6, 11, 17, 29, 30] and monkey [21, 22].

3.4.1 *Histology of Hertwig's Epithelial Root Sheath*

Hertwig [8,9] first suggested the use of the term "epithelial sheath" in 1874 as he felt that the epithelium in the root portion of the tooth had to be differentiated from the coronal portion. This observation was made with a frog tooth but the definition persisted and is now used in mammalian teeth.

Basically, as described earlier, HERS is a sheet-like structure made up of a double layer of epithelial cells, which separates the dental papilla and dental sac. It forms the outline of the root [1,7,14,15]. On closer examination utilising light and electron microscopy, investigators [6,13,14,15,31] have noted some variation in the appearance of the cells of HERS depending on their location along the developing tooth root and also depending on the stage of development of the root.

Owens [14] and in particular, Gurling and Sampson [6] divided the HERS into different zones which assisted the three dimensional visualisation of the sheath along the root. Although, the investigations were performed on different animals, that is, in dogs by Owens [14] and mice by Gurling and Sampson [6], the latter investigators noted that there was little species variability. However, there was more variation within the root during root development. The zones and observations are as follows:

3.4.1.1 Tip of the Diaphragm

In the early phases of development (11-day old mice in the Gurling and Sampson [6] study), the apical extremity of the diaphragm consisted of two to three layers of flat closely packed cells. These epithelial sheath cells were separated from immature follicular and pulp cells by a basal lamina that was more distinct on the inner side. Numerous small intercellular spaces were noted which occasionally contained vascular structures. Both the inner and outer sheath cells were similar in appearance with numerous free ribosomes, several mitochondria, small amounts of rough endoplasmic reticulum (RER) and some tonofilaments. However, compared to cells of the outer layer, the epithelial cells of the inner layer had a lower nuclear-cytoplasmic ratio. The cells at the tip of the outer layer showed well-defined pseudopodial processes which were

directed apically, whilst the cell membranes of the inner layer were irregular in outline and showed some small infoldings [6,14].

3.4.1.2 Middle of the Diaphragm

In the middle segment of the diaphragm, cells of the inner layer were more cuboidal and maintained a lower nuclear-cytoplasmic ratio. Their cytoplasm contained numerous free ribosomes and mitochondriae, but little RER. The cells were closely packed with few intercellular spaces. In contrast, cells of the outer layer were flat, elongated and loosely packed with numerous large intercellular spaces and tonofilaments in their cytoplasm. Tight junctions were noted between adjoining inner-epithelial cells, whilst small desmosome-type junctions joined adjacent outer-epithelial to inner-epithelial cells. A continuous inner and outer basal lamina separated the epithelial layers from adjacent differentiating pre-odontoblasts and follicular cells [6,14].

3.4.1.3 Diaphragm abutting polarizing odontoblasts

At the upper extremity of the diaphragm (just before it becomes associated with dentine), the cells in the outer layer were elongated and had a marked increase in their nuclear-cytoplasmic ratio compared with inner layer cells. Mitochondriae, RER and free ribosomes dominated the inner cells. Intercellular spaces in the inner layer were also more numerous, larger and more irregular in outline. A continuous basal lamina was noted on both surfaces [6,14].

3.4.1.4 Intermediate Lateral Sheath – abutting pre-marginal dentine

Outside the newly formed dentine, the sheath appeared as a continuous unicellular layer. Cells of the inner layer were densely packed and contained fewer organelles. Some of the cells in the outer layer appeared to be breaking off from the sheath and the associated basal lamina was discontinuous [14]. Gurling and Sampson [6] noted that these cells were no longer present or part of the sheath.

At a more coronal level, the basal lamina of the inner layer was penetrated by epithelial cell processes which extended for short distances into the relatively collagen free dentine matrix. The cytoplasm of these processes contained fine fibrils and resembled cytoplasm of adjacent odontoblast processes. Furthermore, there was actual contact between odontoblast processes and the inner basal lamina.

Near the coronal limit of this region, the cytoplasm of some of the inner layer of cells was packed with many free ribosomes, extensive RER and mitochondriae [6,14].

3.4.1.5 Discontinuous Lateral Sheath

At the more apical end, there was complete loss of the inner basal lamina and gross irregularity of the dentine-epithelial boundary. However, the epithelial cells continued to form a complete covering over the dentine.

Owens [14] classified the epithelial cells remaining near the root surface into two types. Type 1 cells, which were relatively electron-lucent with small amounts of RER and a few tonofilaments and Type 2 cells, which were relatively electron-dense with more RER, but less tonofilaments. Junctional complexes were observed between the two cell types.

At more coronal levels, the sheath cells were generally more widely separated and both Type 1 and Type 2 cells were readily identifiable. Collagen fibrils were evident between these cells.

At the most coronal level, a site of sheath severance was noted, with the coronal extremity of the sheath close, but not attached to the apical end of the enamel organ. Epithelial cells were still present in clusters of varying size close, but not attached to the root surface. Type 2 cells could no longer be seen. Collagen was plentiful in the intercellular spaces, but showed no well-defined pattern of fibre organisation. Large ovoid bodies were observed amongst the epithelial clusters. These varied in size and contained fine fibrillar material and a few vesicles. A granular matrix-like material was also noted on the tooth surface [6, 14]. These observations are depicted in Figure 1.

3.4.2 *Fate of Hertwig's epithelial root sheath*

With continuing root development, the outer layer of epithelial cells begins to decrease and appears to shorten. There is much controversy and disagreement regarding the fate of the cells of HERS. Various early investigators [15, 32, 33] believed that the cells either migrated into the PDL where cell degeneration occurred or become incorporated in forming cellular cementum. Other investigators [2, 3, 34] believed that the sheath fragments and any surviving cells form a network of cells termed the "epithelial rests of Malassez" (ERM) in the PDL. It is likely that a combination of these processes occur during root development.

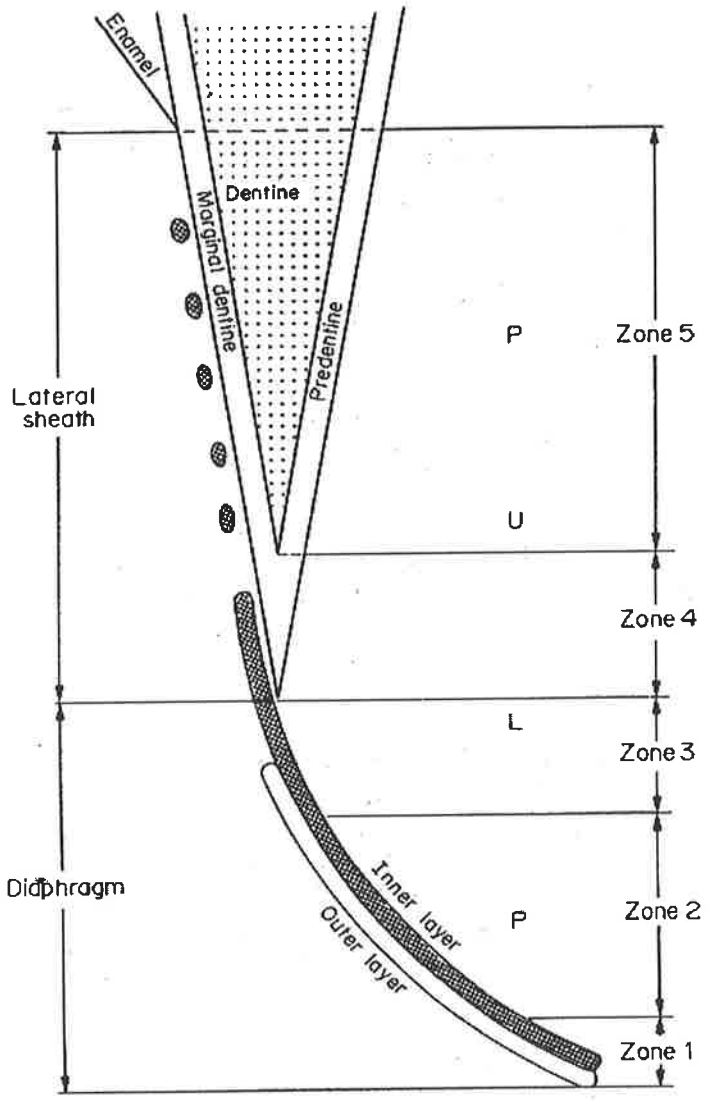

Figure 1

Epithelial Root Sheath Divisions

Zone 1: Tip of epithelial diaphragm, Zone 2: Middle of diaphragm, Zone 3: Diaphragm abutting polarising odontoblasts, Zone 4: Intermediate root sheath and Zone 5: Discontinuous lateral sheath.

(Adapted from Gurling and Sampson , Epithelial root sheath changes during molar formation in the mouse. *Arch Oral Biol.* 1985; 30(11/12): 757-761)

Owens [14] and Gurling and Sampson [6] postulate that with age, HERS unfolds as the epithelial cells of the outer layer migrate apically and add to the apical extremity of the inner layer to maintain a consistent dimension of the apical epithelial foramen. Eventually, the epithelial cells separate from the enamel organ and then the root surface. These become the epithelial rests and are carried occlusally within the developing PDL during tooth eruption [6], where they remain throughout life. This process is depicted in Figure 2.

3.5 Epithelial Rests of Malassez (ERM)

It is widely assumed that the epithelial rests of Malassez (ERM) were first fully described by Malassez in 1885 [35,36] when he examined adult human teeth and found that the epithelial rests formed a network around the tooth root. However, Reitan [37] contends that the term "epithelial rests" was probably first used by Serres in 1817. However, he does credit Malassez with proving that the epithelial rests persist in the adult periodontal membrane.

Much work has been performed on the histology of the ERM through the years in humans and a host of animal teeth. Some differences in the appearance of the ERM between species have been noted.

3.5.1 *Histology of the Epithelial Rests of Malassez*

3.5.1.1 Human Epithelial Rests of Malassez

In conventional histological sections cut perpendicular to the axis of the root, the ERM appear as small, solid circular or oval aggregates or strands from approximately four to twenty cells, with individual clusters dispersed at intervals down the periodontal ligament [2,3,37]. However, in longitudinal sections, these cell rests appear as strands of cells running in close proximity to the cementum surface and on rare occasions, coming into direct contact with it. The strands run further out in the ligament, winding in and out of the fibre bundles [2,3].

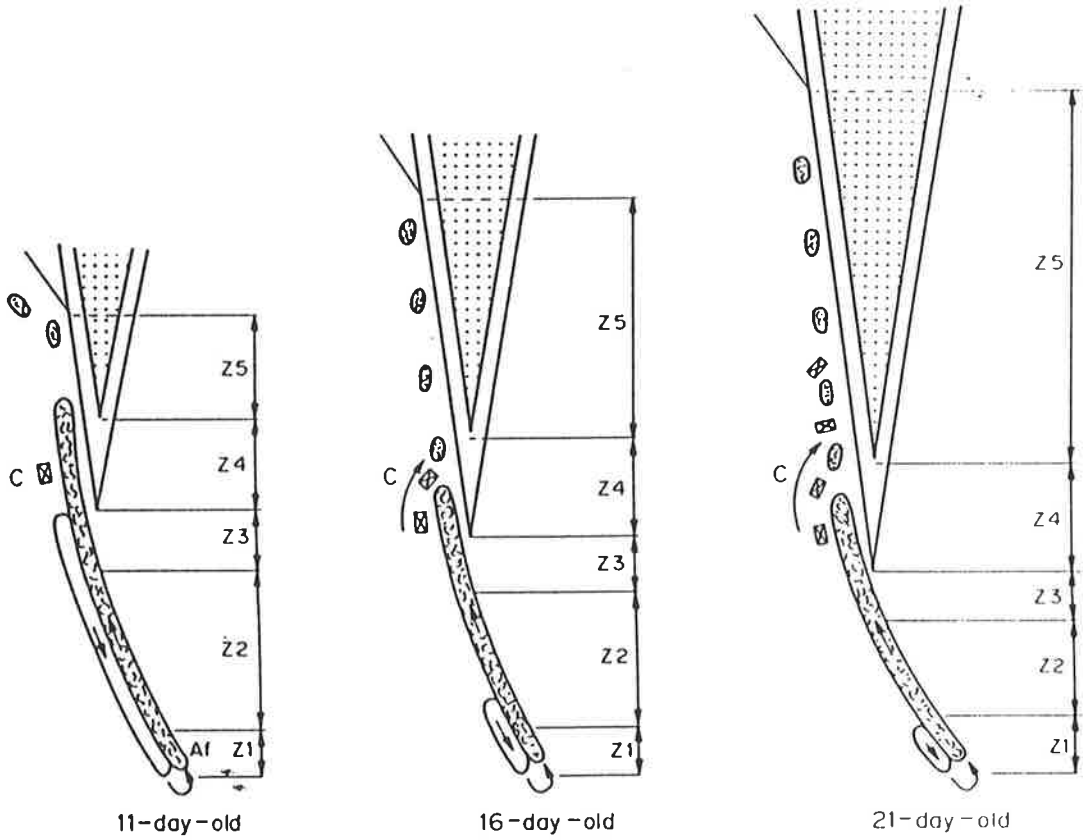

Figure 2

Fate of HERS in mice (from 11 to 21 days)

The outer layer of epithelial cells shortens, transforming the bicellular root sheath to a predominantly unicellular structure at 21-days old. The proposed direction of epithelial cell movement (arrows) favours maintenance of the inner layer. Cementoblast-like cells (c) become interspersed with the fragmenting epithelial cell layer in Zone 5.

(Adapted from Gurling and Sampson. Epithelial root sheath changes during molar formation in the mouse. *Arch Oral Biol.* 1985; 30(11/12): 757-761)

It is generally accepted that the ERM form a network of cells around the periodontal ligament (PDL) [2,3]. However, on performing serial sectioning of human teeth, Lambrichts et.al [38] failed to visualise any interconnection between the islands of ERM cells detected. Fischer 1932 (in Reitan [37]) was of the opinion that such a network could not be produced in human teeth but was much more plausible in teeth of animals like cat and swine, although no reason was provided why this should be so. This fact was disputed by Spouge [2] who confirmed the presence of the ERM network in human PDL tissue.

Under the light microscope, the ERM cells appear to have dark-staining nuclei and little cytoplasm [1,2,3]. Reeve and Wentz [39] studied the periodontal ligament of thirty one human jaws and noted three morphologic types of ERM:

(a) Resting type

These were mostly located close to the cementum, but could occasionally be found in bone marrow spaces of the alveolar septum and beyond the apex of the tooth. Small and large forms were noted.

The small resting ERM were mostly found in young persons, usually in their first and second decade of life. In tangential sections, these ERM appeared to be arranged in strands which formed a netlike arrangement. In cross section, the cells of the strands appeared in oval groups consisting on average of ten polyhedral cells. The surrounding connective tissue did not form a capsule.

The large resting ERM, on the other hand, were found in ovoid or spherical groups composed on average of twenty eight cells. These groups were isolated and did not form strands. The nuclei of these cells were slightly larger than those of the small resting ERM and the chromatin were not stained as deeply. The cells were also not as closely arranged. The connective tissue fibres and cells surrounding these cells had a loose concentric arrangement [39].

(b) Degenerated type

This type was most frequently observed in young persons. The majority of these cells were located in the apical and middle zones of the periodontal ligament in close proximity to the cementum. In cross section, these ERM appeared oval and contained an average of ten cells in each rest. Each cell group had a distinct boundary and a definite shape. The nuclei were dark and pyknotic.

In cases where these cells were noted in older persons (middle-aged subjects), the beginnings of calcifications could be observed in the ERM. The authors thus hypothesised that all ERM of this type would eventually calcify and end up appearing as cementicles in the PDL [39].

(c) Proliferating type

Rests of this type were located close to the cementum as well. However, they were mostly observed in persons in the later decades of life. These rests were the largest, averaging eight to ten times the size of the small resting type.

The nuclei of the cells in these ERM were pale, larger and more vesicular than those of the resting type. There was high variability in the appearance of the nuclei and cytoplasm of the cells. The rests were often found surrounded by a well-differentiated fibrous capsule, with a concentric arrangement of cells and fibres. However, in some instances, the capsule changed into a hyalinized mass where fibres and cells could not be distinguished [39].

Reeve and Wentz [39] also noted that the incidence of all types of ERM seemed to vary with age. They appeared to be more abundant around younger teeth. The greatest frequency of occurrence was in the second decade. After this, there was a reduction in the total number of ERM until in the seventh decade when the incidence was found to be approximately one-fourth the number observed in the first twenty years of life. The authors state that this reduction occurs by degeneration with consequent disappearance, or by degeneration followed by calcification and the formation of cementicles. Spouge [2] seems to agree with this. However, he states that the ERM are often difficult to distinguish with certainty within the tissues of the PDL under the light microscope, thus accounting for the variation in assessment of their presence.

3.5.1.2 Animal Epithelial Rests of Malassez

Numerous experiments have been performed to visualise ERM in various animals. Most have been conducted on mice or rats [40,41]. However, dogs [8] and monkeys [42,43] have also been used. As this study will be performed on rats, it is appropriate to explore mouse and rat ERM further.

Mouse and rat ERM appear similar to human ERM. The rests appear as a network of round to cuboidal structures, composed of cells with relatively large, rounded

nuclei and cytoplasm which stained darker than surrounding fibroblasts [41]. They are either packed in groups or appeared as solitary cells [41].

Wentz et al [44] identified three different morphologic forms of ERM in rat molars:

(a) Small Resting Type

These ERM were found close to the cementum. They consisted on average of 7 to 10 cuboidal cells arranged in spherical groups. The nuclei were ovoid but there were some variations in their location. In some cases, the nuclei were found at the basal end and in other cases, they were located at the distal end of the cells. In some instances, the nuclei appeared pyknotic.

The connective tissue surrounding the epithelial rests was quite variable. In most instances, the connective tissue showed hyalinization. In other instances, the fibroblasts were arranged in an "onion-leaf" arrangement.

In longitudanal sections, the cells of the ERM were arranged in strands of varying diameters, usually 2 to 5 cells wide. In the vicinity of some strands, an irregularity in the contour of the cementum was noted [44].

(b) Proliferating Type

The majority of these ERM were observed close to the cementum. They were generally twice the size of the small resting form. Two variations of this form were further observed:

(i) Smaller Form

These consisted on average of 35 to 40 cells with small ovoid nuclei. They had a connective tissue capsule which contained closely packed hyalinized fibres and stained strongly with eosin.

(ii) Larger form

This form was composed on average of 50 to 100 cells with large, well-formed nuclei. They were usually observed in the interdental spaces and in the cervical third of molar roots [44].

(iii) Differentiating Form

These consisted of ovoid islands of cells which can be found singly or in groups of 2 to 4. There was a distinct difference between cells in the periphery of the islands

compared with cells in the centre. The peripheral cells were cuboidal and arranged regularly on a basement membrane. They had very little cytoplasm which stained more intensely than that of the central cells. The scarcity of the cytoplasm made the nuclei appear closer together than in the central area.

The cells in the central area were more loosely arranged and generally had smaller nuclei with an oval to spherical shape [44].

As with human ERM, rat and mouse ERM tended to decrease in number with age [41,44]. However, Wentz et al [44] stated that this depends on the type of ERM. The proliferating form was found to be fairly constant throughout life. The small resting type decreased whilst the differentiating type increased with age. The authors did not comment on the fate of the larger resting ERM with regard to age changes.

3.5.2 *Ultrastructure of the Epithelial rests of Malassez*

Under the electron microscope, the epithelial cells of the ERM were observed to have a high nuclear-cytoplasmic ratio [40] which corresponded to light microscope observations. The nuclei of the cells were round to ovoid in shape with condensed heterochromatin and one or two poorly developed nucleoli [38,40]. They were irregularly contoured with occasional deep infoldings of the cytoplasmic membrane.

The cytoplasm contained a normal set of organelles, glycogen particles and microfilament bundles [38,40]. Hamamoto et al [40] also noted a high number of mitochondriae, a poorly developed rough endoplasmic reticulum and a Golgi complex which was located close to the nucleus. Coated pits and vesicles were observed at the periphery of the cells and there was a basal lamina which separated the epithelial cells from the surrounding connective tissue [40]. Most authors [38,40,41,45] noted that the cells were connected by desmosomes and gap junctions. However, there was some disagreement amongst the authors as to how well developed these structures were. This could be due to the fact that the authors may have recognised different morphological forms of ERM, as will be described later.

A primary cilium was noted by Hamamoto et al [40] in association with the Golgi complex close to the nucleus. However, the authors were unable to speculate on its possible function in the ERM.

Yamasaki and Pinero [45] went a step further and noted structural differences in the different morphological types of ERM:

3.5.2.1 Resting Epithelial Rests of Malassez

These ERM had an appearance similar to that described above by previous authors. The cells had round to ovoid nuclei with indentations and heterochromatin accumulations. There were a few mitochondriae, a poorly developed rough endoplasmic reticulum and short tonofibrils scattered in scant cytoplasm. Well developed gap junctions were found between cells, but desmosomes were poorly developed.

3.5.2.2 Proliferating Epithelial Rests of Malassez

Conversely, the epithelial cells of these ERM had euchromatic nuclei and abundant cytoplasm containing numerous free ribosomes. There were fewer tonofilaments and they formed tiny, short arrays of fibrils which were dispersed throughout the cytoplasm. Occasionally, however, there were cells present which contained a large amount of tonofilaments. These were normally found in the inner parts of the epithelial islands. Well defined microfilament bundles were noted at the periphery of the cytoplasm. Desmosomes were not conspicuous and gap junctions were not found.

The authors hypothesised that the anatomy of the ERM cells was such to facilitate their motility during proliferation activity.

3.5.2.3 Migrating Epithelial Rests of Malassez

The cells of this form had similar ultrastructural characteristics to basal and prickle cells of the stratified squamous epithelium. Two cell types were identified by the authors [45]. The first type consisted of thin cells with prominent tonofilaments and less conspicuous organelles. These were usually located in the centre of the epithelial islands. The second type were generally thicker cells and tended to contain more cytoplasmic organelles and fewer tonofilaments. They were usually spread out in the ERM. Thus, the authors [45] stated that differentiation and desquamation occurs centripetally in the ERM.

All cells were connected by desmosomes.

Yamasaki and Pinero [45] postulate that the different forms of ERM represented different states of activity. Thus, the presence of different cell forms in the PDL indicated that inactive ERM could be converted to an active state and then proliferate when subjected to certain environmental changes such as inflammation (for example, that produced during orthodontic tooth movement).

3.5.3 *Position of Epithelial Rests of Malassez*

3.5.3.1 Human Epithelial Rests of Malassez

It is generally agreed that the ERM are found within the PDL in close proximity to cementum[1,2,40,46,47] (although Lester[15] believed that they became trapped in cementum during development). However, there is some disagreement as to the distance of the ERM from cementum. This tends to range from 15μm - 50μm[46] to 10μm - 100μm[47]. However, the latter ERM distance, provided by Kittel[47], was of ERM in repairing cementum after orthodontic tooth movement. Generally, most of the ERM were located in the apical third of the root[2,37]. Also, it was noted by Reitan[37] that there were fewer ERM in the bifurcation areas compared to other root surfaces. This was, however, refuted by Yamashiro et al[48] who noted heavier distribution of ERM in the cervical and furcation regions of the rat molar root.

Reeve and Wentz[39] observed that the location of the ERM seemed to shift with age. In the first and second decades, the ERM were most prevalent in the apical third. However, in the third to seventh decades of life, the ERM appeared to spread out, with 53% of the rests found in the cervical third, 26% in the middle third and 21% in the apical third of the root.

Little has been written on the association of ERM to PDL blood vessels. Brice[46] noted that ERM were often found in close association with blood vessels in the apical third of the root. Kittel[47] in attempting to produce a three dimensional reconstruction of the PDL, seemed to concur with this finding. However, he did note that it was often difficult to identify the presence of blood vessels due to their size and collapsed appearance. The significance of this relationship between ERM and neighbouring blood vessels will be discussed later.

3.5.3.2 Mouse Epithelial Rests of Malassez

It was similarly noted by Wesselink and Beertsen[41] that mouse ERM were mostly located close to the cementum. The authors noted that the rests were equally distributed among all root aspects with 58% located in the apical half and 42% in the coronal half. Three to four times more rests were observed on the mesial root of the first molar compared to other root surfaces. However, the authors made no comment on ERM distribution differences between different ages.

3.5.4 *Functions of the Epithelial Rests of Malassez*

When the ERM were first observed, original investigators first thought that they were only epithelial remnants with no physiological function [41]. However, the different morphological forms of ERM observed by previous investigators [39,44,45] suggest that the ERM can be activated and proliferate in the presence of environmental changes. As far back as 1899, Black (in an article by Spouge [2]) suggested that the ERM had an endocrine function due to the observation of a lumen in the rests. However, this existence of a central lumen has been shown to be a misinterpretation [2]. In addition, Valderhaug and Nylen [36] in their observation of ERM discounted the existence of any secretory characteristics in the cytoplasm of the ERM cells.

One of the first studies to allude to the possible role of the ERM in the PDL was performed by Löe and Waerhaug [42] where 58 teeth from four monkeys and six dogs were extracted and then replanted. They noted that a vital periodontal membrane was preserved when ERM were present in the PDL. In these teeth, ankylosis or the tendency of bone to bridge the periodontal space was not observed. Thus, they postulated that the ERM played a role in conserving the periodontal space, thereby preventing ankylosis and limiting root resorption.

Since then, various authors have investigated this protective role of the ERM. In reviewing anatomical relationships, Spouge [2] noted that nowhere in the body is epithelium in direct contact with bone. There is usually at least a thin buffer zone of fibrous connective tissue between them. This appears to be replicated in the PDL where the ERM network acts as a barrier between bone and cementum. Thus, he proposed that these interposing ERM could act as ankylosis inhibitors, supporting the findings of Löe and Waerhaug [42].

There is a strong possibility that developmental and repair processes share a number of cellular and/or molecular aspects [49]. The ERM can be said to have been involved in tooth development via HERS. They have also been implicated in bone resorption [50] and repair of resorption areas during or after orthodontic movement [43, 46, 51].

Brice [46] examined eight extracted first premolars that had undergone orthodontic tooth movement and noted epithelial cell clusters in areas of repairing orthodontic root resorption on the buccal root surfaces. He consistently found these clusters within repairing resorption bays but not within actively resorbing bays. Furthermore, the epithelial clusters present within the areas of repair had ultrastructural features similar to

the proliferating dark ERM described by Yamasaki and Pinero[45]. This led him to conclude that the ERM could be involved in the repair of orthodontic root resorption and the reconstitution of the PDL following orthodontic tooth movement[51].

The ERM have also been implicated in the formation of dental cysts[1,52] due to observations of bone resorption activity by the rests[52,50]. Other authors have likewise noted ERM involvement in bone resorption related to orthodontic tooth movement[36,53].

Thus, it appears that the ERM are plausibly involved in the process of orthodontic tooth movement as they appear to play an important role in the repair of orthodontic root resorption, bone resorption and remodelling, and the maintenance of the PDL which includes re-establishment of the PDL after tooth movement. This involves the formation of new blood vessels to heal any areas damaged during orthodontic tooth movement.

To fully investigate this further, a basic understanding of the vasculature of the PDL is important.

3.6 Vasculature of the Periodontal Ligament

The PDL is a connective tissue with a vascular volume three to seven times that of a normal ligament[54]. This rich vascular supply most likely reflects the high rate of turnover of both its cellular and extracellular constituents[3]. The primary role of the PDL vasculature is to enable blood circulation within the PDL, thus, providing for the exchange of substrate and metabolites between blood and the periodontal tissues[55]. This assists in the maintenance of health and vitality of the cells of the periodontal tissues. The vasculature of the PDL also have an important role in tooth support as it acts as a cushion against forces displacing the tooth, for example during mastication.

The main blood supply to the PDL is from the superior and inferior alveolar arteries. These arteries course intraosteally and give off alveolar branches that ascend within the bone as interalveolar arteries. Numerous branches arise from these vessels to run horizontally, penetrate the bone lining the alveolus, and enter the PDL space. As they enter the PDL they are called perforating arteries. They occur in greater numbers in the PDL of posterior teeth than in anterior teeth, and in greater numbers in mandibular teeth than maxillary teeth. In single rooted teeth, they are found most frequently in the gingival third of the ligament, followed by the apical third[3]. This was in agreement with the findings of Sims[56] and Douvartzidis[57] who noted a progressive increase in blood volume from the cervical to apical regions in the PDL of mice and monkeys. Blaushild et

al[58] calculated that blood vessels occupy 47 ± 2 percent in the apical portion of the PDL compared to 4 ± 2 percent at the incisal end.

Once within the PDL, the arteries occupy areas or bays of loose connective tissue called interstitial areas found between principal fibre bundles and form an arcading pattern closer to bone surface than to cementum surface[3].

Many arterio-venous anastomoses occur in the PDL. In fact, most of the PDL vessel types have been classified as post-capillary venules[59, 60]. Venous drainage is achieved by axially directed blood vessels that drain into the apical portion of the ligament[3, 54].

3.7 Role of Periodontal Ligament Vessels in Inflammation and Wound Healing

3.7.1 *Inflammation*

When a stimulus results in cell injury, a complex reaction known as inflammation is provoked. It is fundamentally a protective response whose ultimate goal is to rid the body of the initial cause of injury (such as microbes or toxins) and the consequences of such injury, that is necrotic cells and tissues. The inflammatory response involves both cellular and vascular responses that are mediated by chemical factors derived from plasma or cells. Two types of inflammations have been recognised. Firstly, acute inflammation, which is of relatively short duration (lasting from a few minutes to several hours or a few days) whose main characteristics are exudation of fluid and plasma proteins, and the emigration of leucocytes, predominantly neutrophils. The action of the activated leucocytes may result in the release of toxic metabolites and proteases extracellulary, potentially causing both endothelial and tissue damage (for example, root resorption). The second type of inflammation is chronic inflammation, which is of longer duration and associated histologically with the presence of lymphocytes and macrophages, and also the proliferation of blood vessels (known as angiogenesis) and connective tissue[61].

Inflammation is closely interwoven with the process of repair. Inflammation serves to destroy, dilute or wall off the injurious agent. It also sets off a series of events to heal the damaged tissue[61].

3.7.2 *Wound Healing*

The PDL is a specialised form of connective tissue and as such should respond very much like connective tissue to trauma. This response involves different stages as described below:

3.7.2.1 Haemostasis

Immediately following an injury, haemorrhage occurs into the tissue defect, with an aggregation of platelets and subsequently, coagulation to form a clot. This clot not only serves as a haemostatic barrier but also unites the wound margins and eventually provides a scaffold for the subsequent migration of reparative cells [62].

3.7.2.2 Inflammation

Neutrophils are the first inflammatory cells to invade the wound. They appear within a few hours of injury, reaching a maximum after twenty-four hours. They have a short life span at the wound site before degenerating. Their main function is to control bacterial invasion and hence infection. If a wound is not infected, the absence of neutrophils will not hinder the repair process.

Macrophages enter the wound after about forty-eight hours and remain for around five days. Their main function is to mop up foreign and damaged materials, but they also secrete a variety of biologically active proteins or peptides that include a mitogen specific for fibroblasts. In the absence of macrophages, fewer fibroblasts are stimulated during wound healing. Thus, rate of repair is slowed and the amount of repair tissue reduced [62].

3.7.2.3 Repair

The body's ability to repair damage induced by local injury and replace dead cells is critical to survival. Generally, this occurs by two distinct processes: (1) regeneration of injured tissue by cells of the same type, sometimes leaving no residual trace of the previous injury and (2) replacement by connective tissue, or fibroplasia, which in its permanent state constitutes a scar [63].

Regeneration of Injured Tissue

In the PDL, the first stage involves the proliferation of fibroblasts, induced by growth factors such as epidermal growth factor (EGF), platelet-derived growth factor (PDGF), fibroblast growth factors (FGF), transforming growth factors (TGF) α and β and various cytokines, such as interleukin-1(IL-1) and tumour necrosis factor (TNF). These

are released by a host of cells including macrophages, which are abundant in healing wounds.

TGF-β, in particular stimulates fibroblast chemotaxis and the production of collagen and fibronectin, at the same time inhibiting collagen degradation, all of which are effects that favour fibrogenesis. IL-1 and TNF are mitogenic and chemotactic for fibroblasts. They also stimulate the synthesis of both collagen and collagenase by fibroblasts. They are known as fibrogenic cytokines. The FGFs are capable of inducing all the steps necessary for new blood vessel formation, known as angiogenesis[63]. This process will be elaborated on later.

The fibroblasts for wound healing are derived from two sources: (1) by division of undamaged fibroblasts at the periphery of the wound and (2) by the differentiation and proliferation of undifferentiated perivascular cells[62].

Replacement by Connective Tissue

In the body, the next step in the repair process involves the replacement of non-regenerated cells by connective tissue, which in time produces a scar. The resulting daughter cells from proliferated fibroblasts described in the first stage migrate into the wound defect to form the collagen of scar tissue[62,63]. In the PDL, this scar tissue is almost immediately remodelled by the fibroblasts of the ligament to restore its normal architecture. Thus, PDL repair occurs without the formation of a scar[62].

Part of this process also involves the budding or sprouting of new vessels from pre-existing blood vessels. This process as mentioned above is termed angiogenesis and is an important biologic process contributing to the regeneration of damaged tissue.

3.7.3 *The Process of Angiogenesis*

Angiogenesis is the term used to describe the formation and ingrowth into an area of new capillary blood vessels. It usually occurs during biologic events such as tissue regeneration and the repair of wounds (which occurs in the PDL and during alveolar bone remodelling subsequent to orthodontic tooth movement), the cyclical proliferation of the nutrient-rich endometrium in preparation for the implantation of the fertilised egg, and the development of the embryo and its supporting structures[64,65]. It can also occur pathologically during the growth of tumours[66-69].

Angiogenesis occurs as a response to angiogenic factors released from (1) ischemic tissues, (2) tissues that are growing rapidly or (3) tissues that have excessively

high metabolic rates[64]. The target vessels for the angiogenic factors are the post-capillary venules and small terminal venules. These consist of flattened endothelial cells that lie upon a basal lamina, surrounded by an interrupted layer of pericytes and smooth muscle cells and invested in an extracellular matrix[64].

One of the first steps in angiogenesis involves disruption of focal contacts between adjacent endothelial cells, pericytes and smooth muscle cells. The endothelial cells then degrade and migrate through their basement membrane and extracellular matrix. Then, they undergo alterations in their expression of cell-cell and cell-matrix adhesive molecules, exhibit re-organisation of cytoskeletal elements, and express cell surface adhesion molecules such as integrins and selectins[64,65,70].

These 'activated' endothelial cells also generate proteolytic enzymes that enable them to degrade their extracellular matrix and migrate away from their parent vessel. This process initiates the formation of capillary buds that continue to grow and mature into functioning vessels. Vessel maturation involves re-establishment of the basement membrane and lumen formation. Anastomosis of these developing buds occurs with other growing buds or pre-existing vessels resulting in the formation of intact capillary loops. Once formed, these new capillaries stabilise and persist for as long as the metabolic demands of the tissue necessitate their presence. They may continue to persist as capillaries or may go on to differentiate into mature venules and arterioles[64,65,70]. This process is summarised in Figure 3.

3.7.3.1 Mediators of Angiogenesis

Angiogenesis is initiated by angiogenic mediators which may act directly on the endothelial cells to stimulate motility and mitosis, or indirectly by attracting and activating accessory cells such as inflammatory macrophages, and inducing them to produce other angiogenic mediators which then target endothelial cells[64,66]. An important feature of these mediators is that none of them are endothelial-cell specific and thus unique to the angiogenesis process. Most of them have a wide range of functions and target cells[66], some of which, as has been mentioned previously, are also involved in wound repair. Some of these angiogenic mediators include:

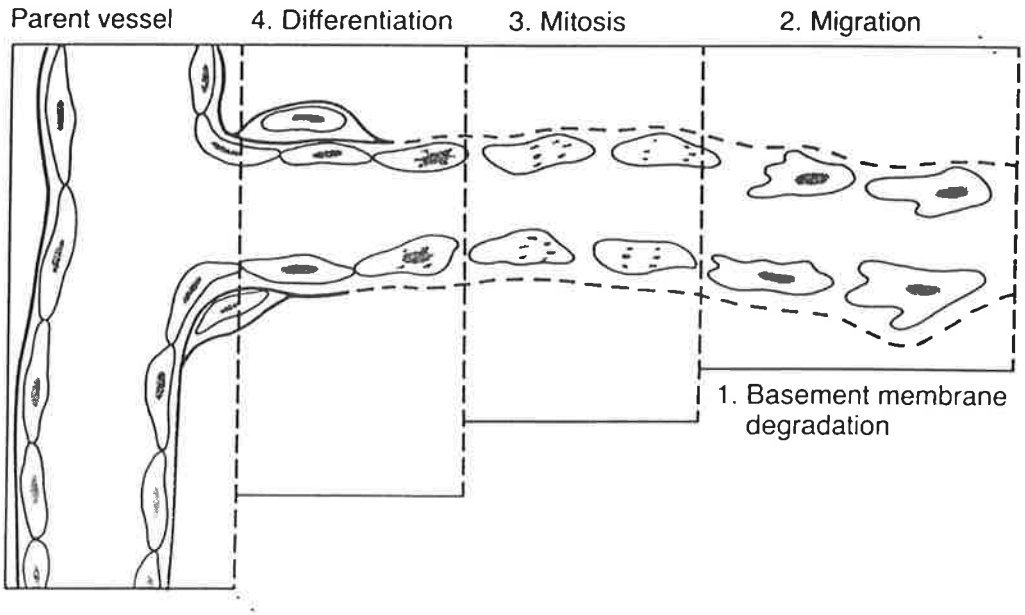

Figure 3

The Process of Angiogenesis.

Parent mature vessel is on the left. 1. Basement membrane and extracellular matrix degradation. 2. Endothelial migration. 3. Endothelial proliferation (mitosis). 4 Organisation and maturation.

(Adapted from Kumar, Cotran and Robbins. Repair: Cell growth, regeneration, and wound healing. **In** Basic Pathology. Ed. Kumar, Cotran and Robbins. Publ. WB Saunders, Philadelphia. Pp 47-60)

(a) Transforming Growth Factors (TGF)

TGF-α is released by macrophages. It has a proliferative effect on endothelial cells *in vitro* [71].

TGF-β has been shown to be angiogenic *in vivo* and *in vitro* [64]. However, it has also been shown to inhibit angiogenesis *in vitro* and *in vivo*. The actions of TGF-β on endothelial cells depend on its concentration and organisation of the extracellular matrix (ECM). Higher concentrations inhibit migration and proliferation of endothelial cells, whereas lower concentrations support proliferation or tube formation of microvascular cells [64,70].

(b) Tumour Necrosis Factor - α (TNF-α)

As with TGF-β, the actions of TNF-α are largely dose dependent. Low doses of TNF-α induce angiogenesis whilst high doses inhibit it [64].

(c) Fibroblast Growth Factor (FGF)

These can be divided into acidic FGF (aFGF or FGF-1) and basic FGF (bFGF or FGF-2). Both act directly on endothelial cells to induce endothelial cell growth and angiogenesis [64]. Basic FGF has also been found to stimulate directed migration and proliferation on cultured endothelial cells, as well as promoting the formation of differentiated capillary tubes [70].

(d) Interleukins (IL)

The main cytokine involved in angiogenesis is interleukin-8 (IL-8) [64, 70, 71]. It is a heparin-binding cytokine which is produced by most cell types. IL-8 is chemotactic for endothelial cells and induces their proliferation. It has been found to induce angiogenesis in cornea assays *in vivo* [64,70]. Norrby [71] injected rats with IL-8 and noted that statistically increased *de novo* angiogenesis occurred. Similar findings have also been noted by other authors [64,70,72]. However, Cockerill et.al [64] in a literature review also noted that very high concentrations of IL-8 did not seem to produce angiogenesis, suggesting that its actions, like TGF-β and TNF-α, are dose dependant.

IL-6 has also been implicated in the regulation of angiogenesis, although there is some disagreement as to its functions. Cohen et.al [73] found that IL-6 promoted

angiogenesis through the induction of vascular endothelial growth factor (VEGF) expression. VEGF is a potent angiogenic agent which acts on vascular endothelial cells. However, Hu et.al[72] found no effect on angiogenesis with IL-6 administration into their rats. Other authors have claimed that IL-6 has an inhibiting effect on angiogenesis[74,75]. It is most likely that its actions are dose dependent too.

Other biologic mediators which have been implicated in angiogenesis include angiogenin[64], substance P[70], prostaglandins[70] and platelet derived - growth factor[70].

3.8 Relationship of ERM to PDL Blood Vessels

Brice[46], Kittel[47] and Leedham[43] observed that ERM were often found in close proximity to blood vessels of the PDL. Brice[46, 51] noted that the ERM were found only in repairing root resorption bays but not in actively resorbing bays, leading him to the conclusion that the ERM were most likely involved in the repair of orthodontic root resorption and following this, the reconstitution of the periodontium. Leedham[43] also found ERM within repairing resorption areas and suggested that resorption repair occurs via ERM stimulation of reparative cementoblasts to form repaired cementum in the resorption lacunae.

In a three-dimensional reconstruction of ERM in relation to tooth surface and surrounding blood vessels, Kittel[47, 74] observed that these blood vessels were usually positioned between the tooth surface and epithelial cells in areas that were undergoing active root resorption. This led him to postulate that inflammatory reactions produced as a result of orthodontic force application caused PDL hyalinisation which in turn caused destruction of the ERM network allowing blood vessels to migrate into the area between the ERM and tooth surface.

The work of Löe and Waerhaug[42] alluded to the protective function of the ERM against root resorption. Root resorption can arise as a result of various traumatic stimuli. These stimuli, which can be exogenous or endogenous, initiate an inflammatory reaction in the PDL. One of the effects of inflammation is the proliferation of blood vessels to increase blood into the injured area. This results in the release of a host of inflammatory mediators which can lead to tissue destruction or repair of the area. It is this author's proposal that the ERM form a barrier around the root, protecting it against tissue damage, that is resorption. If the traumatic stimulus is large enough, this barrier is broken

and denudation of root tissue occurs. Should this occur, the ERM may also play a role in promoting repair of the resorption area.

To investigate this, immunohistochemical staining procedures will be utilised to aid in the demonstration of blood vessel and ERM structures within developing rat tissue sections.

3.9 Immunohistochemistry

Immunohistochemistry involves the use of antibodies to locate antigens in tissue. As these antigenic molecules are restricted to specific cell types, the ability to identify them through antigenic sequences has become a powerful technique in diagnostic practice. It is used by localising antigens to sections of tissue or surfaces of cells for visualisation at the light microscope level. The majority of antigens are macromolecules. Within these macromolecules, short regions known as epitopes provide a binding site for an antibody raised to that particular antigen [76]. This method is mostly used in diagnostic pathology for the detection of neoplasms. However, it can also be utilised in histology to assist in the detection of particular cellular components [76, 77].

Various immunohistochemical techniques have been developed over the years. One of the most popular techniques is the avidin-biotin technique, which will be utilised in this study. The procedure relies on the high affinity of binding between biotin and avidin. This affinity is greater than any other antigen-antibody binding [77, 78].

3.9.1 *The Avidin-Biotin Technique*

Biotin is a low molecular weight vitamin that can be covalently linked to a primary antibody to produce a biotinylated conjugate, which, when added to a section localises to the sites of an antigen. Avidin is a basic glycoprotein commonly found in eggwhites. It has four binding sites for biotin. When avidin, conjugated to horseradish peroxidase (HRP) is added to a biotinylated antibody, a tight bond is rapidly produced, thus locating the peroxidase moiety at the site of the antibody antigen reaction [77, 78]. This system is depicted in Figure 4

In 1981, Hsu et al [77-79] developed this technique further and introduced the avidin-biotin-peroxidase (ABC) complex system. This system employs a preformed complex of avidin bound to biotinylated peroxidase molecules. It is largely used as an indirect technique, whereby the primary antibody is linked to the avidin-biotin-peroxidase

conjugate by a biotinylated secondary antibody. The complex is a lattice-like, three-dimensional formation and serves to localise several molecules of horseradish peroxidase at the site of antigen in the section (refer Figure 5), thus making this technique more sensitive[77, 78].

Since then, the ABC procedure has been further refined with the introduction of streptavidin. Streptavidin is a protein with four identical subunits (each with a biotin-binding site) derived from the bacterium *Streptomyces avidinii*. It has a neutral charge and thus supposedly produces less background staining. In contrast, eggwhite avidin, which has a positive charge at physiological pH is theoretically more predisposed to greater non-specific staining[77, 78].

By utilising this technique, together with immunohistochemical markers for the ERM and endothelial cells, this study will attempt to further investigate the development of the ERM and their relationship to the blood vessels of the PDL.

d.1.1 Antigen Retrieval

Numerous authors have commented on the inconsistent results produced by formalin-fixed paraffin sections[77, 78, 80-84]. In immunohistochemistry, the aim of fixation is: (1) inactivation of autolytic mechanisms, with retention of tissue architecture, (2) immobilization of molecules to prevent artifact relocalization to other cell compartments or to prevent diffusion from the tissue, and (3) to increase rigidity of tissue for sectioning[77]. The current method of tissue processing (with formalin) and paraffin-embedding reduces the amounts of immunohistochemically detectable antigen[78]. However, True[77] discovered protein losses of up to 6% with 10% formalin whilst Leong[78] found that antigen preservation was inversely related to the duration of exposure to formalin. He found that there was a distinct reduction in the staining of some antigens after three days fixation and of most antigens after seven days fixation. He also noted that it was possible to detect changes of antigen staining in tissues fixed in formalin for a period as short as thirty minutes. Due to these facts, he conceded that tissues fixed in formalin "may not be useful for immunoperoxidase staining"[78].

However, it is still possible to salvage antigens of routinely fixed tissue through various antigen retrieval methods. As stated above, fixation with formalin can result in weak or false negative immunostaining. Various authors[80-83, 85] have explained that this occurrence is due to the fact that formalin produces cross-linking of proteins and this in turn inhibits the immunostaining reaction.

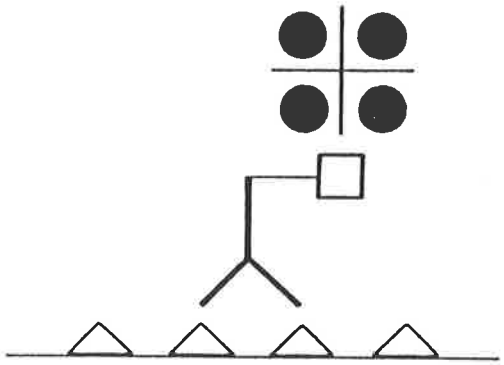

Figure 4

Avidin-Biotin Technique

Biotin (represented by the open square, is covalently linked to the primary antibody which binds to the tissue antigen (represented by triangles). Avidin (represented by +) has four binding sites for biotin and can be chemically conjugated to horseradish peroxidase (represented by solid circles). The addition of peroxidase-conjugated avidin as a secondary reagent will allow tight binding of the complex to the biotinylated primary antibody, localising to the site of the antibody-antigen reaction.

(Adapted from Leong. Immunohistochemistry – theoretical and practical aspects. **In** Applied Immunohistochemistry for the Surgical Pathologist. Ed. Leong. Publ. Edward Arnold, London. 1993. Pp1-22)

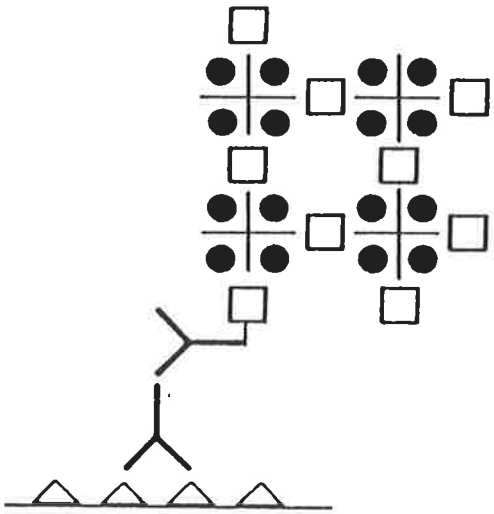

Figure 5

Avidin-Biotin-Peroxidase Complex (ABC) Technique

This technique employs a primary antibody with specificity against the antigen under study, a secondary biotinylated antibody, and a tertiary, ABC complex. The latter comprises a complex, lattice-like three-dimensional formation of avidin-biotin-peroxidase molecules which serves to localise several molecules of horseradish peroxidase at the site of antibody-antigen reaction in the tissue section.

(Adapted from Leong. Immunohistochemistry – theoretical and practical aspects. **In** Applied Immunohistochemistry for the Surgical Pathologist. Ed. Leong. Publ. Edward Arnold, London. 1993. Pp1-22)

For many years, protease pretreatment (of formalin sections) was the main antigen retrieval method [85]. It was thought that protease digestion freed antigen sites masked by formaldehyde [86, 87]. The literature [86-88] is in agreement that pretreatment of sections with protease digestion enhanced immunostaining significantly. However, for maximum effectiveness, the duration of digestion must be adjusted according to the duration of fixation [67], as according to Battifora and Kopinski [88], it is possible to over-digest tissues. This will result in deterioration of cytologic detail, thus reducing rather than enhancing immunoreaction.

According to Hautzer et.al [87], the most effective protease was trypsin, although Battifora and Kopinski [88] noted no noticeable advantage of one proteolytic enzyme over another.

Recently, investigators [80-88] have discovered that high temperature especially via microwave irradiation is capable of reversing the cross-linking of proteins produced by formalin, thus resulting in positive immunostaining of antigens. Von Wasielewski et al [85] found that 58% of the antibodies they tested showed better immunostaining results after microwave heating. Cuevas et al [83] also had similar results with 41 out of 80 antibodies tested showing significant improvement.

The method of using microwave heating to retrieve antigens was first utilized by Shi et al [80]. They heated tissue sections in a microwave oven in the presence of distilled water and metal ions. They found that the antibodies they were testing showed increased intensity of immunostaining in the presence of both solutions. Nonetheless, intensity of staining was stronger with the metal solutions. Also, best immunostaining results were obtained when slides were heated in two 5-minute cycles with an interval of one minute between cycles.

Later, Evers and Uylings [82] and Shi et al [81] discovered that the pH of the antigen retrieval solution can significantly influence immunostaining. The pH of the solution used is dependent on the antigens that are to be retrieved. Shi et al [81] discovered that an antigen retrieval solution at high pH should be employed for most of the antibodies used in surgical pathology whilst strongest immunostaining results for nuclear antigens were achieved when an antigen retrieval solution of low pH was used.

Generally, the antigen retrieval medium predominantly used by investigators [81, 82, 84, 85] at the moment is sodium citrate buffer (0.01M, pH 6). It is widely acclaimed for its

ability to enhance immunostaining with many antibodies. Although distilled water has also been shown to produce improved immunostaining, Shi et al [81] do not advocate its use as its pH value changes after heating.

There was, however, disagreement between the investigators on the optimal duration for the heat treatment. Shi et al [80, 81] recommended two 5-minute cycles on the highest power with an interval of one minute between cycles. Von Wasielewski et al [85] found that best results were obtained by continuous heating for 20-35 minutes. Cuevas et al [83] suggested irradiating the tissue sections for 5 minutes on medium power, replacing any evaporated buffer and repeating the cycle up to three times.

By utilising antigen retrieval methods during immunohistochemical staining, it is hoped that a strong, positive result may be obtained with markers used to identify ERM and blood vessels in this project.

3.9.2 *Immunohistochemical staining technique*

In summary, the steps involved in immunohistochemical staining of deparaffinized tissue involve several basic steps [77, 89]. Firstly, any endogenous peroxidase activity is blocked with a solution of 0.5% hydrogen peroxide diluted in methanol for a period of thirty minutes. This produces specific localisation of the cells or structures to be studied by reducing background staining. The tissue sections can then treated to a variety of antigen retrieval methods discussed above to improve marker efficiency.

Non-specific immunoglobulin sites are then blocked by incubating the tissues for thirty minutes in a solution of 3% animal serum (such as, horse serum) in which the primary and secondary antibodies will be diluted in. All incubations are to be performed in a moist chamber to prevent drying out of tissues.

The tissues are then incubated with the primary antibody marker (which binds to antigen receptor sites on the tissue) diluted in animal serum at an optimal working concentration. The incubation period is dependent on the concentration of the antibody.

Later, the tissues are incubated for thirty minutes with the secondary reagent, that is, the biotinylated antibody directed against whole immunoglobulins of the animal species in which the primary antibody was generated. Finally, the tissues are incubated in the tertiary reagent, that is, the avidin (or streptavidin)-biotin-peroxidase complex for an hour. This mixture binds tightly to the biotinylated secondary antibody and serves to localise molecules of horseradish peroxidase (HRP) at the site of the antibody-antigen reaction in the tissue section (this has been previously summarised in Figure 5).

A chromogen, usually 3, 3'-Diaminobenzidine Tetrahydrochloride, commonly known as DAB, is then applied to the tissue. It is utilised to detect the presence of peroxidase in a substrate or tissue section, thus demonstrating sites where HRP is present [77, 78]. In the presence of peroxidase, DAB is oxidised and converted into a stable, insoluble brown precipitate that can be visualised under the microscope [77, 78]. The development of the chromogen is timed by viewing under the microscope to optimise the stain:background ratio. However, it is essential to note that DAB is a potential carcinogen [90]. Scopsi and Larrson [90] advise that safety measures such as masks, gloves and a fume-hood be used when DAB is being utilized. In addition, both DAB solutions and contaminated glassware should be treated with either sodium hypochlorite or a mixture of potassium dichromate (or permanganate) and sulphuric acid to degrade the DAB [89, 90].

Upon completion of staining the slides are lightly counter-stained with a nuclear dye, usually haematoxylin. This increases the ability to visualise tissue architecture surrounding the immuno-stained structures, which in this case are ERM and blood vessels.

Various markers have been utilised in the literature to illustrate ERM and blood vessels immunohistochemically.

3.10 Markers for Epithelial Rests of Malassez

There have been some immunohistochemical studies performed to determine ERM markers. Investigators [91-94] have noted a positive reaction to cytokeratins.

3.10.1 Keratins and Cytokeratins

Keratins are a group of water-insoluble fibrous proteins which constitute tonofilaments in the cytoplasm of almost all true epithelial cells or tissues [95, 96]. The intracellular fibrous proteins are also known as intermediate filaments. These intermediate filaments have been recognised as major components of the cytoskeleton, and in most cells are shown to extend as fibrillar arrays between the cell membrane and nucleus. It is, therefore, hypothesised that they function as anchoring elements for the nucleus and cellular organelles, and serve as general mechanical integrators of the intracellular space [97].

The intermediate filaments can be divided into five major subclasses, each found in different types of cells: (1) desmin, found in mesenchymal myogenic cells, (2) vimentin in mesenchymal nonmyogenic cells, (3) neurofilaments in neural cells, (4) glial fibrillary acidic protein in glial cells and (5) or keratin in epithelial cells [97].

Cytokeratin was a term coined by earlier researchers to describe the keratin-like proteins of various nonepidermal epithelia [98]. However, Sun et al [95] found that the different classification of proteins into epidermis-specific "keratins" versus non-epidermal "cytokeratins" problematic and impractical as they referred to identical substances. Thus, the two terms may be used inter-changeably.

In human epithelial cells, the cytokeratins consist of at least nineteen different polypeptides which are classified into two families, one containing the relatively large and neutral-basic polypeptides, which are cytokeratins numbers one to eight; and the other smaller, more acidic poplypeptides, cytokeratins numbers nine to nineteen. The pattern of cytokeratin expression within a particular epithelium varies with its anatomical location, developmental stage, and state of differentiation. Thus, epithelial cells can be characterised by the specific pattern of keratin polypeptides they express [91]. Based on this, monoclonal antibodies with specificity for individual keratin polypeptides have been generated to enable identification of keratins at the single cell level by immunohistochemical methods [91, 97, 99].

Some investigators have used these antibodies in attempts to uncover an immunohistochemical marker for the ERM [91-94]. The results have generally been similar, but there is some discrepancy in determining the exact polypeptides contained in the ERM. Furthermore, some investigators [94] did not utilise the same nomenclature for the cytokeratin polypeptides.

Gao et al [91] noted a strong staining reaction to cytokeratin 5 and especially, cytokeratin 19. Staining with cytokeratins 3, 4, 7 and 8 were either absent or very weak. They also noted that proliferating ERM (such as those in periapical granulomas) strongly expressed keratin 14, and subsequently keratin 13, and some keratin 4. Peters et al [92] detected cytokeratins 5, 7, 8, 14, 15, 17, 18 and 19 in their immunohistochemical experiments on the ERM. Berkovitz et al [93] also noted positive staining reactions with cytokeratins 5, 6, 8, 17 and 19. They found no reactions with 1, 4, 10, 11 and 18. The slightly dissimilar results obtained by the different investigators may be due to the fact that the experiments were performed on different animals – Gao et al [91] on humans,

Peters et al [92] on rabbits and humans and Berkovitz et al [93] on cows. There were no studies performed on rat ERM. The cytokeratins which appear to overlap in the above studies include cytokeratins 5, 19 and possibly 17 (Gao et al [91] did not include this cytokeratin in their experiment).

A group of investigators [95, 96] have developed 3 monoclonal antibodies, AE1, AE2 and AE3, against human epidermal keratins. They found that AE1 antibody reacted predominantly with 50 and 56 kd keratins, AE2 reacted with 56 kd and 65 to 67kd proteins whilst AE3 reacted with 58kd and 65 to 67kd keratins. Thus, AE1 and AE3 in combination can recognise almost all known keratin species. Keratins of the AE1 family are in general more acidic than those of the AE3 family.

The monoclonal antibody combination of AE1-AE3 has successfully been used by investigators to demonstrate the presence of epithelial cells [100-102] and ERM [43], and thus will be utilised in this study to demonstrate ERM in rat tissue sections.

3.11 Markers for Blood Vessels

The inner lining of blood vessels is formed by a uniform layer of cells known as endothelial cells. These cells provide a protective, non-adherent surface and transport various substances from or into the bloodstream [103]. Much work has been done on endothelial cell markers. However, most of these have been performed on tumours such as angiosarcoma and a variety of carcinomas. This is due to that fact that one of the requirements for tumour growth is the occurrence of angiogenesis [104], signified by the increased production of endothelial cells.

Another complicating factor in the use of such markers is that endothelial cells are not the same throughout the entire cardiovascular system [103]. There are also differences between different species of animals. Endothelial cells may differ in morphology between different sites, for example, continuous endothelial cells are found in most capillaries, whilst fenestrated endothelial cells are found in glomerular capillaries and flat endothelial cells are found in many vessels except postcapillary venules of lymph nodes where cuboidal cells are found. Also, "activated" endothelial cells are more prominent or plumper than ordinary endothelial cells [103].

There are other less obvious differences, for instance, Weibel-Palade bodies (associated with secretion of von Willebrand factor (vWF)) are present in the endothelium of rats, humans and other primates but are absent in other species, prominently so in

mice. Thus, monoclonal antibodies against human vWF do not react or react poorly with endothelial cells of other species. Even within species vWF is not uniformly distributed. In humans, it can be found (by immunologic staining) in endothelial cells of arterioles, capillaries and venules of several tissues, but is absent in glomerular capillaries. The proliferative rate of endothelial cells is also quite variable. Finally, different populations of cells differ in their normal functions and also in their response to injury [103].

The markers which have been used in the literature include von Willebrand factor (also known as Factor VIIIA-related antigen or FVIII-RA), *Ulex europaeus* I agglutinin (UEA), CD31, CD34 [104-108] and rat endothelial cell antigen–1 (RECA-1) [109]. Different authors have demonstrated different results with each marker, most likely due to the variability of endothelial cells discussed above.

3.11.1 *Von Willebrand Factor (Factor VIIIA-related antigen)*

Von Willebrand factor (vWF) is a plasma protein that is important for platelet agglutination and thus, blood coagulation [108]. It is actively synthesised by virtually all non-lymphatic endothelial cells and is localised to the secretory apparatus of the cells, that is the Weibel-Palade bodies, Golgi complex and rough endoplasmic reticulum [108,107,110]. However, the main vWF storage area in endothelial cells is the Weibel-Palade bodies [110]. These rod-shaped structures are unique to endothelium. They measure 0.1μm in diameter, up to 4μm in length and are surrounded by a unit membrane [110]. Although they were first described in large blood vessels, Ewenstein and Handin [110] note that these structures have since been found in virtually all vascular and lymphatic endothelial cells, thus making vWF a good marker for endothelial cells. Commercially available monoclonal and polyclonal antibodies with proven specificity for this protein are available for labelling non-neoplastic endothelial cells, and cells of benign endothelial lesions.

However, several authors have reported variable intensity of staining with this method. Hollingsworth [104] and Poblet et al [106] in a comparison of different endothelial markers found that vWF tended to understain tissue sections. On the other hand, Siitonen et al [107] found that although vWF produced a high amount of background staining, it was their preferred choice for staining microvessels. Other authors [67-69] have successfully utilised vWF to clearly demonstrate endothelial cells in microvessels of various tumours.

The reason for this discrepancy may be due to endothelial cell variation. Another explanation was provided by True [108], who stated that the staining intensity of vWF is dependent on vessel caliber. He noted that endothelial cells of smaller vessels tended to stain more intensely with this antibody than larger vessels.

3.11.2 *Ulex europaeus I agglutinin (UEA)*

Ulex europaeus I agglutinin (UEA) is a lectin glycoprotein derived from gorse seeds. It specifically agglutinates erythrocytes of blood group O. It has a high affinity for the sugar group α-L-fucose. Human blood group O contains significant quantities of α-fucosyl groups, which accounts for their agglutination by UEA. UEA also has a high affinity for vWF, and thus, to endothelial cells [106, 108].

UEA stains most endothelial cells in vessels of all sizes. However, it lacks specificity and has been known to also stain epithelial cells of the skin, pancreas and lung [108]. Furthermore, Hollingsworth [104] also noted understaining of endothelial cells in their specimens with UEA compared with CD34.

3.11.3 *CD31*

CD31 is a glycoprotein present in endothelial cells, platelets, granulocytes and monocytes. This molecule is identical to the platelet-endothelial cell adhesion molecule, also known as PECAM-1 [106]. There is not as much work in the literature regarding this molecule (compared to CD34), although Poblet et al [106] favoured it as the most reliable marker for angiosarcoma.

3.11.4 *CD 34 (QBEnd 10)*

CD34 is also known as human haematopoietic progenitor cell antigen. It is a heavily glycosylated transmembrane protein expressed in immature human haematopoietic precursor cells from normal bone marrow [105, 106]. It is primarily used in the recognition of acute leukemias. However, it has also been shown to positively detect vascular endothelium, endothelial cell tumours and human umbilical vein endothelium. These findings suggest that CD34 may be expressed selectively in endothelial cells during angiogenesis. Nevertheless, it can also serve as a very good marker for normal endothelial cells [104, 105]. In the study by Hollingsworth [104] the reaction produced by CD34 was so much better than the other markers used (vWF and UEA) that results from the other markers were discounted and only results from CD34 used.

Traweek et al [105] noted that CD34 tended to produce a stronger staining reaction with neoplastic endothelial cells compared with adjacent benign cells. They suggested that the CD34 protein was expressed at higher levels in neoplastic cells than in non-neoplastic cells, which was consistent with their theory that CD34 functions better during endothelial cell proliferation, that is during angiogenesis.

The above experiments were all carried out on human biopsies. So far, these markers do not appear to have been utilised for rat endothelial cells. As this experiment will be conducted in rat tissue, an antigen specific for rat tissue or human antigens which can cross-react with rat tissue need to be utilised. One particular antigen which has specifically been developed as a marker for rat endothelial cells is RECA-1.

3.11.5 *Rat endothelial cell antigen-1 (RECA-1)*

In 1992, Duijvestin et al [109] in the search for antibodies that would react with rat endothelial cells developed two monoclonal antibodies which they named RECA-1 and RECA-2. These antibodies were tested in a variety of frozen sections of rat tissue. The investigators noted that only RECA-1 appeared to be endothelial cell-specific (RECA-2 cross-reacted with other cell types). They also noted that RECA-1 could be successfully applied to formalin fixed tissue. As yet, there has been no known work conducted on decalcified tissue.

Since then, various investigators [111, 112] have successfully utilised RECA-1 to identify endothelial cells in rat tissue, although not rat PDL. However, according to the manufacturers, RECA-1 cannot be successfully utilised with paraffin-embedded tissue, making it unsuitable for this current experiment (despite Duijvestin et al's [109] claims otherwise).

3.12 Double Immunohistochemical Staining

To visualise both ERM and blood vessel markers simultaneously in a single section, a double immunohistochemical staining protocol must be developed. This can be accomplished using several combinations of chromogens or metal precipitates. Antigen-coated gold granules of different sizes have been used to reveal antibodies which they bind to. It has the drawback of needing a labeled antigen preparation for each substance to be localised [113].

Recently, Vector Laboratories® have introduced an array of chromogens in a variety of colours to assist in the double detection of antigens. These include Vector blue (or immunoalkalinephosphatase), Vector VIP (purple), Vector red and Vector SG (blue-gray). These have been utilised by a several investigators including Mori et al [114], Zhou and Grofova [115].

Mori et al [114] found that the combination of immunoalkaline phosphatase with Vector blue and DAB, counter-stained with methyl green, produced the best results, providing an excellent contrast between positive and negative cells.

Before this method was available, the only way to visualise the presence of two antigens in a single section was via immunofluorescence. The advantage of this method over immunofluorescence is that the sections can be examined with the use of an ordinary light microscope and can be stored without loss of quality for long periods. Moreover, the immunoperoxidase method is more sensitive than immunofluorescence [114].

For this project, the double immunohistochemical method was utilised using a combination of markers for both ERM and endothelial cells to investigate the relationship between them.

4 MATERIALS AND METHODS

4.1 Introduction

A preliminary study was conducted prior to commencement of the main observational study to determine the markers which were to be utilised in the main study. Once the markers were chosen, the remaining tissues were then used to ascertain the optimum concentrations required to best visualise ERM and blood vessels simultaneously in each tissue section. These markers were then utilised in the main study at the established concentrations.

4.2 Ethics Approval

Permission for the use of rats in this observational study was granted by the Ethics Committee of the Adelaide University; Approval Number: S/51/98

4.3 Preliminary Study

Six Sprague-Dawley rats were sacrificed at each age of 2 days, 1 week, 2 weeks, 3 weeks, 4 weeks and 7 weeks of age. Maxillae and mandibles were dissected out and fixed overnight in 10% neutral buffered formalin (pH7) (Appendix 1). Following fixation, the tissues were decalcified in EDTA dissolved in phosphate buffered saline (pH 7) (Appendix 2). After radiographic confirmation of decalcification, the tissues were processed and embedded in paraffin (Appendix 1). Blocks were oriented to enable longitudinal sectioning, thus allowing investigation of epithelial rests of Malassez and blood vessel distribution along the length of the root.

Serial sections 0.5μm thick were cut with a microtome (Reichert-Jung), and then mounted on silane (2% APT) treated glass slides. These sections were utilised in various immunohistochemical staining runs in an attempt to determine the optimum working concentration for AE1-AE3, the epithelial cell marker (Cell Marque), CD34 and Factor VIII, endothelial cell markers (Dako). Several runs were conducted especially for Factor VIII, which also required microwave antigen retrieval for optimal endothelial cell identification.

Initially, the microwave antigen retrieval protocol originally developed by the Institute of Medical and Veterinary Sciences, Adelaide[89] was utilised. This involved microwaving the tissues in 250mL of sodium citrate solution for ten minutes on High power (Toshiba 1000W), then 10 minutes on Low power (NEC 750W). However, this proved too intense for the decalcified tissues. Most of the decalcified tissue lifted off the slides and were lost to the sodium citrate solution during the process.

Subsequently, tissues were immersed in 200ml of sodium citrate solution pH 6.3 (Appendix 4) and microwaved using different combinations of time and microwave power levels (Sharp 700W). These preliminary trials also utilised different concentrations of Factor VIII.

Once optimum concentration levels (1:2000 for AE1-AE3 and 1:10 000 for Factor VIII) and microwave antigen retrieval times (2 minutes 15 seconds on Medium High power and 3 minutes on Low power) were determined, the main experiment was commenced. (CD34 was not utilised as it did not clearly stain the blood vessels).

4.4 Main Experiment

Two pregnant Sprague-Dawley rats were obtained and their pups utilised for this study. Four Sprague Dawley rat pups were obtained at each developmental period of 2 days, 1 week, 2 weeks, 3 weeks, 4 weeks and 6 weeks of age, making a total of 24 rats. These intervals were selected to enable observation of development the first molar from commencement of crown formation (at 2 weeks) to completion of eruption into the oral cavity (6 weeks). The rats were sacrificed in a carbon dioxide gas chamber. Their maxillae were dissected out and fixed overnight in 10% neutral buffered formalin. Following fixation, the maxillae were decalcified in 4% EDTA dissolved in phosphate buffered saline (pH 7). Full decalcification was confirmed radiographically. The tissues were then processed through alcohols and Clearene (Surgipath) (refer to Appendix 1) and embedded into paraffin blocks. In each age group, 2 maxillae were oriented to enable longitudinal sections to be cut, whilst the remaining 2 were oriented to generate transverse sections. Maxillae to be oriented longitudinally were first cut in half before being mounted into paraffin blocks to ease orientation and sectioning. This is summarised in Figure 6 and Table 2.

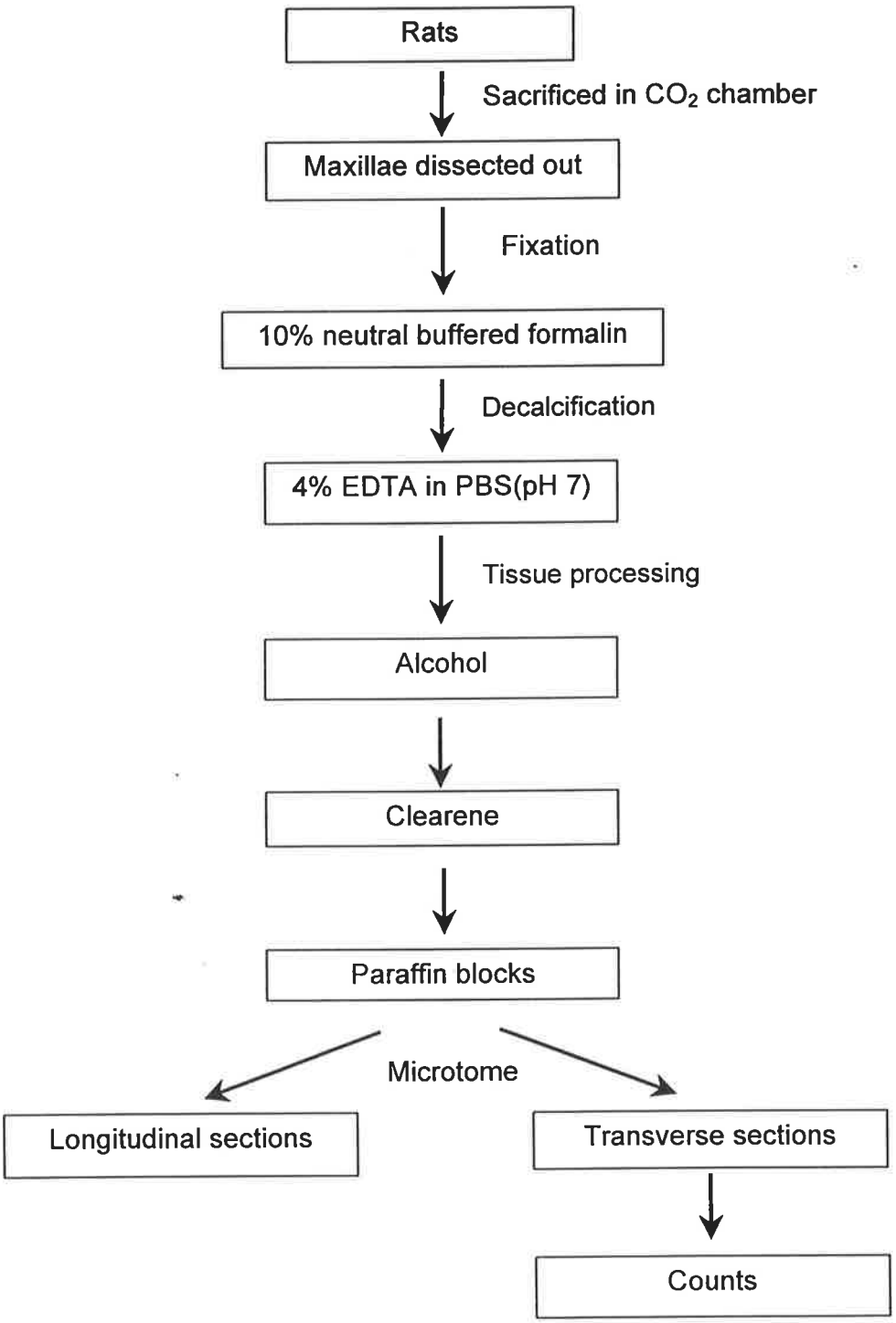

Figure 6

Flow chart depicting the processes involved in obtaining ERM and blood vessels counts

		Number of blocks in each orientation			Total
		Transverse	Longitudinal (right half)	Longitudinal (left half)	
Age	2 days	2	2	2	6
	1 week	2	2	2	6
	2 weeks	2	2	2	6
	3 weeks	2	2	2	6
	4 weeks	2	2	2	6
	6 weeks	2	2	2	6
Total		12	12	12	36

Table 2

Number of paraffin blocks in each maxillary orientation

This table shows the number of maxillae observed at different ages in various orientations to enable three dimensional visualisation of the distribution of the ERM and blood vessels within the periodontal ligament. This produced a total of thirty six paraffin blocks for sectioning.

0.5μm thick serial sections were cut with a microtome (Reichert Jung) and mounted on 2% APT treated slides. Three sections were mounted per slide. Every sixth slide was selected for investigation. These were then stained using a double immunohistochemical protocol developed during the preliminary experiment to allow simultaneous demonstration of both epithelial rests of Malassez and blood vessels in the same section, thus enabling investigation of a possible relationship between these structures. The protocol developed was as follows:

4.4.1 *Protocol for double immunostaining of epithelial rests of Malassez and endothelial cells with AE1-AE3 and Factor VIII*

1 De-wax sections in xylene and take to absolute alcohol.

2 Block endogenous peroxidase with 0.5% H_2O_2 in methanol — 30 minutes
- 3.32ml H_2O_2 in 200ml methanol

3 Rinse in Phosphate Buffered Saline (PBS) (Appendix 2) — 2 x 3 minutes

4 Antigen retrieval
- 200ml citrate
  - Microwave — 2 minutes 15 seconds Medium High + 3 minutes Low (Sharp 700 Watts)
  - Allow to cool
- Trypsin II — 3 minutes
  0.0625g Trypsin II (Sigma) in 250ml PBS pre-warmed to 37°C

5 Rinse in PBS — 2 x 3 minutes

6 Circle section with PAP pen and incubate in 3% normal horse serum (NHS) — 30 minutes
- 3% NHS = 1ml horse serum to 29ml PBS

7 Drain NHS and incubate with AE1-AE3 (at concentration 1:2000) — overnight

8 Rinse in PBS — 2 x 3 minutes

9 Incubate with anti-mouse IgG (MG) (Vector Laboratories) — 30minutes
4μL MG / 1ml NHS

10 Rinse in PBS — 2 x 3 minutes

11 Incubate with streptavidin peroxidase (SPC) (Pierce) — 60 minutes
1μL SPC / 1ml NHS

12 Rinse in PBS — 2 x 3 minutes

13 Apply Vector SG™ according to instructions — 5 minutes
Neutralise with $KMnO_4$ + Sulfuric Acid

14 Rinse in PBS	3 x 3 minutes
15 Incubate in 3% NHS	30 minutes
16 Drain NHS and incubate with Factor VIII (conc 1:10 000)	overnight
17 Rinse in PBS	2 x 3 minutes
18 Incubate with anti-rabbit IgG (AR) (Vector Laboratories)	30 minutes
4μL MG / 1ml NHS	
19 Rinse in PBS	2 x 3 minutes
20 Incubate with streptavidin peroxidase (SPC)	60 minutes
1μL SPC / 1mL NHS	
21 Rinse in PBS	2 x 3 minutes
22 Apply DAB (Vector Laboratories)	5 minutes
Neutralise with $KMnO_4$ + Sulfuric Acid	
23 Rinse in PBS	3 x 3 minutes
24 Lightly counter-stain with 2% methyl green	3 dips
2% methyl green = 2g methyl green / 100ml distilled water	
25 Dehydrate in absolute alcohol	2 dips / 30 seconds
26 Clear in xylene and mount	

Upon completion of immunohistochemical staining, the sections were then examined microscopically to determine the possibility of a relationship between the ERM and blood vessels.

4.4.2 *Microscopic examination*

Rats have three maxillary posterior teeth, each with five or more roots. It was decided that the first molar tooth would be studied in this investigation with the largest root, that is the mesiobuccal root, examined for ERM and blood vessel distribution.

4.4.2.1 Longitudinal sections

These sections were utilised purely for orientation purposes to enable better three dimensional visualisation of the distribution of ERM and blood vessels during tooth development.

4.4.2.2 Transverse sections

In each section, each first molar mesiobuccal root on the left and right sides of the maxillae were visually separated into four quadrants: mesial, distal, buccal and palatal. The periodontal ligament in each quadrant was subsequently visually separated into

three sections: tooth third, middle third and bone third along its width. The number of ERM cells and clusters, and blood vessels within each section was counted and recorded. HERS cells were not counted. To differentiate HERS and ERM cells, HERS cells were considered as those cells still adherent to the cementum surface, whilst ERM cells were those that were not adherent to the cementum, that is, there was some PDL tissue between the ERM cell and cementum.

The counts were recorded on spreadsheets. ERM cells and clusters, as well as blood vessel numbers in each periodontal ligament third and root surface quadrant along the length of the mesiobuccal root were tabulated to investigate a possible relationship between ERM and blood vessels. This can be summarised by the diagrams in Figure 7 to Figure 10. An example of the spreadsheets used is depicted in Appendix 5.

The presence of resorption lacunae on the root surfaces and along the root were also recorded and enumerated (refer to Appendix 5).

4.4.3 *Statistical Analysis*

As there were only two animals per time period, it was not possible to perform any sophisticated statistical analysis to adequately analyse the relationship between ERM cells, clusters and blood vessels along the tooth root, between surface quadrants and periodontal ligament thirds; and also to the incidence of root resorption.

Mean counts were obtained for the ERM cells, clusters and vessels for each PDL third, root third and root surface quadrant. Mean resorption lacunae per root surface quadrant and along the length of the root were also recorded. These were analysed to obtain a summary of the relationship in each area studied.

4.4.4 *Intra-Operator Error Assessment*

To calculate intra-operator error in measurement of counts, ten percent of the counts were re-counted and analysed using a paired-t test to determine if there was any systematic error due to the equipment used. The Dahlberg statistic was also performed to compute the magnitude of any errors made during counting.

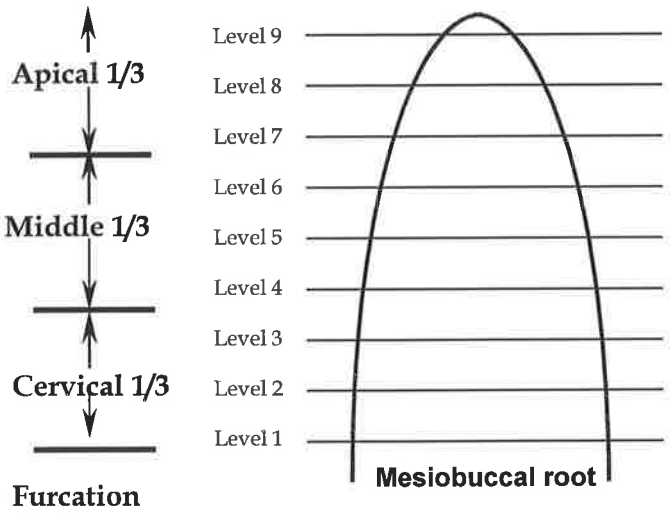

Figure 7

Root levels

Schematic diagram illustrating the division of the mesiobuccal root of the first molar into vertical thirds (cervical, middle and apical) and the levels at which sections were obtained for immunostaining and observation of ERM and blood vessel relationship

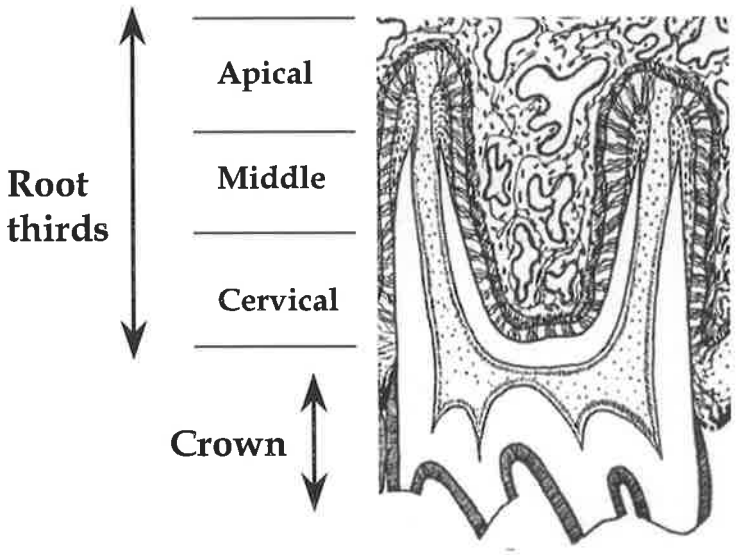

Figure 8

Mesiobuccal root thirds

This depicts the division of the mesiobuccal root of the first rat molar into thirds – cervical, middle and apical thirds

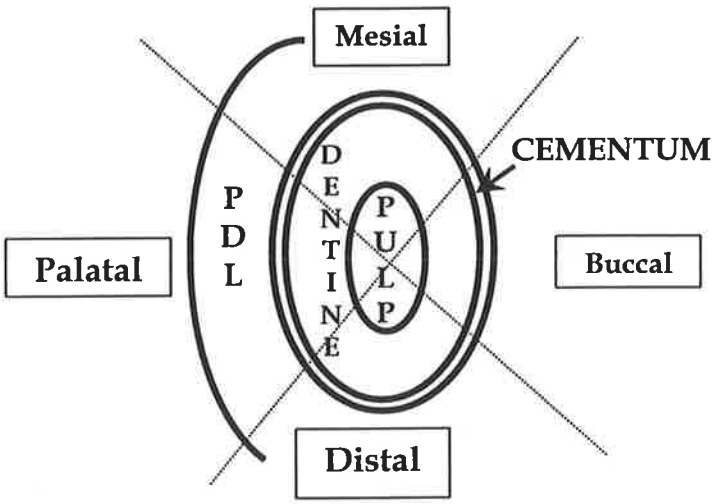

Figure 9

Root surface quadrants

A schematic diagram depicting a transverse section of the mesiobuccal root with the root surface divided into four quadrants – mesial, buccal, distal and palatal.

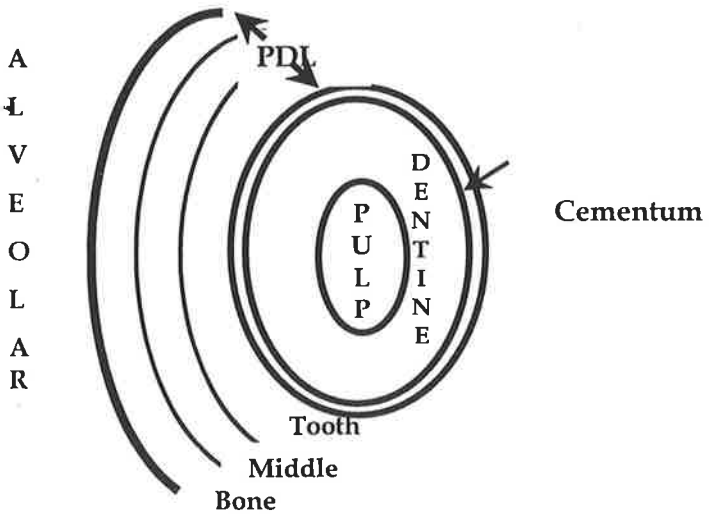

Figure 10

Periodontal ligament thirds

A schematic diagram depicting a transverse section of the mesiobuccal root with the periodontal ligament divided into thirds – tooth, middle and bone thirds.

5 RESULTS

5.1 Double Immunohistochemical Staining

AE1-AE3 (at a concentration of 1:2000) successfully demonstrated the epithelial cells of the gingival epithelium, inner and outer epithelial layers of the developing enamel organ at the early stages of crown development, and the epithelial cells of HERS and ERM. Together with the chromogen Vector SG™ the technique produced clear blue stained areas with no background staining. However, the blue colour that was produced was not obvious when sections were counter-stained with haematoxylin. Thus, sections had to be counter-stained with methyl green to enable better visualisation of cells. The author feels that the contrast between the two colours (that is, blue and green) was not as good as that which could have been obtained between DAB and haematoxylin (that is, brown and purple).

CD34 did not demonstrate the blood vessels of the PDL as well as Factor VIII. Thus, Factor VIII was the antibody of choice for the experiment. Factor VIII (at a concentration of 1:10 000) together with the chromogen DAB also produced a clean brown staining reaction with minimal background staining after microwave and trypsin II antigen retrieval. However, upon closer examination of sections, it was noted that some blood vessel-like structures had not been stained with the antibody. Either these structures were not Weibel-Palade containing vessels, were not blood vessels at all or the antibody was not labelling the cells efficiently.

The 1:10 000 concentration utilised for Factor VIII only positively demonstrated blood vessels after microwave and trypsin antigen retrieval was performed. Without antigen retrieval, the stains obtained at this concentration level were very pale and not many blood vessels were demonstrated. At higher concentrations, a high level of background staining was evident making identification of blood vessels very difficult. The period during which the sections were microwaved was also crucial. When placed too long at the high power setting, much of the decalcified tissue was lost off the slide. The final microwaving period determined for this experiment was enough to just break the protein cross-links produced by formalin, but not enough to destroy the tissue.

However, on close inspection of sections, some tissue damage was noted in a few of the sections, especially the longitudinal sections of older rats where large decalcified tooth material was present.

Nevertheless, the results of the double immunohistochemical staining protocol developed enabled sufficient simultaneous visualisation of both ERM cells and blood vessels in each tissue section and allowed investigation of rat first molar development and the relationship between these structures within these developing molars.

5.2 Two Day Old Rats

At this age, the first molar was in the bell stage of crown development. The external and internal epithelium layers of the enamel organ were clearly stained with AE1-AE3. Factor VIII demonstrated some early developing blood vessels in the dental papilla. The stellate reticulum and stratum intermedium cells could be clearly seen. An example of this is depicted in Figure 11.

5.3 One Week Old Rats

The first molar was now further into bell stage and was just commencing the early phase of the crown stage of development. The external and internal epithelial layers were still very clearly visible, and could be seen extending into the cervical loop. There were still some stellate reticulum cells in the dental organ. This can be seen in Figure 12.

5.4 Two Week Old Rats

The crown had nearly completed formation and the cervical loop was starting to elongate to commence root development. The epithelial cells of the internal and external epithelium were proliferating and a double layer of cells forming Herwig's epithelial root sheath (HERS) was starting to become visible. Refer to Figure 13. In some sections, a break was noted in the gingival epithelium which might be an indication of commencement of tooth eruption.

Figure 11

Two day crown
This depicts the first (**M1**) and second (**M2**) molars of a two day old rat in the bell stage of development. Note the dark blue stain of AE1-AE3 (with Vector SG) staining the internal and external epithelium. (Original magnification = 4X)

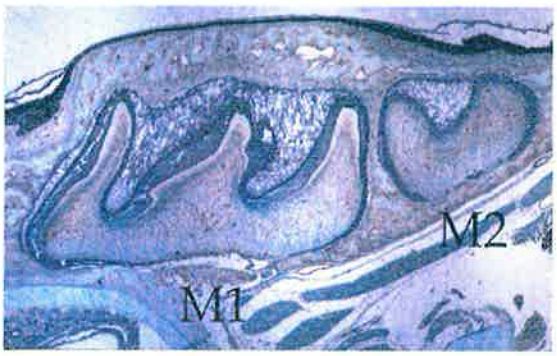

Figure 12

1 week crown
This depicts the appearance of the first molar in a one-week-old rat. It is still in the late bell stage of development. (Original magnification = 4X)

Figure 13

2 week crown
This depicts the appearance of the first molar in a two-week-old rat. The crown has nearly completed formation and root development has commenced. Note the presence of the cervical loop. Also, the tooth has started erupting and appears closer to the gingival margin than the previous diagrams. (Original magnification = 4X)

5.5 Three Week, Four Week and Six Week Old Rats

5.5.1 *Observations*

At three weeks, HERS continued to produce elongation of the molar root (only the mesiobuccal (MB) root will be concentrated on). The epithelial diaphragm was still present. In some areas, ERM were starting to appear along the root.

The root continued to develop during the four-week period and had nearly completed development at six weeks. Some HERS cells were still noted along the root at six weeks (though, the number of ERM was much larger) and the sheath diaphragm was very much still present in the apical third. There was some difference in developmental stages of the root between surfaces. The diaphragm was still present, usually on the mesial and occasionally palatal surfaces, but not on the buccal or distal surfaces at the apical ends of the roots in both four and six-week-old rats. These changes can be seen in Figure 14, Figure 15, Figure 16 and Figure 17.

ERM cells and clusters were found from three weeks onwards and a network made up of a combination of ERM and HERS cells was observed around the root. In transverse sections (Figure 15 and Figure 16) the ERM presented as single round or ovoid cells (Figure 18) or as clusters of multiple cells (Figure 19). In longitudinal sections, the cells were observed to form a network that ran parallel to the length of the root.

With age, there was an increasing number of ERM cells and clusters which, although still in the tooth third of the PDL, appeared further away from the cementum surface. Also noted in the older animals (that is, four-week and six-week-old rats) was an increasing number of cells in the apical third which were trapped within the cementum. These cells were not included in the counts. (Figure 20)

PDL blood vessels were observed mainly in the middle and bone third of the PDL in all ages. However, it was noted that the vessels located in the bone third were much larger in diameter than those found in the middle third.

Figure 14

3 week tooth

At three weeks of age, the crown was fully developed but the root was still developing. The tooth was nearly fully erupted. The tooth appeared very similar at four and six weeks of age.
(Original magnification = 2X)

Figure 15

Three week root - transverse section

This depicts a three-week first molar cut in a transverse direction. The rat maxillary first molar has five roots. The mesiobuccal (**MB**) root which is the largest, buccal (**B**) roots and two palatal (**P**) roots. (Original magnification = 4X)

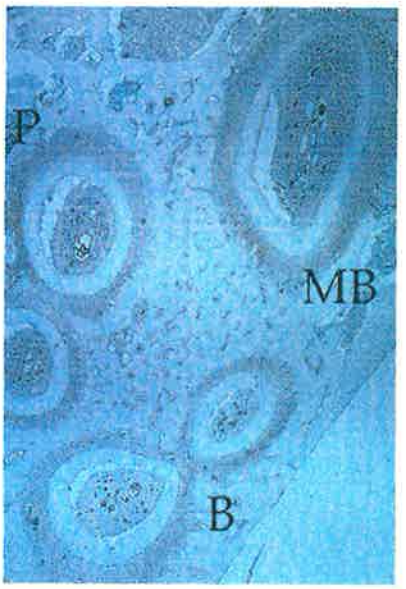

Figure 16

HERS and ERM network

This depicts the distal surface of a three-week-old mesiobuccal root with a network made up of ERM and HERS cells on the surface. Although the magnification is not high enough, the HERS cells are those attached to the tooth root cementum (**T**), whilst the ERM cells are are not. This photograph also shows the simultaneous demonstration of epithelial cells and blood vessels (**bv**) stained utilising the double immunostaining technique.
(Original magnification =20x)

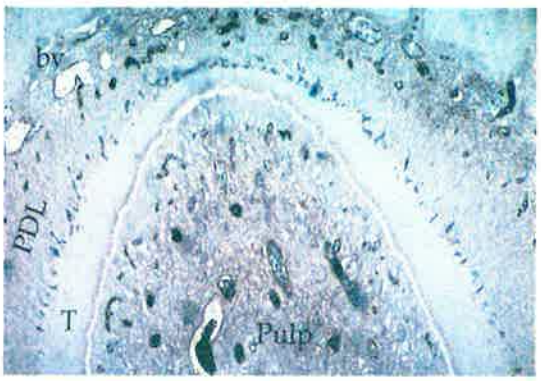

Figure 17

Diaphragm on mesial surface of root

The difference in developmental levels between the root surfaces is shown here. The diaphragm of HERS (**D**) is still present on the mesial root surface of the mesiobuccal root but not on any of the other surfaces. (Original magnification = 10x)

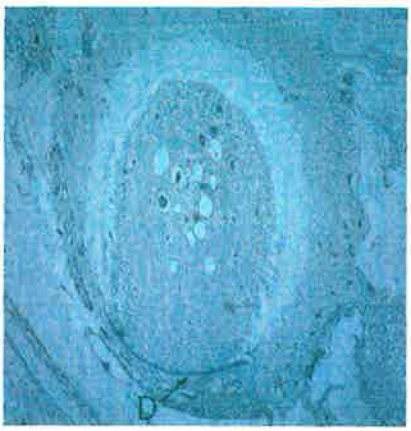

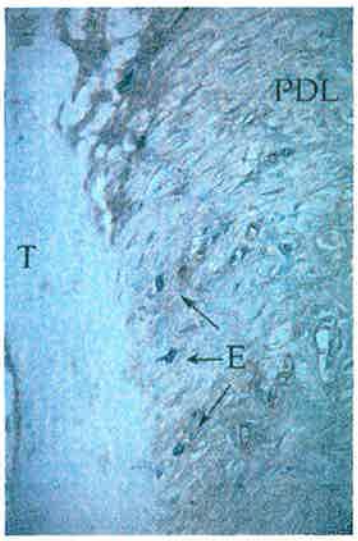

Figure 18

ERM cells

This picture depicts the appearance of ERM which presented as single cells (**E**) in a transverse section of root. (**T** = Tooth, **PDL** = periodontal ligament). (Original magnification = 40x)

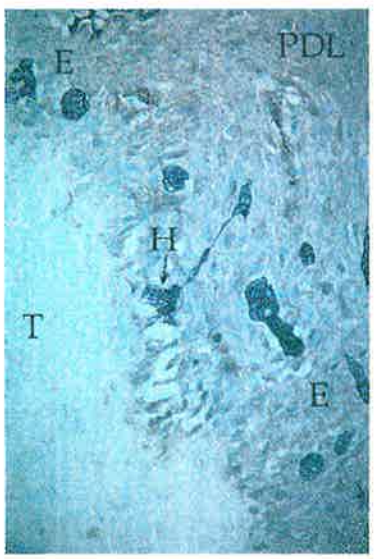

Figure 19

ERM clusters

This depicts the appearance of ERM (**E**) which presented as clusters of multiple cells in a transverse section of a root. Note the presence of HERS (**H**) on the surface of the tooth root (**T**) cementum. (Original magnification = 40x)

By the age of three weeks, the first molar was nearly fully erupted in the oral cavity. During the four week period, there was an increase in the number of ERM cells and clusters and also blood vessels which also appeared to invade the tooth third of the PDL. Root resorption was also an important feature as demonstrated by an increasing number of resorption lacunae along the root surfaces of both four and six-week-old molars (Figure 21).

5.5.2 *Counts*

ERM and blood vessel counts were obtained for three, four and six week old rats; and their distribution along the PDL was investigated, together with their relationship to resorption lacunae.

5.5.2.1 Distribution of Epithelial Rests of Malassez

As mentioned previously, the ERM presented in two forms along the PDL. Some appeared as single cells and others were present in clusters. Thus, counts were differentiated into "single cell" and "cluster" groups. From the transverse sections, the number of cells and clusters in each section were further divided into root surface quadrants (buccal, mesial, palatal and distal) and into which horizontal third of the periodontal ligament area there were noted. The total counts were divided by the number of sections to obtain a mean ($\bar{x}$) number of ERM cells and clusters for each PDL third, vertical root third and root surface quadrant along the mesiobuccal root of the first molar. Counts from the root surface quadrants were further divided into which vertical root third the cells or clusters were noted. This is shown in Table 3, Table 4, Table 5 and Table 6. All of the ERM cells and clusters were found on the tooth third of the PDL.

Distribution along vertical mesiobuccal root thirds (Table 3 and Table 4)

At three weeks, the mean ERM single cell counts were higher ($\bar{x}$ = 7.14 $\pm$ 3.67) in the middle third of the root, slightly lower ($\bar{x}$ = 6.89 $\pm$ 3.55) in the cervical and apical third ($\bar{x}$ = 6.0 $\pm$ 2.39) in (Table 3). However, ERM clusters were more numerous in the cervical third ($\bar{x}$ = 3.11 $\pm$ 1.53), slightly lower in the middle ($\bar{x}$ = 2.43 $\pm$ 1.99) and lowest ($\bar{x}$ = 2 $\pm$ 1.6) in the apical third of the root (Table 4).

At four weeks, there were larger numbers ($\bar{x}$ = 17.71 $\pm$ 4.3) of single ERM cells in the middle of the root, followed by the apical third ($\bar{x}$ = 11.5 $\pm$ 8.37) and a much lower number ($\bar{x}$ = 8.7 $\pm$ 3.5) in the cervical third. ERM clusters were once again higher ($\bar{x}$ = 4.5

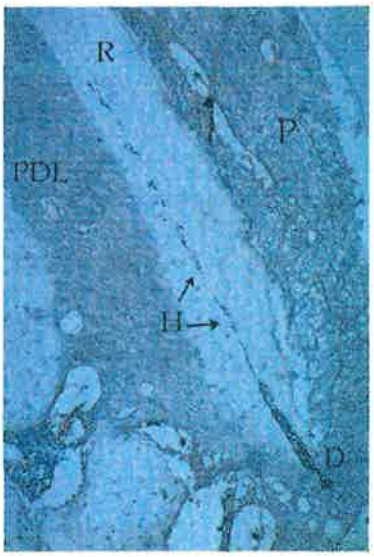

Figure 20

HERS cells trapped in cementum

This depicts HERS cells (**H**) which become trapped in forming cementum of the root (**R**) during root development. These cells do not go on to form ERM. (**P** = pulp, **D** = diaphragm, **PDL** = periodontal ligament). (Original magnification = 20x)

Figure 21

Resorption lacuna

This depicts a resorption lacuna (**R**) on the distal surface of a six-week-old mesiobuccal root. Note the break in the ERM network (**E**) and the invasion of blood vessels (**bv**) across the PDL towards the root surface. (Original magnification =20x)

ERM cell counts			
Age of rats	Root thirds	Mean ($\bar{x}$) counts	Standard deviation (SD)
3 weeks	Cervical	6.89	3.55
	Middle	7.14	3.67
	Apical	6.0	2.39
4 weeks	Cervical	8.7	3.5
	Middle	17.71	4.3
	Apical	11.5	8.37
6 weeks	Cervical	17.67	3.83
	Middle	6.44	4.75
	Apical	2.75	2.87

Table 3

Mean and standard deviation of ERM single cell counts along the first molar root in the tooth third of the PDL of 3, 4 and 6 weeks rats

ERM clusters			
Age of rats	Root thirds	Mean ($\bar{x}$) counts	Standard deviation (SD)
3 weeks	Cervical	3.11	1.54
	Middle	2.4	2.00
	Apical	2.00	1.64
4 weeks	Cervical	4.50	1.96
	Middle	3.57	2.07
	Apical	2.63	3.38
6 weeks	Cervical	11.50	3.27
	Middle	1.78	1.99
	Apical	1.00	0.71

Table 4

Mean and standard deviation ERM clusters along the first molar root in the tooth third of the PDL of 3, 4 and 6 weeks rats

± 1.96) in the cervical third, slightly lower ($\bar{x}$ = 3.57 ± 2.07) in the middle and lowest ($\bar{x}$ = 2.63 ± 3.38) in the apical third.

At six weeks, both single and clusters of ERM cells were very much higher ($\bar{x}$ = 17.67 ± 3.83 and $\bar{x}$ = 11.5 ± 3.27) in the cervical third area, reducing to means of 6.44 ± 4.75 and 1.78 ± 1.99 respectively in the middle third area and were low ($\bar{x}$ = 2.75 ± 2.87 and $\bar{x}$ = 1 ± 0.71) in the apical third area.

The above counts were converted into graphs in Figure 22, Figure 23, Figure 24 and Figure 25. When the counts were combined the graph produced can be seen in Figure 26.

Thus, in summary, at three weeks, ERM cell counts were highest in the apical third of the root and lowest in the cervical third. All counts showed some increase at the four-week period, with apical and middle counts experiencing a greater increase compared to cervical counts. However, by six weeks, middle and apical cell counts were greatly decreased whilst cervical counts were greatly increased to the extent of showing the highest counts for the time period.

The number of ERM clusters was usually lower than the number of single cells in each root third. For all time periods, cervical counts were higher than middle or apical counts (which were the lowest for all time periods). At the six-week period, there was a big increase in cluster counts compared to increases in the middle and apical vertical thirds of the mesiobuccal root.

Distribution around root surface quadrants (Table 5 and Table 6)

Due to the variability in counts along the vertical length of the root, ERM counts from the four surface quadrants between the root thirds were analysed according to root thirds:

Cervical third

At three weeks of age, the greatest number of ERM cells were noted on the distal surface ($\bar{x}$ = 2.40 ± 2.19), followed by the buccal and mesial surfaces ($\bar{x}$ = 2.11 ± 1.62 and $\bar{x}$ = 2.11 ± 2.2 respectively) with the least found on the palatal surface ($\bar{x}$ = 1.33 ± 1.12). After four weeks, there was a general slight increase in the number of cells noted on all surfaces. The greatest number of cells was noted on the distal ($\bar{x}$ = 3.38 ± 2) and buccal ($\bar{x}$ = 2.5 ± 1.08), with smaller amounts on the mesial ($\bar{x}$ = 2.1 ± 2.23) and palatal ($\bar{x}$ = 1.4 ± 1.35).

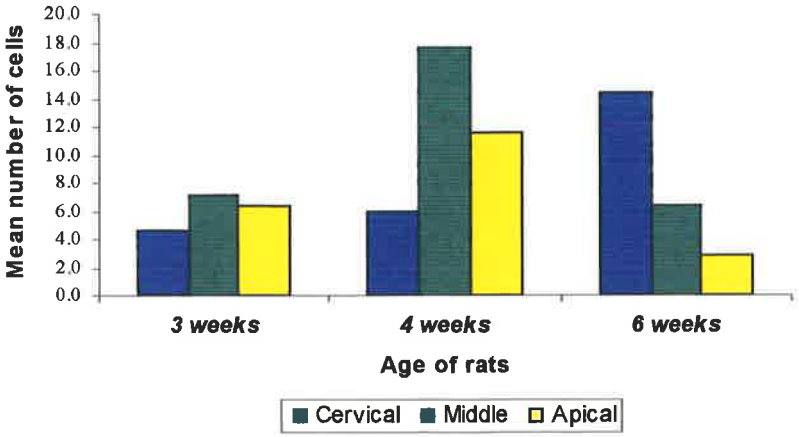

Figure 22
ERM cells along mesiobuccal root
Mean ERM cell counts along the tooth root thirds in the tooth third of the PDL of 3, 4 and 6-week-old rats

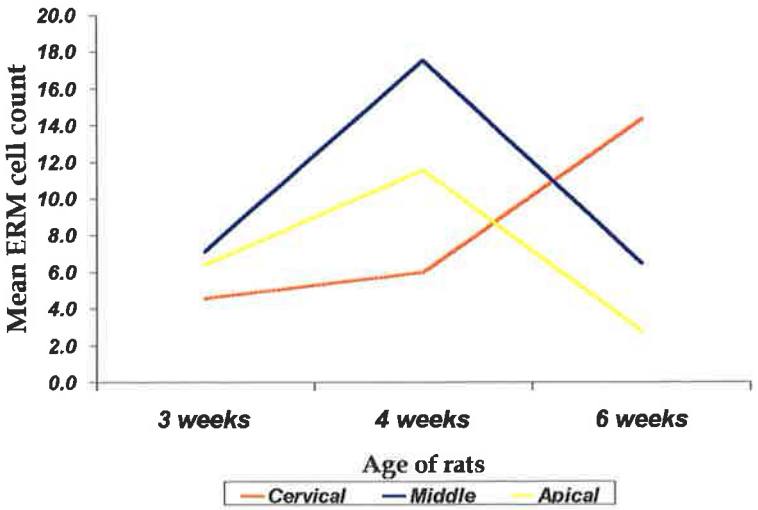

Figure 23
ERM cells along mesiobuccal root
Mean ERM cells along the tooth root thirds in the tooth third of the PDL of 3, 4 and 6-week-old rats

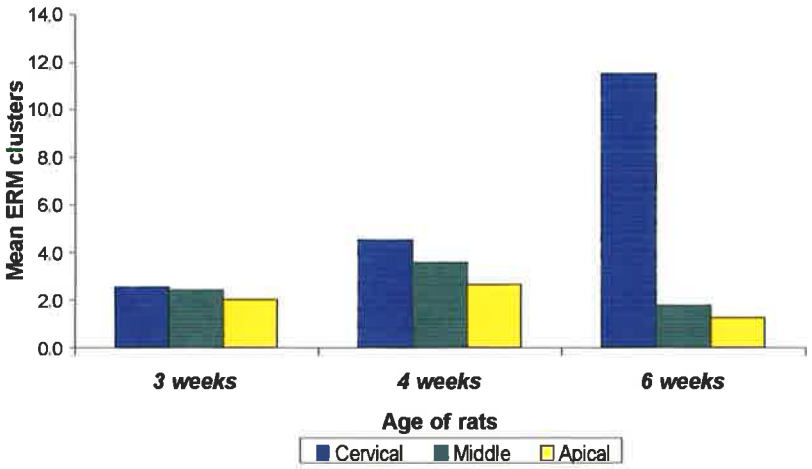

Figure 24
ERM clusters along mesiobuccal root
Mean ERM clusters along the tooth root thirds in the tooth third of the PDL of 3, 4 and 6-week-old rats

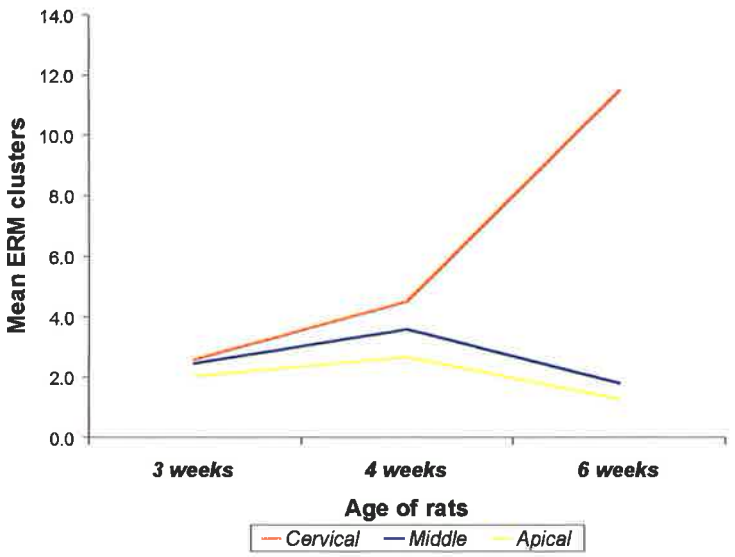

Figure 25
ERM clusters along mesiobuccal root
Mean ERM clusters along the tooth root thirds in the tooth third of the PDL of 3, 4 and 6-week-old rats

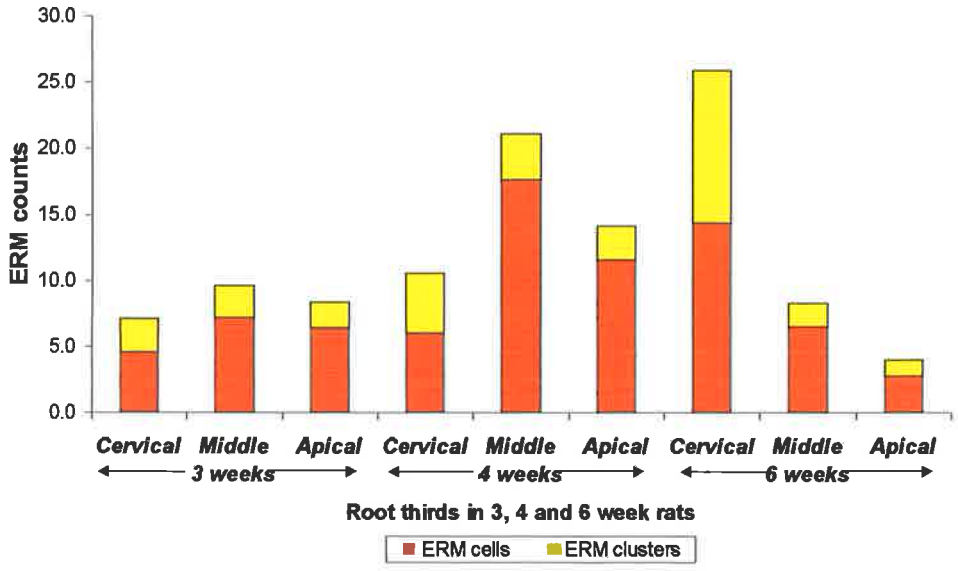

Figure 26

ERM cells and clusters along mesiobuccal root

Mean ERM cells and clusters along the tooth root of 3, 4 and 6-week-old rats

ERM cells							
Root thirds	Surface quadrants	Age of rats					
		3 weeks		4 weeks		6 weeks	
		Mean	SD	Mean	SD	Mean	SD
Cervical	Buccal	2.11	1.62	2.50	1.08	5.00	2.45
	Mesial	2.11	2.20	2.10	2.23	5.17	4.31
	Palatal	1.33	1.12	1.40	1.35	4.17	1.72
	Distal	2.40	2.19	3.38	2.00	4.00	2.34
Middle	Buccal	1.29	1.38	3.57	1.27	1.33	1.66
	Mesial	2.71	2.81	8.29	4.23	1.22	1.92
	Palatal	1.29	0.95	2.86	1.07	1.56	1.74
	Distal	1.86	1.07	3.00	1.63	2.56	2.18
Apical	Buccal	2.13	0.84	3.00	2.39	0.50	0.58
	Mesial	1.50	0.71	11.50	0.71	2.00	0.00
	Palatal	1.25	0.71	2.50	2.14	1.25	1.50
	Distal	2.63	2.61	3.50	1.96	0.50	1.00

Table 5

Mean and standard deviation of ERM cell counts around the root surfaces in the tooth third of the PDL of 3, 4 and 6 weeks rats

ERM clusters							
Root thirds	Surface quadrants	Age of rats					
		3 weeks		4 weeks		6 weeks	
		Mean	SD	Mean	SD	Mean	SD
Cervical	Buccal	1.22	1.30	1.20	1.82	3.50	3.83
	Mesial	0.89	1.54	0.10	0.32	1.17	1.6
	Palatal	0.22	0.44	0.00	0.00	3.00	1.41
	Distal	1.40	1.52	4.00	1.85	4.60	1.34
Middle	Buccal	0.57	0.82	0.86	1.22	0.11	0.33
	Mesial	0.86	1.09	0.71	1.11	0.11	0.33
	Palatal	0.43	0.84	0.71	0.76	0.56	0.88
	Distal	0.57	0.82	1.29	1.50	1.00	1.50
Apical	Buccal	0.38	0.74	0.63	1.41	0.75	0.89
	Mesial	0.50	0.71	2.00	2.84	1.00	0.00
	Palatal	0.25	0.46	0.63	0.74	0.00	0.00
	Distal	1.25	1.28	0.88	1.46	0.25	1.50

Table 6

Total and mean ERM cell counts around the root surfaces in the tooth third of the PDL of 3, 4 and 6 weeks rats

By six weeks, the number of cells had increased again on all the surfaces. The greatest number of cells was found on the mesial surface ($\bar{x}$ = 5.17 ± 4.31) and secondly on the buccal surface ($\bar{x}$ = 5.0 ± 2.45). Less cells were noted on the palatal ($\bar{x}$ = 4.17 ± 1.72) and distal ($\bar{x}$= 4 ± 2.34) surfaces.

At three weeks, the highest number of ERM clusters was noted on the distal ($\bar{x}$ = 1.4 ± 1.52) and buccal ($\bar{x}$ = 1.22 ± 1.3) and the lowest on the mesial ($\bar{x}$= 0.89 ± 1.54) and palatal ($\bar{x}$ = 0.22 ± 0.44) surfaces. After four weeks, the number of ERM clusters on the distal surface increased to $\bar{x}$ = 4 ± 1.85. The clusters on the other surfaces did not differ greatly from three weeks. The mesial surface contained $\bar{x}$ = 1.2 ± 1.82 clusters whilst the mesial had $\bar{x}$ = 0.1 ± 0.32. None were noted on the palatal surface.

The number of clusters appeared to be larger at six weeks of age. The highest number was noted on the distal ($\bar{x}$ = 4.6 ± 1.34) and buccal ($\bar{x}$ = 3.5 ± 3.83). The palatal had slightly less clusters ($\bar{x}$ = 3 ± 1.41 with the least noted on the mesial surface ($\bar{x}$ = 1.17 ± 1.6).

Generally, in the cervical third of the mesiobuccal root, a higher proportion of cells was noted on the buccal surface. However, a larger proportion of clusters was noted on the buccal and distal surfaces. There was an increase in the number of cells and clusters with age.

Middle third

At three weeks, the highest number of cells was noted on the mesial ($\bar{x}$ = 2.71 ± 2.81 and distal ($\bar{x}$ = 1.86 ± 1.07). The buccal and palatal surfaces had similar counts ($\bar{x}$ = 1.29 ± 1.38 and $\bar{x}$ = 1.29 ± 0.95 respectively). Cell numbers increased at four weeks with a large number noted on the mesial surface ($\bar{x}$ = 8.29 ± 4.23). Fewer cells were noted on the buccal ($\bar{x}$ = 3.57 ± 1.27), distal ($\bar{x}$ = 3.0 ± 1.63) and palatal ($\bar{x}$ = 2.86 ± 1.07) surfaces.

By six weeks, cell numbers had decreased slightly with the largest number of cells on the distal having a mean of only $\bar{x}$ = 2.56 ± 2.18. Counts for the other surfaces were $\bar{x}$ = 1.56 ± 1.74 on the palatal, $\bar{x}$ = 1.33 ± 1.66 on the buccal and $\bar{x}$ = 1.22 ± 1.92 on the mesial.

There were fewer clusters in the middle third compared to the cervical third. At three weeks, the highest mean count was on the mesial surface ($\bar{x}$ = 0.86 ± 1.09). The buccal and distal surfaces had similar counts and standard deviations ($\bar{x}$ = 0.57 ± 0.82), and the lowest count was on the palatal ($\bar{x}$ = 0.43 ± 0.84). Counts were slightly higher at four weeks. The highest count was on the distal this time ($\bar{x}$ = 1.29 ± 1.5). The buccal

surface had a mean of $\bar{x}$ = 0.86 ± 1.22, whilst the mesial and palatal surfaces had counts of $\bar{x}$ = 0.71 ± 1.11 and $\bar{x}$ = 0.71 ± 0.76 respectively.

Just like the ERM cells, cluster counts decreased slightly after six weeks with a mean of $\bar{x}$ = 1 ± 1.5 on the distal surface. The second highest count was on the palatal with $\bar{x}$ = 0.56 ± 0.88. The lowest counts were noted on the buccal and mesial surfaces, both with $\bar{x}$ = 0.11 ± 0.33.

Generally, in the middle third of the root, a higher proportion of cells and clusters was noted on the distal surface. However, a very large number of cells was noted on the mesial surface after four weeks. The number of cells and clusters increased from three to four weeks, but decreased again at six weeks.

Apical third

At three weeks of age, the largest number of cells was noted on the distal ($\bar{x}$ = 2.63 ± 2.61) and buccal surfaces ($\bar{x}$ = 2.13 ± 0.84). Fewer cells were noted on the mesial ($\bar{x}$ = 1.5 ± 0.71) and palatal ($\bar{x}$ = 1.25 ± 0.71). The number of cells in all surfaces increased at four weeks. Once again, there appeared to be a very large number on the mesial ($\bar{x}$ = 11.5 ± 0.71) surface. This was followed by the distal ($\bar{x}$ = 3.5 ± 1.96), buccal ($\bar{x}$ = 3 ± 2.39) and palatal ($\bar{x}$ = 2.5 ± 2.14).

Similar to the middle third of the root, cell numbers decreased at six weeks. The largest number of cells was noted on the mesial ($\bar{x}$ = 2 ± 0) followed by the palatal ($\bar{x}$ = 1.25 ± 1.5). Fewer cells were found on the distal and buccal surfaces ($\bar{x}$ = 0.5 ± 1 and $\bar{x}$ = 0.5 ± 0.58 respectively).

At three weeks, the largest number of clusters was noted on the distal surface ($\bar{x}$ = 1.25 ± 1.28) followed by the mesial ($\bar{x}$ = 0.5 ± 0.5). The buccal and palatal surfaces had counts of $\bar{x}$ = 0.38 ± 0.74 and $\bar{x}$ = 0.25 ± 0.46 respectively. At four weeks, the largest counts of clusters ($\bar{x}$ = 2 ± 2.84) was noted on the mesial surface as well. This was followed by the distal ($\bar{x}$ = 0.88 ± 1.46), buccal ($\bar{x}$ = 0.63 ± 1.41) and palatal ($\bar{x}$ = 0.63 ± 0.74) surfaces.

By six weeks, the number of ERM clusters had reduced with the highest mean ($\bar{x}$ = 1 ± 0) found on the mesial surface. The second highest ($\bar{x}$ = 0.75 ± 0.89) was noted on the buccal surfaces. This was followed by the distal surface ($\bar{x}$ = 0.25 ± 1.5) with no clusters noted on the palatal.

In the apical third, there was a variation in distribution of ERM cells between the surfaces between the ages. However, the largest number of clusters was generally noted on the mesial surface and the least on the palatal. Cells and clusters also appeared to

increase in number from three to four weeks, but appeared to reduce again after six weeks. This was similar to the presentation at the middle third of the root.

These counts are depicted graphically in Figure 27, to Figure 38.

5.5.2.2 Distribution Of Blood Vessels

Unlike the ERM, the blood vessels were spread out along the width of the PDL. Most were found on the bone and middle third of the PDL and there were some that appeared to invade into the tooth third. The distribution of the blood vessels will be discussed below and is listed in Table 7,Table 8, Figure 8 and Figure 7. It is summarised graphically in Figure 39, Figure 40, Figure 41 and Figure 42.

Distribution across vertical root thirds (Table 7)

In the three-week-old rats, no blood vessels were noted in the tooth third of the PDL. Generally, there were more vessels on the bone third than the middle. The middle third of the root had the highest number of vessels ($\bar{x}$ = 31.57 ± 16.14 in the middle and $\bar{x}$ = 50.29 ± 11.06 in the bone third of the PDL). This was followed by the apical third with $\bar{x}$ = 29.17 ± 12.69 in the middle and $\bar{x}$ = 44.83 ± 13.7 in the bone third. The cervical third of the root had the lowest count ($\bar{x}$ = 26.5 ± 7.33 in the middle and $\bar{x}$ = 44.25 ± 8.43 in the bone third). Nonetheless these counts did not vary greatly from each other.

The blood vessels encroached into the tooth third of the PDL at four weeks of age. The cervical third of the root had the highest number of vessels in the tooth third ($\bar{x}$ = 4.2 ± 3.91) and also a large number of vessels in the middle ($\bar{x}$ = 47.2 ± 21.04) and bone thirds ($\bar{x}$ = 44.8 ± 13.94) as well. The middle third had slightly lower counts with only a mean of 1.75 ± 2.19 in the tooth third, 38 ± 14.35 in the middle and 47.5 ± 16.9 in the bone thirds of the PDL. The apical third had similar counts with $\bar{x}$ = 0.8 ± 1.03 in the tooth third, $\bar{x}$ = 35.1 ± 35.1 in the middle and $\bar{x}$ = 43.9 ± 16.92 in the bone third.

At six weeks, the number of blood vessels in the tooth third of the PDL decreased. None were found in the tooth third of the cervical third of the root. Counts in the middle third ($\bar{x}$ = 47 ± 19) was higher than the bone third ($\bar{x}$ = 42.33 ± 21.48). In the middle of the root, there was a mean of 0.17 ± 0.41 in the tooth third, whilst the middle had 38.17 ± 14.25 which was lower than the cervical and the bone third with 55.5 ± 16.74 was higher than the cervical third. The apical third of the root had the highest blood vessel counts in the middle ($\bar{x}$ = 40.25 ± 18.91) and bone ($\bar{x}$ = 53.25 ± 15.12) thirds, but only $\bar{x}$ = 0.88 ± 1.64 in the tooth third.

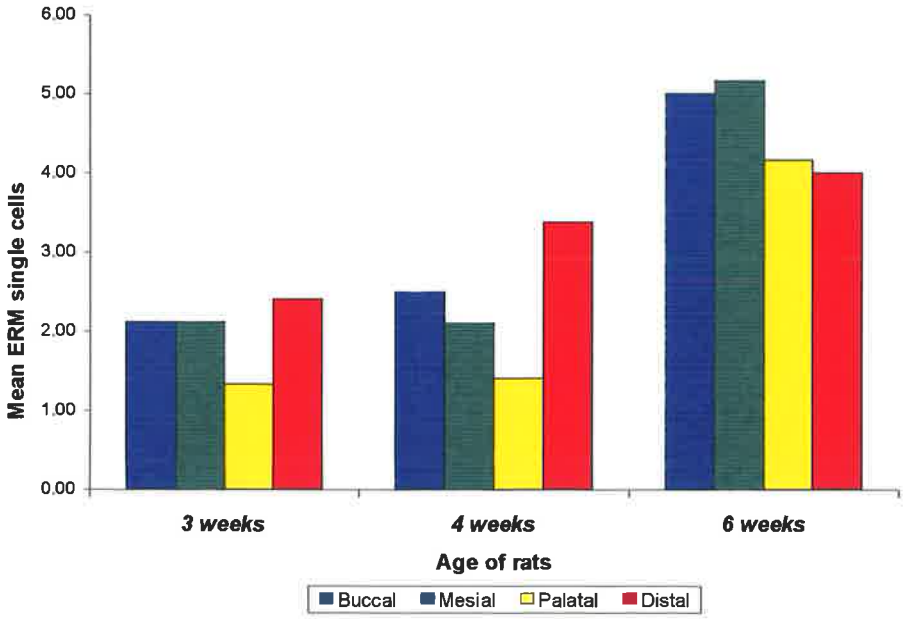

Figure 27
ERM cells around root surfaces (cervical third)
Mean ERM cells around the root surface quadrants at the cervical third level of the mesiobuccal root in 3, 4 and 6-week-old rats

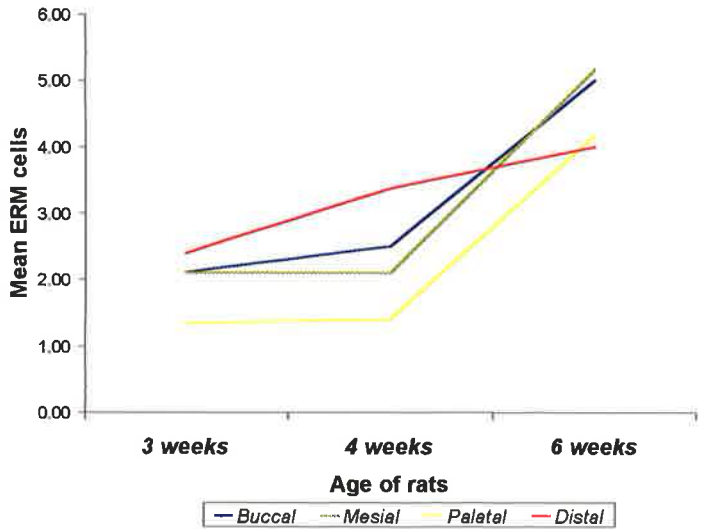

Figure 28
ERM cells around root surfaces (cervical third)
Mean ERM cells between the different surface quadrants in the cervical third of the mesiobuccal molar root of 3, 4 and 6-week-old rats

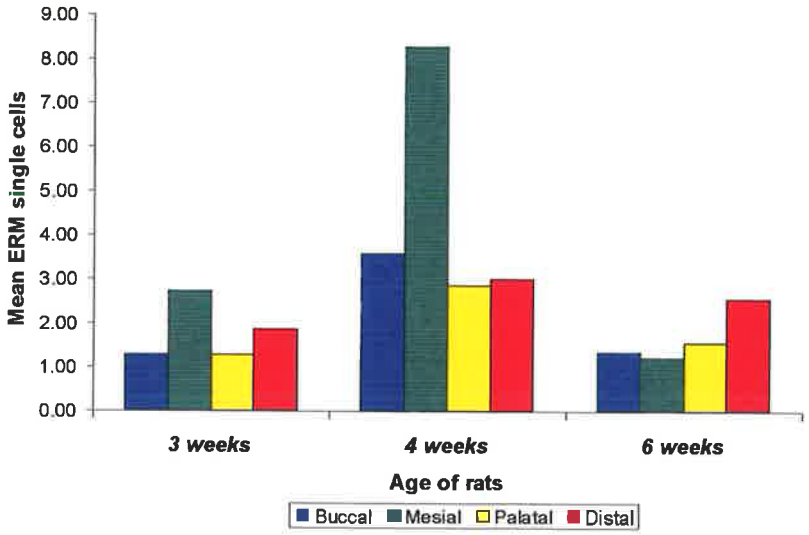

Figure 29

ERM cells around root surfaces (middle third)

Mean ERM cells around the root surface quadrants at the middle third level of the mesiobuccal root in 3, 4 and 6-week-old rats

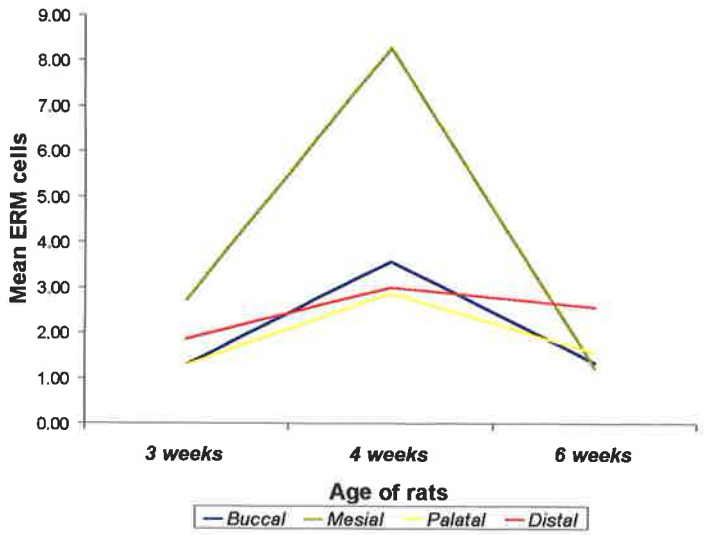

Figure 30

ERM cells around root surfaces (middle third)

Mean ERM cells between the different surface quadrants in the middle third of the mesiobuccal molar root of 3, 4 and 6-week-old rats

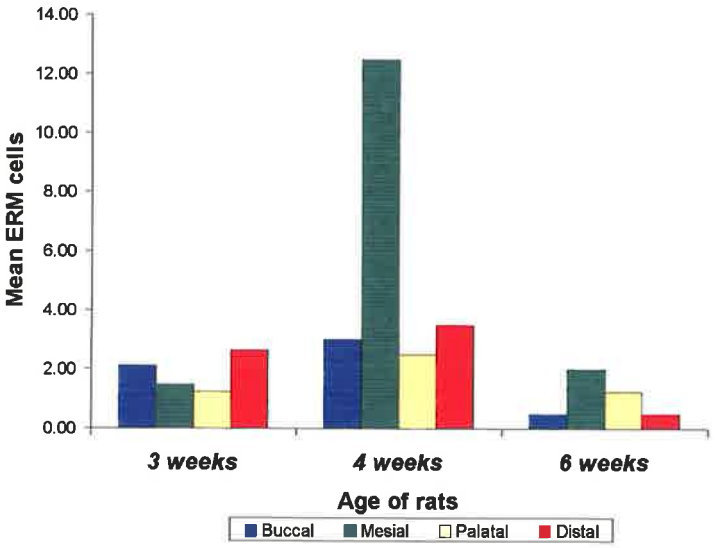

Figure 31
ERM cells around root surfaces (apical third)
Mean ERM cells around the root surface quadrants at the apical third level of the mesiobuccal root in 3, 4 and 6-week-old rats

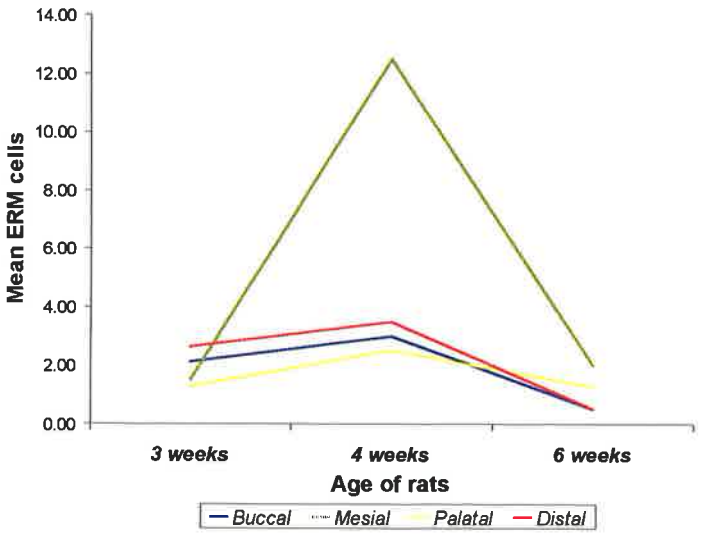

Figure 32
ERM cells around root surfaces (apical third)
Mean ERM cells between the different surface quadrants in the apical third of the mesiobuccal molar root of 3, 4 and 6-week-old rats

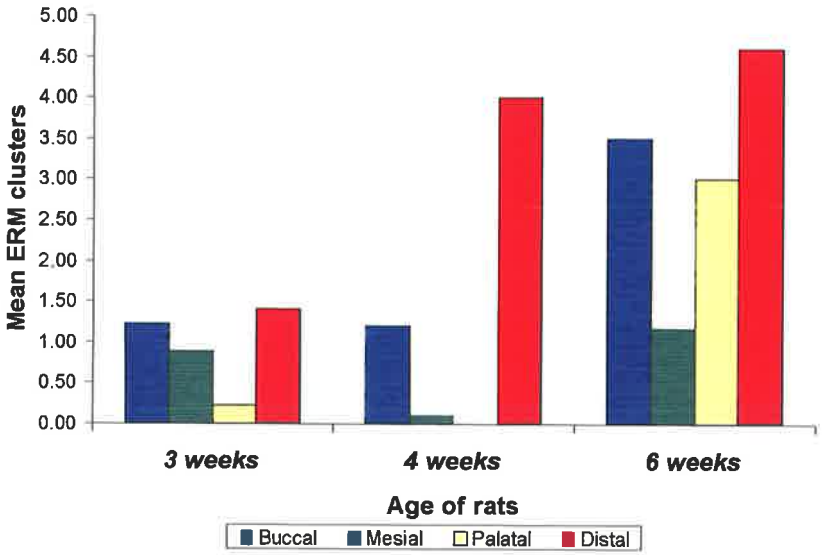

Figure 33
ERM clusters around root surfaces (cervical third)
Mean ERM clusters around the root surface quadrants at the cervical third level of the mesiobuccal root in 3, 4 and 6-week-old rats

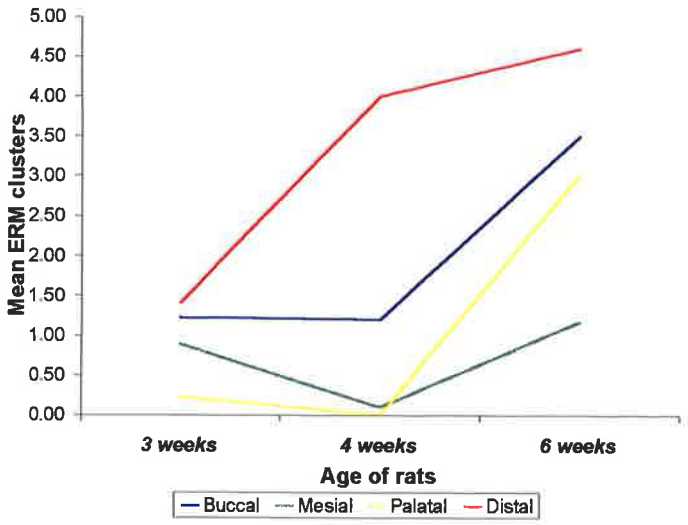

Figure 34
ERM clusters around root surfaces (cervical third)
Mean ERM clusters between the different surface quadrants in the cervical third of the mesiobuccal molar root of 3, 4 and 6-week-old rats

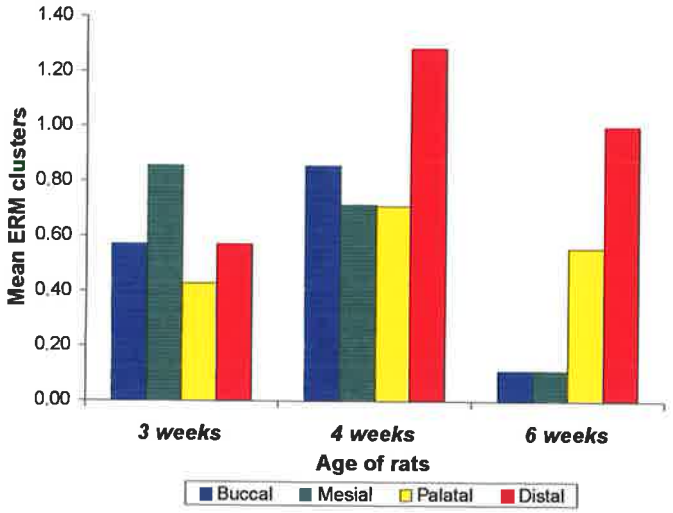

Figure 35

ERM clusters around root surfaces (middle third)

Mean ERM clusters around the root surface quadrants at the middle third level of the mesiobuccal root in 3, 4 and 6-week-old rats

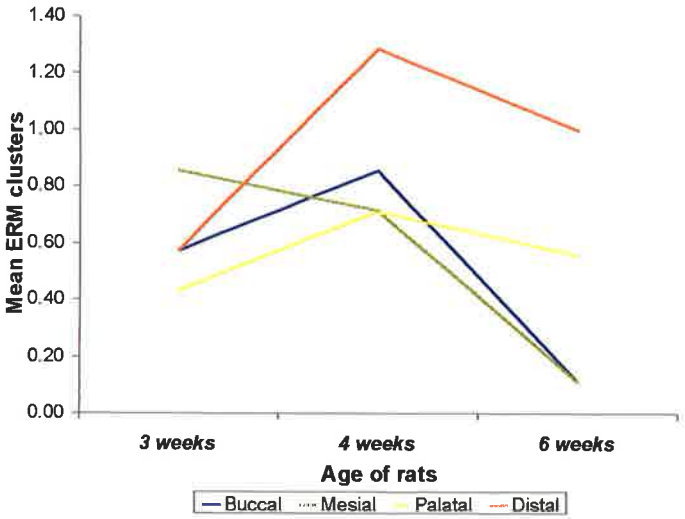

Figure 36

ERM clusters around root surfaces (middle third)

Mean ERM clusters between the different surface quadrants in the middle third of the mesiobuccal molar root of 3, 4 and 6-week-old rats

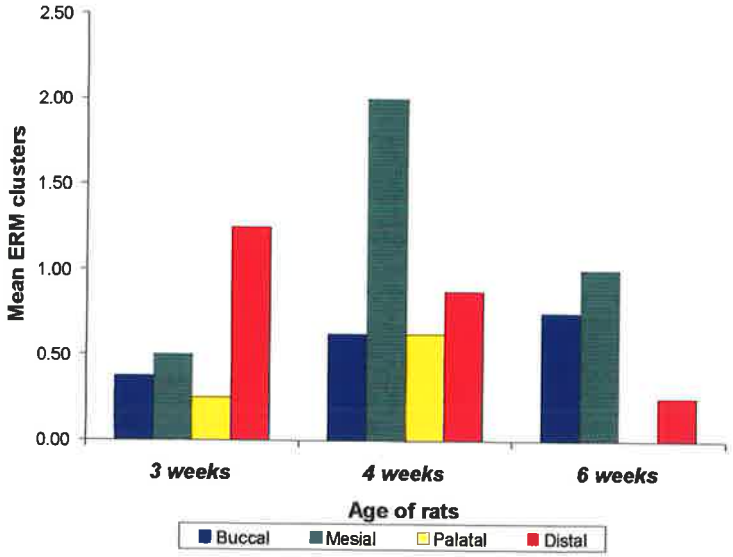

Figure 37

ERM clusters around root surfaces (apical third)

Mean ERM clusters around the root surface quadrants at the apical third level of the mesiobuccal root in 3, 4 and 6-week-old rats

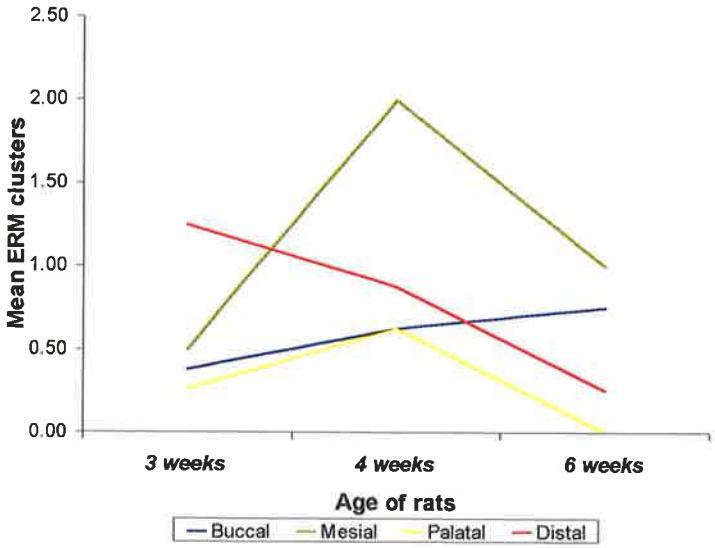

Figure 38

ERM clusters around root surfaces (apical third)

Mean ERM clusters between the different surface quadrants in the apical third of the mesiobuccal molar root of 3, 4 and 6-week-old rats

Blood vessels							
		Age of rats					
		3 weeks		4 weeks		6 weeks	
Root thirds	PDL thirds	$\bar{x}$	SD	$\bar{x}$	SD	$\bar{x}$	SD
Cervical	Tooth	0	0	4.2	3.91	0	0
	Middle	26.5	7.32	47.2	21.04	47	19
	Bone	44.25	8.43	44.8	13.96	42.33	21.49
Middle	Tooth	0	0	1.75	2.19	0.17	0.41
	Middle	32.57	16.14	38	14.35	38.17	14.25
	Bone	50.29	11.06	47.5	16.9	55.5	16.74
Apical	Tooth	0	0	0.8	1.03	0.88	1.64
	Middle	29.17	12.69	35.1	31.56	40.25	18.91
	Bone	44.83	13.7	43.9	16.92	53.25	15.11

Table 7

Mean and standard deviation of blood vessel circumferential counts across the PDL thirds along the vertical thirds of the mesiobuccal root.

Distribution around root surface quadrants (Table 8, Table 9 and Table 10)

The blood vessel distribution around the root surfaces was also analysed:

Cervical third

At three weeks, no blood vessels were noted in the tooth third of the PDL on any of the root surfaces. In the middle third of the PDL, the largest number of vessels was noted on the distal surface ($\bar{x}$ = 13 ± 5.89), followed by the buccal ($\bar{x}$ = 9.57 ±·8.92) and palatal ($\bar{x}$ = 8.75 ± 4.86) surfaces. The mesial had the least number of vessels with $\bar{x}$ = 2.88 ± 2.85. In the bone third of the PDL, the highest number of vessels was once again noted on the distal surface ($\bar{x}$ = 15.75 ± 5.74), followed by the buccal and mesial surfaces ($\bar{x}$ = 13 ± 5.8 and $\bar{x}$ = 13 ± 4.63 respectively. The least number of vessels was noted on the palatal surface ($\bar{x}$ = 12.75 ± 4.13).

At four weeks, some vessels were noted in the tooth third of the PDL. The highest number was noted on the distal ($\bar{x}$ = 2.38 ± 2.19) and buccal surface ($\bar{x}$ = 1.6 ± 1.96). Very few were noted on the palatal ($\bar{x}$ = 0.6 ± 1.27) or mesial ($\bar{x}$ = 0.1 ± 0.32) surfaces. There was a slight increase in blood vessels in the middle third of the PDL (compared to three weeks). The highest number of vessels was noted on the mesial surface ($\bar{x}$ = 15.6 ± 8.84). This was followed by the buccal ($\bar{x}$ = 11.6 ± 7.04) and distal surfaces (11.25 ± 5.8), with the least being on the palatal surface ($\bar{x}$ = 8.7 ± 5.81). Mean vessel counts in the bone third was also noted to be highest on the mesial surface ($\bar{x}$ = 13.5 ± 5.91, followed by the buccal ($\bar{x}$ = 12.5 ± 3.5) and distal ($\bar{x}$ = 11.5 ± 5.1) surfaces. The smallest number of vessels was found on the palatal ($\bar{x}$ = 9.6 ± 3.34).

By six weeks of age, no vessels were noted on the tooth third of the PDL and the number of vessels in both the middle and bone third had increased. In the middle third of the PDL, the highest number of vessels was noted on the buccal surface ($\bar{x}$ = 33 ± 10.41) followed by the mesial ($\bar{x}$ = 21.5 ± 8.21). A smaller number were found on the distal ($\bar{x}$ = 16 ± 1.41) and palatal ($\bar{x}$ = 12 ± 5.02). In the bone third, however, the largest number of vessels was noted on the distal ($\bar{x}$ = 25 ± 0.71) and buccal ($\bar{x}$ = 22.75 ± 8.98) surfaces. Counts on the other surfaces included $\bar{x}$ = 19.25 ± 5.78 on the palatal and $\bar{x}$ = 15.25 ± 5 on the mesial.

Thus, the spread of blood vessels across the surface quadrants appeared quite variable. Generally, vessel counts did not appear to increase from three to four weeks. However, there was a large increase of vessels from four to six weeks of age. The vessels appeared to invade into the tooth third of the PDL at four weeks of age, however,

the number of vessels noted in this area disappeared by six weeks. Generally, a larger proportion of vessels was noted on the buccal surface in all age groups.

Middle third

Once again, no vessels were found in the tooth third of the PDL at three weeks. In the middle third, the largest number was noted the mesial ($\bar{x}$ = 11.14 ± 8.12) with the next highest in the buccal ($\bar{x}$ = 9.29 ± 7.7). Fewer vessels were noted on the distal ($\bar{x}$ = 6.86 ± 4.85) and palatal ($\bar{x}$ = 4.29 ± 4.23). In the bone third of the PDL, the highest number of vessels was found on the distal ($\bar{x}$ = 17.29 ± 5.77) followed by the buccal ($\bar{x}$ = 12.29 ± 5.68). Slightly fewer vessels were noted on the mesial ($\bar{x}$ = 12 ± 4.74) and even fewer were found on the palatal ($\bar{x}$ = 7.71 ± 4.99).

At four weeks, vessels appeared to invade into the tooth third of the PDL with the highest mean noted on the distal surface ($\bar{x}$ = 1.38 ± 1.85). A small number were noted on the palatal ($\bar{x}$ = 0.25 ± 0.46) and mesial ($\bar{x}$ = 0.13 ± 0.35). None were found on the buccal. In the middle third of the PDL, the largest mean number of vessels was noted on the mesial ($\bar{x}$ = 12.13 ± 6.77) and distal ($\bar{x}$ = 11.13 ± 4.91). This was followed by the buccal ($\bar{x}$ = 8 ± 5) and palatal ($\bar{x}$ = 7.63 ± 2.39) surfaces). Vessel distribution in the bone third was similar to the middle third with the highest number of vessels noted on the mesial ($\bar{x}$ = 15.75 ± 8.17) and distal (15.63 ± 5.66) surfaces. A smaller number was noted on the buccal ($\bar{x}$ = 9.13 ± 4.67) followed by the palatal (7 ± 1.31).

By six weeks of age, some vessels could still be found on the distal ($\bar{x}$ = 1.4 ± 1.29) and palatal ($\bar{x}$ = 0.2 ± 0.38) surfaces in the tooth third of the PDL. None were noted on the buccal or mesial. The number of vessels did not appear to increase much from four weeks, in the middle third of the PDL. The highest mean number of vessels was noted on the distal surface ($\bar{x}$ = 16 ± 5.03) followed by the buccal ($\bar{x}$ = 14.4 ± 5.82). Similar counts were noted on the mesial ($\bar{x}$ = 10.2 ± 6.02) and palatal ($\bar{x}$ = 10.2 ± 8.11). There was, however, a slight increase in mean vessel count from four to six weeks in the bone third of the PDL. The highest mean count was found on the distal ($\bar{x}$ = 20.8 ± 4.57) followed by the mesial ($\bar{x}$ = 19.4 ± 6.14). Slightly lower counts were noted on the palatal ($\bar{x}$ = 16.8 ± 6.14) and buccal ($\bar{x}$ = 14.4 ± 4.96) surfaces.

Once again, blood vessel distribution across the surfaces appeared variable in the middle third of the root. Mean vessel counts did not change much from three to four weeks of age. There was however, an increase in vessel number in the bone third of the PDL from four to six weeks. Vessels appeared to invade into the tooth third of the PDL at four weeks with some remaining in the area at six weeks. Generally, a larger proportion

of counts were noted on the distal surface (except for the middle third of the PDL in three week rats) whilst the smallest proportion of vessels was usually noted on the palatal.

Apical third

At three weeks, no vessels were found on the tooth third of the PDL. In the middle third, the highest mean vessel count was noted on the mesial ($\bar{x}$ = 10 ± 9.21) and distal surfaces ($\bar{x}$ = 9 ± 4.73). Smaller counts were noted on the buccal ($\bar{x}$ = 5.67 ± 4.03) and palatal ($\bar{x}$ = 4.5 ± 3.21). In the bone third of the PDL, highest mean vessel count was noted on the distal ($\bar{x}$ = 19 ± 4.34) followed by the buccal ($\bar{x}$ = 10.83 ± 5.98). The mesial ($\bar{x}$ = 9.17 ± 4.36) and palatal ($\bar{x}$ = 6.67 ± 4.93) had a smaller number of vessels.

After four weeks, vessels were only noted on the distal surface ($\bar{x}$ = 0.8 ± 1.03) in the tooth third of the PDL. Vessel counts in the middle third of the PDL included $\bar{x}$ = 10.3 ± 8.69 on the buccal, $\bar{x}$ = 10.1 ± 11.64 on the mesial, $\bar{x}$ = 8.7 ± 7.42 on the palatal and $\bar{x}$ = 6.6 ± 7.11 on the distal. In the bone third of the PDL, the highest number of vessels was noted on the distal ($\bar{x}$ = 16.6 ± 5.13) and mesial ($\bar{x}$ = 11 ± 4.74). The buccal surface had slightly less vessels ($\bar{x}$ = 10.5 ± 6.72) whilst the palatal had the least ($\bar{x}$ = 5.8 ± 4.85).

By six weeks of age, the only vessels noted in the tooth third of the PDL were once again on the distal surface ($\bar{x}$ = 1 ± 1.51). The number of vessels had increased from the four-week period. In the middle third of the PDL, the largest number of vessels was noted on the mesial surface ($\bar{x}$ = 24.75 ± 6.09). This was followed by the palatal ($\bar{x}$ = 17.25 ± 4.88), distal ($\bar{x}$ = 15 ± 5.77) and buccal ($\bar{x}$ = 14.75 ± 8.7) surfaces. In the bone third of the PDL, the highest mean vessel count was noted on the distal surface ($\bar{x}$ = 27.5 ± 3.59) followed by the mesial ($\bar{x}$ = 24.5 ± 6.11). The mesial ($\bar{x}$ = 20.75 ± 6.47) and palatal ($\bar{x}$ = 20.25 ± 8.02) had similar counts.

Vessel distribution was variable in this vertical third of the root with no specific pattern detected. It was however, noted that once again vessel number did not appear to increase much from three to four weeks. However, there was an increase in vessel numbers from four to six weeks of age in both the middle and bone thirds of the PDL. Vessels appeared to invade into the tooth third of the PDL after four weeks, but only on the distal surface and numbers were small.

These counts can be depicted graphically in Figure 39, Figure 40, Figure 41 and Figure 42.

Blood vessels							
		PDL thirds					
Root thirds	Root surfaces	Tooth 1/3		Middle 1/3		Bone 1/3	
		Mean	SD	Mean	SD	Mean	SD
Cervical	Buccal	0	0	9.57	8.92	13.00	5.80
	Mesial	0	0	2.88	2.85	13.00	4.63
	Palatal	0	0	8.75	4.86	12.75	4.13
	Distal	0	0	13.00	5.89	15.75	5.74
Middle	Buccal	0	0	9.29	7.70	12.29	5.68
	Mesial	0	0	11.14	8.12	12.00	4.74
	Palatal	0	0	4.29	4.23	7.71	4.99
	Distal	0	0	6.86	4.85	17.29	5.77
Apical	Buccal	0	0	5.67	4.03	10.83	5.98
	Mesial	0	0	10.00	9.21	9.17	4.36
	Palatal	0	0	4.50	3.21	6.67	4.93
	Distal	0	0	9.00	4.73	19.00	4.34

Table 8

Table of mean and standard deviation blood vessel counts between PDL thirds along the root thirds in 3 week-old rats.

Blood vessels							
		PDL thirds					
Root thirds	Root surfaces	Tooth 1/3		Middle 1/3		Bone 1/3	
		Mean	SD	Mean	SD	Mean	SD
Cervical	Buccal	1.60	1.96	11.60	7.04	12.50	3.50
	Mesial	0.10	0.32	15.60	8.84	13.50	5.91
	Palatal	0.60	1.27	8.70	5.81	9.60	3.34
	Distal	2.38	2.19	11.25	5.80	11.50	5.10
Middle	Buccal	0.00	0.00	8.00	5.00	9.13	4.67
	Mesial	0.13	0.35	12.13	6.77	15.75	8.17
	Palatal	0.25	0.46	7.63	2.39	7.00	1.31
	Distal	1.38	1.85	11.13	4.91	15.63	5.66
Apical	Buccal	0.00	0.00	10.30	8.69	10.50	6.72
	Mesial	0.00	0.00	10.10	11.64	11.00	4.74
	Palatal	0.00	0.00	8.70	7.42	5.80	4.85
	Distal	0.80	1.03	6.60	7.11	16.60	5.13

Table 9

Table of mean and standard deviation blood vessel counts between PDL thirds along the root thirds in 4 week-old rats.

Blood vessels							
		PDL thirds					
Root thirds	Root surfaces	Tooth 1/3		Middle 1/3		Bone 1/3	
		Mean	SD	Mean	SD	Mean	SD
Cervical	Buccal	0.00	0.00	33.00	10.41	22.75	8.98
	Mesial	0.00	0.00	21.50	8.21	15.25	5.00
	Palatal	0.00	0.00	12.00	5.02	19.25	5.78
	Distal	0.00	0.00	16.00	1.41	25.00	0.71
Middle	Buccal	0.00	0.00	14.40	5.82	14.40	4.96
	Mesial	0.00	0.00	10.20	6.02	19.40	5.61
	Palatal	0.20	0.38	10.20	8.11	16.80	6.14
	Distal	1.40	1.29	16.00	5.03	20.80	4.57
Apical	Buccal	0.00	0.00	14.75	8.70	20.75	6.47
	Mesial	0.00	0.00	24.75	6.09	24.50	6.11
	Palatal	0.00	0.00	17.25	4.88	20.25	8.02
	Distal	1.00	1.51	15.00	5.77	27.50	3.59

Table 10

Table of mean and standard deviation blood vessel counts between PDL thirds along the root thirds in 6 week-old rats.

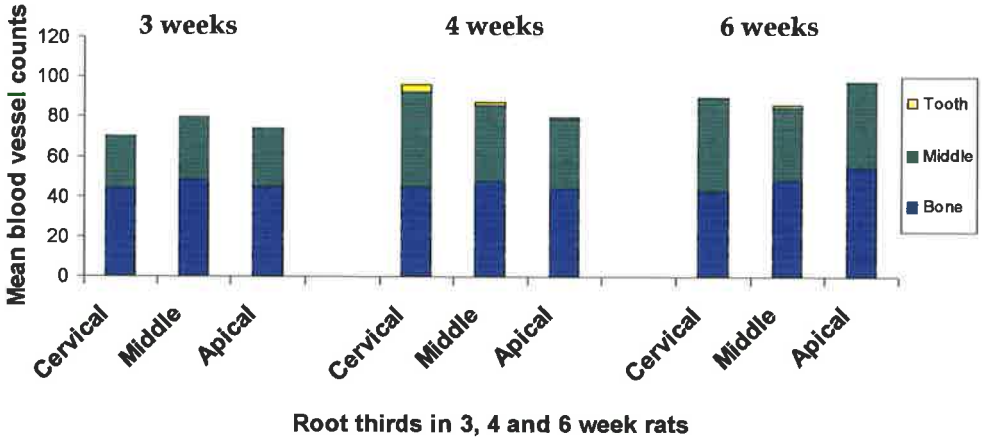

Figure 39
Blood vessel distribution along root thirds
Distribution of blood vessels in PDL thirds along the mesiobuccal root of 3, 4 and 6 week-old rats

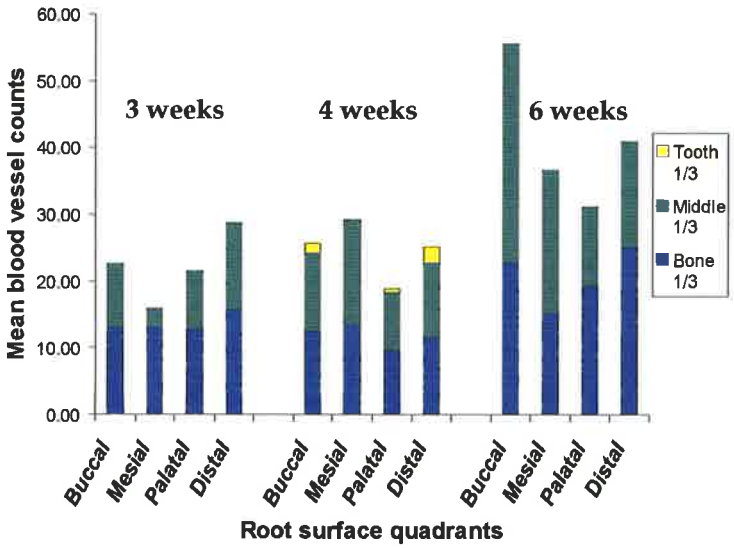

Figure 40
Blood vessel distribution between root surface quadrants (cervical third)
Distribution of blood vessels between the root surface quadrants in the cervical third of the mesiobuccal root of 3, 4 and 6 week-old rats

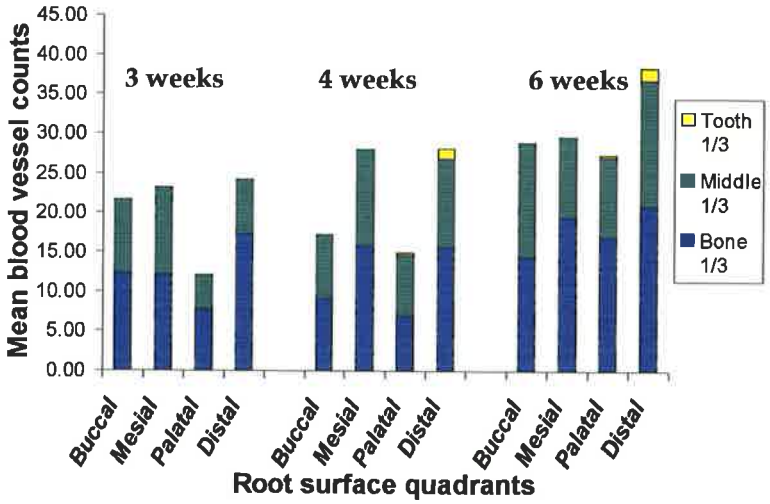

Figure 41
Blood vessel distribution between root surface quadrants (middle third)
Distribution of blood vessels between the root surface quadrants in the middle third of the mesiobuccal root of 3, 4 and 6 week-old rats

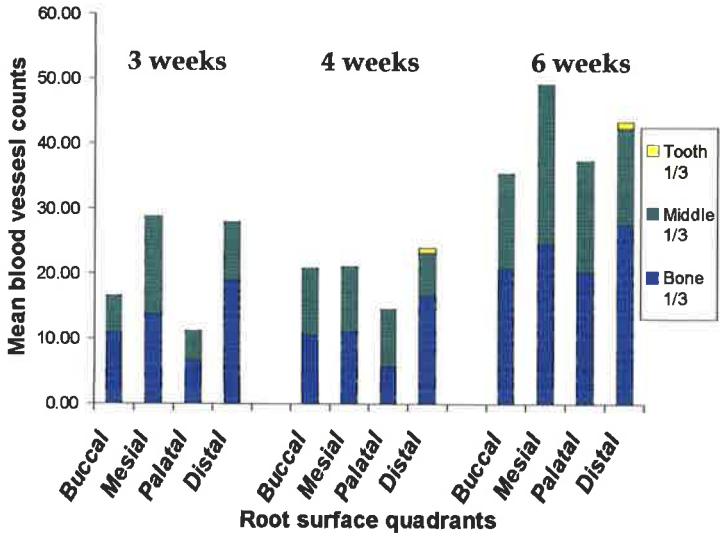

Figure 42
Blood vessel distribution between root surface quadrants (apical third)
Distribution of blood vessels between the root surface quadrants in the apical third of the mesiobuccal root of 3, 4 and 6 week-old rats

5.5.3 *Intra-operator Error Assessment*

Ten percent of the ERM cell and cluster counts as well as the blood vessel counts were re-counted from slides selected at random from the slides containing three, four and six-week-old rat maxilla sections. A two-tail paired t-test was performed on the count to determine if there were any systematic errors during the counting process. The calculated two-tail t value for the ERM cells was 0.288, which was less than the critical t value (at $p<0.05$ level) of 2.02. Thus the null hypothesis, that is that there was no significant difference between the counts, was retained. The two-tail t value for ERM clusters was 0.904, which was also lower that the critical t value (at $p<0.05$ level of 2.02, thus indicating no significant difference in counts due to systematic error. The two-tail t value for the blood counts was 0.54. It too was lower than the critical t value of 1.99, once again indicating no significant difference in counts due to systematic error.

A Dahlberg statistic was also performed to determine the magnitude of any intra-operator error. The Dahlberg statistic for the ERM cells and clusters was 1.09 and 1.1 respectively, indicating that the magnitude of intra-operator error for the cell and cluster counts was one cell between the two counting periods. The Dahlberg statistic for blood vessels counts was a little higher, that is 2.58, indicating an intra-operator error of two to three blood vessels.

5.5.4 *Root Resorption Areas*

Many of the blood vessels in the tooth third area were associated with resorption lacunae on the root surface. In fact, most of these vessels were found inside the resorption lacunae. All the lacunae were found on the distal surface of the mesiobuccal root (Table 11).

The highest mean number of resorption lacunae occurred in the cervical and middle third of the root in four and six week old animals. A small number were found in the apical third of the root in four-week-old rats. No resorption was noted in the three-week-old rats (Figure 43).

Although the ERM were found adjacent to the resorption lacunae, none were found directly over them. It appeared as though there was a break in the continuity of the ERM network wherever root resorption was present. As stated previously, in these areas, blood vessels were noted to invade into the tooth third of the PDL. However, none were found directly in between the ERM and tooth surfaces. They were either on the bone side of the ERM or were in the resorption lacunae themselves (where there were no ERM).

		Resorption lacunae					
		Mean			SD		
		3 weeks	4 weeks	6 weeks	3 weeks	4 weeks	6 weeks
Root thirds	Cervical	0	0.5	0.5	0	0.76	0.71
	Middle	0	0.5	0.29	0	0.53	0.49
	Apical	0	0.2	0	0	0.42	0

Table 11

Table of total and mean number of resorption lacunae on the distal surfaces along the length of the mesiobuccal root in 3, 4 and 6-week-old rats

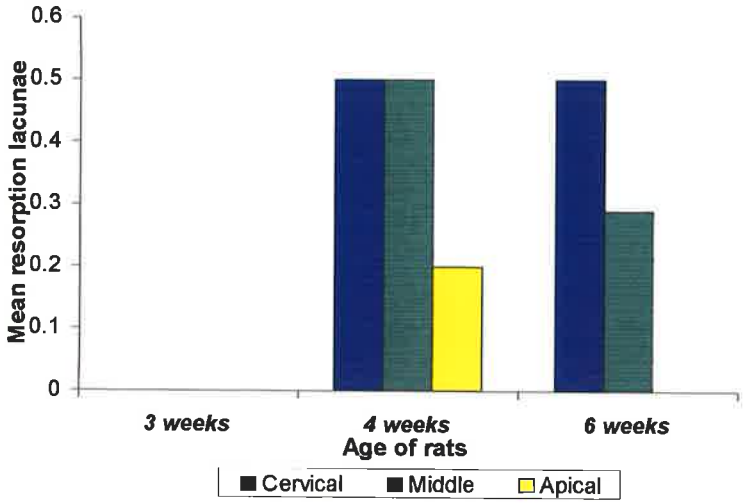

Figure 43

Mean root resorption lacunae along the root thirds

Distribution of root resorption lacunae on the distal surface along the root thirds of the mesiobuccal molar root in 3, 4 and 6 week-old rats

6 DISCUSSION

6.1 Development of the rat first molar

Initiation (which begins with the first appearance of the dental lamina) of the first molar tooth of the rat commences on the thirteenth day *in utero* [4]. At the age of two days, when this study was commenced, crown development had already commenced and was in the "bell stage" of development. The enamel organ consisted of two layers of dark blue stained epithelial cells, that is, the external and internal epithelium which were separated by stellate reticulum and stratum intermedium cells. Developing blood vessels could also be noted in the dental papilla which will later form the pulp of the tooth.

The crown continues to develop into the one-week period and entered into the early phase of the "crown stage" of development. At the lower border of the enamel organ, the external and internal epithelial layers combined to form the cervical loop which eventually elongated to form the tooth root. However, at this stage of development, no root development was evident.

At two weeks, crown development is virtually complete and root formation commences. However, McLean [30] and Davey [11] believe that crown formation is still ongoing during root development in contrast to conventional literature [1, 4]. At this stage, the external and internal epithelia of the cervical loop commence formation of Hertwig's epithelial root sheath (HERS). The apical portion of the sheath bends horizontally across the base of the dental papilla, narrowing the wide cervical opening of the tooth germ into the primary apical foramen. It is termed the epithelial diaphragm. Proliferation of HERS epithelium results in elongation of the root. However, there is still no agreement on where this proliferation occurs and exactly how the epithelial cells produce this root elongation [6, 11, 29]. At this stage, the crown is also starting to erupt within the alveolar bone, with the tips of the crown just apparent in the oral cavity. At three weeks the crown was nearly fully erupted and full occlusion was most probably achieved at four weeks. This is summarised in Figure 44.

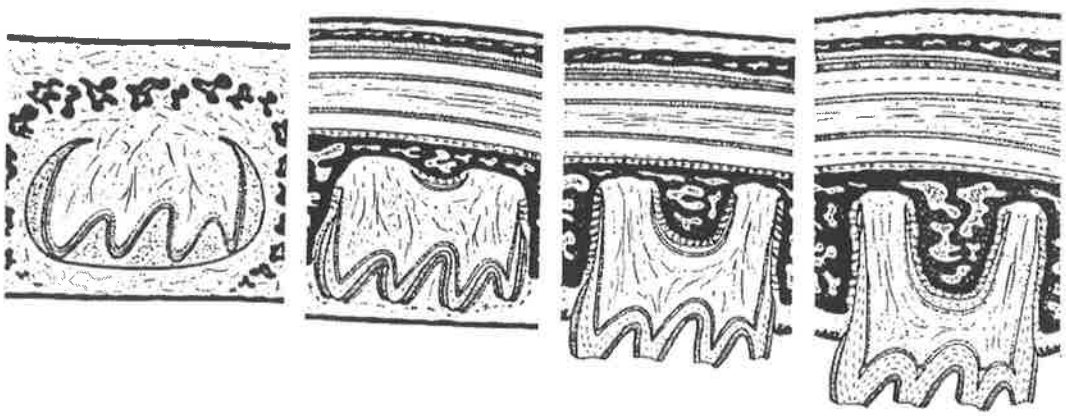

Figure 35

Rat tooth development

Stages of rat tooth development and eruption into the oral cavity from 2 days to 6 weeks.

(Adapted from Schour, I and Massler M, 1971. The Teeth. **In** The Rat in Laboratory Investigation. Ed Farris EJ and Griffith JQ, Hafner Publishing Co, New York. pp104-165

6.1.1 *Mesiobuccal Root Development*

In three-week-old rats, the epithelial diaphragm of HERS continued to produce elongation of the mesiobuccal root. At this stage, some fragmentation of the sheath occured and ERM cells began to appear in the PDL along the length of the root. These together with the HERS cells formed a network around the root presenting as single cells or clusters of multiple cells. An abundant amount of blood vessels were also present in the developing PDL. (The distribution of these will be discussed in the following sections). Also, at this time, the tooth was starting to erupt with part of the crown emerging in the oral cavity.

The root continued to develop and elongate at four-weeks of age and had almost completed development at six weeks. A larger amount of ERM and blood vessels could be demonstrated in the PDL along the length of the root. Nevertheless, the epithelial diaphragm of HERS was still noticed at the apical end of the six-week roots especially on the mesial surfaces and occasionally on the palatal surfaces. This is similar to the findings of Davey [11] who noted a difference in developmental levels between different root surfaces.

Root resorption is a common occurrence in rats and considered as part of root development. It is noticeable once the teeth come into occlusion, that is, from four weeks of age. Belting et al [116] and Weinmann and Schour [117] noted a higher occurrence of resorption on the distal surfaces of roots in the first molars of rats. They attributed this to trauma produced by occlusal and interproximal attrition. These observations match the ones made in this study where all resorption lacunae were noted on the distal surfaces of the roots. Furthermore, these were only observed at four and six weeks when the teeth were in functional occlusion, lending credence to the theory that resorption was relatable to the occlusal forces generated during function.

The distribution of ERM cells and clusters as well as blood vessels appeared to vary with the different ages, moreover, there appeared to be a relationship between these cells with the occurrence of root resorption along the root.

6.2 Distribution of the Epithelial Rests of Malassez

In this study, the ERM were classified according to their presentation in the PDL; that is, as "single cells" or "clusters". In the past, various investigators have attempted to classify the ERM according to their histological [36, 39, 44] or ultrastructural [45] appearance, or according to their location [6].

The "single cell" ERM in the transverse sections of this experiment (which would appear as a strand of cells in longitudinal sections) are equivalent to the "resting type" ERM described by Wentz et al [44] and Reeve and Wentz [39] and to the "strands of cells" described by Valderhaug and Zander [36]. They also correlate to Gurling and Sampson's [6] type II ERM cells.

The ERM "clusters" in this study would be equivalent to the "proliferating type" and "differentiating type" of ERM described by Wentz et al [44] and Reeve and Wentz [39], Valderhaug and Zander's [36] "islands of cells" and also Gurling and Sampson's [6] type I cells as they were mostly noted in the cervical third of the root. However, these clusters were also noted along the middle and apical thirds of the root in all age periods, though in smaller numbers. According to Wentz et al [44] these different presentations of ERM represent different stages of proliferation of rests when stimulated by traumatic factors.

All "cells" and "clusters" were observed in the tooth third of the PDL, although some appeared a little further away from the cementum after four and six weeks. The distribution of these "cells" and "clusters" varied according to root thirds and surface quadrants which may give an insight into the development of the ERM with age.

6.2.1 *Distribution Along Length Of Root*

Most of the earlier investigations on ERM development and distribution were conducted in either older rats [44, 118] or different animals, such as humans [36, 39], mice [6, 29, 30, 41] or sheep [119]. This makes comparisons to previous findings difficult.

In the current study, the spread of ERM cells and clusters along the mesiobuccal root of the first rat molar is summarised in Figure 22 and Figure 23. From these line graphs, it would appear that in younger rats, a greater number of single cell ERM ("resting type" or "strands") were found in the middle third of the root, with the second highest in the cervical and the lowest amount in the apical third at three weeks. All cell counts increased at four weeks, but by the age of six weeks cells were most numerous in the cervical third and least in the middle. The clusters ("differentiating type" or "islands")

were always most numerous in the cervical third and least in the middle third. In the older animals (six weeks), the number of clusters in the cervical third far outnumbered those found in the middle and apical thirds. The findings in older animals are in agreement with Hamamoto et al [40] and Wentz et al [44] who also noted a greater number of ERM in the cervical region of the root in older rats. The spread of ERM in younger rats has not been reported in the literature until now. In contrast, Wesselink and Beertsen [41] and Lambrichts et al [38] noted a higher number of ERM in the apical portion of the root compared to the coronal. These differences may be due to their use of different animal material. Furthermore, Wesselink and Beertsen [41] only divided the root into two halves, confounding comparison between this study and theirs.

There still exists controversy regarding the formation and fate of the ERM with age. Some early investigators [32, 33, 120] believed that ERM did not form in rodent PDL with the opinion that the cells of HERS either degenerate or become encapsulated in cellular cementum during root formation, thus not forming ERM. This has since been disproved by others who have detected ERM in the rat [40, 44, 118] and mouse [6, 11, 29, 30, 121]. It is now generally agreed that the ERM are derived from HERS [2, 19, 122].

According to Spouge [2], during active root formation, root elongation occurs as a result of cell proliferation occurring at the innermost tip of the sheath diaphragm, with newly formed cells passing outwards to assume a new position in the vertical portion of the sheath. This focus of intense mitotic activity is accompanied by equivalent proliferation in the adjacent connective tissue cells both on the inner (pulp side) and outer surfaces (PDL side). Newly formed "pulpal" cells differentiate into odontoblasts and begin secretion of dentine matrix. These cells together with the increasing amount of dentine matrix move progressively outwards, until they come to lie along the future dentino-cemental junction. At this stage the outer layer of the dentine matrix starts to calcify. As this happens, the HERS cells separate from the dentine surface and breaks occur in the sheath. The resulting network is referred to as the ERM [2]. However, this may not be the sole method of ERM formation. Wentz et al [44] were of the opinion that some of the ERM may also be derived from tooth epithelial attachment or from epithelial cells of the gingiva. This may help explain the larger number of cells and clusters noted in the cervical third of the root.

Most investigators agree that the ERM decrease with age either through degeneration [39] or become incorporated into forming cellular cementum [13, 15]. However,

Wentz et al [44] were of the opinion that only the resting cells decreased with age. The differentiating ERM actually increased with age, with rests detected in rats 1088 days old, which is equivalent to nearly three years of age. The results of the present study partly agree with their findings in that the ERM cells (resting type) of the middle and apical third of the root did decrease with age whilst the ERM clusters (differentiation type) increased with age. However, ERM cells in the cervical third and clusters in the middle and apical third behaved in the opposite manner.

It would appear that the cells and clusters in the cervical third increased with age, whilst those in the middle apical areas decreased with age. These results are similar, but not identical to those of Reeve and Wentz [39]. They noted a larger number of ERM in the apical region during the adolescent years in humans. However, by the third to seventh decade of life, a larger number of rests were found in the cervical region compared to the apical. The authors postulated that this change in distribution might be due to the presence of persistent gingival inflammation in older humans. The stimulation of ERM by inflammation has been well documented [34, 53, 123, 124]. Due to the lack of oral hygiene practices in the rats, there most likely exists a constant state of gingival inflammation around the teeth which would result in the proliferation of ERM cells and clusters in the cervical third region.

However, Wentz et al's [44] theory that some ERM may be derived from tooth epithelial attachment or from epithelial cells of the gingiva could not be discounted. Thus, it is also possible that the ERM cells and clusters of the middle and apical thirds of the root degenerate with age or become incorporated into forming cellular cementum (demonstrated in this study). However, the rests in the cervical third may increase due to the extra source of rests from the attachment and gingival epithelium. This increase may have been initiated by the presence of inflammation in the supraalveolar region.

Gurling [29] and Gurling and Sampson [6] propose that the cells of the ERM are carried occlusally within the PDL during tooth eruption and cells found in the apical region are in fact, cells of HERS which have been retarded in their occlusal movement. The results of this study appear to concur with this theory as, according to Figure 23 and Figure 25, there is an increase in the number of ERM cells and clusters in the cervical third of the root with age. This was accompanied by a decrease of cells and clusters in the middle and apical root thirds as the rats became older.

Thus, the variation in cell and cluster distribution along the vertical length of the mesiobuccal root could due to ERM stimulation from inflammation produced during the

root formation and eruption process in the earlier stages followed by the presence of gingival inflammation in the older animals. The distribution of the cells and clusters could also be affected by eruption of the tooth, resulting in the ERM being carried occlusally within the PDL.

Variation in ERM distribution also occurred between the four root surfaces along the mesiobuccal root.

6.2.2 *Distribution Around Root Surfaces*

In the current investigation, it was noted that the highest number of single ERM cells occurred on the distal and secondly on the mesial surface whilst the highest number of clusters were found on the distal and secondly buccal surfaces. The number of cell counts increased at four weeks but decreased by six weeks. The spread of ERM clusters in the three age periods was more variable.

Not as much work has been performed on the distribution of ERM around root surfaces as there has been on distribution along the length of the root. Wentz et al [44] noted a larger amount of differentiating ERM in the bifurcation of the root which corresponds to the distal surface of the mesiobuccal root in this experiment. The results of this study did indeed correlate to Wentz et al's [44] findings in that a very high number of clusters were noted on the distal surface. The literature is sparse on the distribution of ERM on the other root surfaces or the distribution of other types of ERM.

From the line graphs in Figure 28 and Figure 34, it can be noted that in the cervical vertical third of the mesiobuccal root, the largest mean cell and cluster counts were on the distal surface. Cell number increased from three to four weeks, but decreased slightly from four to six weeks. Cluster number increased with age. The highest number of clusters in the middle third of the root was also noted on the distal surface (Figure 36). However, in the other root thirds, the highest mean cell and clusters were noted on the mesial surface (Figure 30, Figure 32 and Figure 38). The distribution appeared very similar, that is, there was an increase in numbers from three to four weeks. However, counts decreased from the four to six week period.

The lowest cell and cluster counts in all vertical root thirds for the three and four week period was on the palatal surface. However, the variable cell and cluster distribution of the six-week rats resulted in higher counts on the palatal surface.

It is possible that the distribution of ERM around the root surfaces may be related to the activity of the rests and the distribution of resorption lacunae. In this experiment, all

the root resorption lacunae were noted on the distal surface of the root in four and six-week-old rats. The highest mean resorption lacunae occurred in the cervical third of the root in both four and six week old rats. This corresponded to the larger number in ERM cells and clusters on the distal surface in the cervical third of the root at four and six weeks. Further down the lower vertical thirds of the root (middle and apical thirds), the number of cells and clusters were lower on the distal compared to the mesial surface, corresponding to a decreasing incidence of resorption lacunae down the length of the root. This finding may point to a possible protective and/or reparative function on the part of the ERM against root resorption on these surfaces (which is in agreement with the work of Brice et al [46, 51]. Thus, the greater likelihood of root resorption on the distal surface, the more likely the proliferation of ERM to protect the root surface against further resorption and also possibly to commence the reparative process once active resorption has ceased.

The large number of cells on the distal surface may also be related to the presence of periodontal inflammation. The distal surface of the cervical third of the root corresponds to the root furcation area. It is one of the main foci of periodontal inflammation and thus may have the potential to stimulate ERM proliferation [48].

Furthermore, the inflammatory reaction may also be related to the emergence of the tooth in the oral cavity. According to Dreyer [125], rodent teeth erupt in an occlusal and distal direction. This would explain the large number of ERM cells and clusters on the distal in the cervical third of the root, and on the mesial surface in the apical third of the root. As the crown (and cervical third) tipped distally with tooth eruption, the root of the tooth would be tipped mesially, increasing ERM proliferation in these areas. According to Bosshardt and Schroeder [27], the speed of root elongation slows down with increasing root length. At four weeks of age, the first molars of the rats in this study had commenced eruption into the oral cavity. At this age, the mesiobuccal root was most likely undergoing a period of rapid development. By six weeks, however, the speed of root development would have slowed down, thus possibly explaining the large increase in ERM numbers from three to four weeks, followed by a decrease in numbers from four to six weeks.

6.3 Distribution of Blood Vessels

The PDL is a highly vascular structure and much work has been undertaken in the past in an attempt to characterise its vasculature [54, 57, 59, 60, 126]. The greatest number of

vessels was found in the bone or alveolar third of the PDL. There were slightly less vessels in the middle third and very few were noted in the tooth third. This result was found in all the tissue sections of the three, four and six-week-old animals. This was in conflict with the findings of Foong [59] who noted that the largest number of blood vessels were noted in the middle third. He did however, agree that the tooth third of the PDL contained the least number of vessels. This discrepancy in findings may be due to the fact that Foong's [59] study was performed on humans and not on rats. Most of the other studies [127, 128] investigating the distribution of blood vessels across the PDL have divided the PDL into halves (bone and tooth halves), making comparisons difficult. These have noted that there are more blood vessels on the bone half compared to the tooth half. However, dividing the PDL into halves does not give as detailed a description of blood vessel distribution as dividing it into thirds.

There was some variability in the counts between the three ages which could not be solely attributed to growth. Blood vessels in the bone third remained virtually unchanged throughout the time periods. There is an increase in the number of vessels in the middle third from three to four weeks, but this remained fairly stable at six weeks. No vessels were noted in the tooth third at three weeks. The number increased at four weeks and decreased slightly at six weeks. Nevertheless, the number of vessels detected in the tooth third was very much lower than those found in the middle or bone third of the PDL. Furthermore, there were no blood vessels detected directly between any of the ERM cells or clusters and the root surface.

The increase in blood vessel counts in the middle third at four weeks can partly be due to the angiogenic process occurring during growth and development of the rat molar. However, it is not the only explanation. A large number of the blood vessels that were noted in the tooth third of the PDL were found in root resorption lacunae. Thus, the increase in blood vessels volume may also be an indication of an active inflammatory reaction occurring in the area.

6.3.1 *Along Length of Root*

Götze [129], Weekes and Sims [126], Douvartzidis [57] and Foong [59] all noted that the apical third of the molar root contained the highest number of blood vessels. Such a distribution was only noted in the six-week-old rats in this study. This was most likely due to the fact that the PDL blood vessels develop occlusally and spread apically with root

development [130]. As such, Birn [131] and Foong [59] noted a decrease in number of blood vessels from the apical to cervical third of the root.

There was an increase in the blood vessel count of the apical third region from three weeks to six weeks which appears to support the theory that blood vessels develop in an occluso-apical direction. However, there was no concomitant decrease of blood vessels in the cervical third. These vessels appeared instead to increase at four weeks and decrease slightly at six weeks. The number of blood vessels in the middle third did not appear to change much throughout the observation periods. Thus, by six weeks the highest numbers of vessels were noted in the apical region, secondly in the cervical region, with the least vessels located in the middle third area. This observation does not appear to support molar PDL blood vessel distributions observed by previous authors [57, 59, 126, 129]. The distribution of PDL blood vessels in this study appear to more nearly match the distribution of blood vessels in the PDL of incisors [131, 132].

The larger than predicted (by the literature) proliferation of blood vessels in the cervical third may be due to angiogenesis owing to the growth process as the root and PDL are still developing at the age of six weeks. Earlier work [57, 59, 126, 129] performed on molar blood vessel distribution was done on different animals or animals that were much older than the animals used in this study. Furthermore, the method of observation was different. This study utilised an immunohistochemical label whilst earlier studies did not.

The increase in the mean number of blood vessels in the cervical third at the four week period could also be the result of increased vessel proliferation due to inflammatory reactions in the gingival tissue produced during tooth development and/or by gingival penetration during eruption. This may also be the reason why blood vessel levels in the cervical third do not reduce below of that in the middle third at six weeks. Furthermore, although the main sources of blood supply to the PDL are from intraosseal and periosteal sites of adjacent bone, the PDL also receives blood vessels from the gingival tissue in the cervical third, and the pulp via the apical foramen in the apical third [133]. This would explain the larger number of vessels in the cervical and apical thirds and why the middle third contains the lowest amount.

6.3.2 *Around Root Surfaces*

Götze [129] observed that the buccal and lingual surfaces of human mandibular premolar teeth had a higher blood supply compared to the mesial and distal surfaces. Douvartzidis [57] noted more blood vessels on the lingual surfaces of marmoset mandibular

molars compared to other surfaces. These findings were not replicated in this study. Firstly, the animals used were different. Secondly, only the mesiobuccal root was examined in this study. Thus, only the mesial and buccal surfaces of the root correspond to the mesial and buccal surfaces of the molar tooth. The palatal and especially, the distal surfaces of the root do not correspond to the equivalent surfaces on the molar tooth itself. Thirdly, maxillary molars were observed in this study instead of mandibular molars. Therefore, results obtained in this study are not comparable to those of previous investigations.

Figure 39 to Figure 42 indicate that the distribution of blood vessels across the root surface quadrants along the vertical thirds of the mesiobuccal root in all three ages appeared highly variable. Thus, a straightforward relationship between ERM and blood vessels distribution could not be determined.

The number of vessels in the surface quadrants did not appear to increase from the three to four week period. However, there was a general increase in vessel numbers from four to six weeks of age. Except for the cervical third area in three and six-week old rats, the highest number of vessels were noted on the mesial and distal surfaces of the root. For the other two surfaces, the highest vessel numbers occurred on the buccal and distal surfaces. Thus, the highest proportion of vessels appeared to be on the distal, which was also the surface that had the highest incidence of resorption in the later ages, pointing to a relationship between vessel distribution and the incidence of resorption. Furthermore, as mentioned earlier, the distal surface of the root also corresponds to the furcation area of the root. In the cervical third of the root, especially, gingival inflammation is common to the furcation region, which in turn may result in the proliferation of blood vessels. However, it is also possible that anatomically, the PDL in the furcal area has more vessels compared to other PDL areas around the root.

According to the graphs, the lowest proportion of vessels was noted on the palatal surfaces in all vertical thirds of the root and across all ages. Once again, it is possible that anatomically, the PDL on the palatal surface has the lowest concentration of vessels compared to the other surfaces.

Another complication in analysing the blood vessel distribution across the root surfaces and also along the vertical thirds of the root is that Factor VIII may not have identified all possible vessels in the tissues observed. If this were true, the true distribution of vessels might be different to that which was observed in this study.

6.4 Relationship of the Epithelial Rests of Malassez to Blood Vessels of the Periodontal Ligament

6.4.1 *Functions of the Epithelial Rests of Malassez and Blood Vessels*

The primary role of the vasculature of the PDL is to provide blood circulation within the PDL, providing for the exchange of substrate and metabolites between blood and periodontal tissues and dentine. It helps to maintain periodontal cell health and vitality [55]. The vessels also play an important role in tooth support as they act as a cushion against forces displacing the tooth, for example during mastication [59]. However, the vessels also have a pathological function. In cases where there has been trauma to the PDL, whether physiologic (such as from the forces of mastication, occlusion or eruption) or pathologic (such as those induced by periodontal disease or orthodontic forces), blood vessels proliferate to enable transport of inflammatory cells (such as neutrophils and macrophages) and mediators (such as cytokines) to the injured area [63]. The result of such interactions may either be tissue destruction or repair, of which root resorption is an example.

The functions of the ERM are not as clear-cut as those of blood vessels.

Ever since the ERM were first discovered by Malassez [35], controversy has existed on what possible role or function they may serve in the PDL. Early investigators originally dismissed them as vestigial structures with no active role. Ten Cate [134] suggested that the presence of glycogen in the rests, together with the presence of a pentose shunt and anaerobic glycolytic pathway was indicative of a metabolism requiring little energy, thereby concluding that the ERM were functionless.

However, since 1899, when Black (cited in Spouge [2]) postulated on the glandular function of ERM due to his observation of a lumen within the ERM, there has been a general belief that the ERM do possess a role within the PDL. Grant and Bernick [135] suggested a possible role in periodontal pocket formation. It was further suggested by Johansen [136] that the ERM might be responsible for the formation of the epithelium of periodontal pocket walls in periodontal disease and also the epithelial lining of radicular cysts. Valderhaug [123] experimentally induced radicular cysts in monkeys and further confirmed the role of the ERM as one of the sources of epithelium in periapical cysts. Various other investigators also agreed upon this pathological role of the ERM [34, 124].

In a review on the pathogenesis of dental cysts, Harris and Toller [137] came to the conclusion that the ERM had in fact a protective role when provoked by periapical sepsis. The ERM appeared to form a barrier, isolating pulpal irritants from surrounding tissue. They postulated that the existence of periodontal cysts was instead associated with a continuous irritant stimulus rather than the action of the ERM. Nevertheless, the ERM do not only perform a pathological function in the PDL. Many investigators [42, 43, 46, 51] also believe that the ERM do possess a protective role, that is the protection of the root surface against root resorption and possibly even repair the root after resorption has occurred.

6.4.2 *Role in Root Resorption*

Root resorption is a common occurrence in rat teeth. It begins to occur in the roots as soon as the teeth come into occlusion and is provoked by any form of trauma to the teeth including occlusal trauma from occlusal attrition and interproximal attrition [116, 117] and can be iatrogenically introduced through the application of orthodontic forces. However, it is not a rampant occurrence. Belting [116] noted that only twenty six root surfaces out of an entire group of seventy four animals showed signs of root resorption. The results of the present study are further confirmation of this showing a mean distribution of less than one ($\bar{x} < 1$) resorption lacuna per root third, indicating a relatively low incidence of root resorption along the mesiobuccal root of the rat maxillary molar. This low incidence may be due to some protective mechanism which prevents extensive resorption from occurring as a result of potential sources of trauma including masticatory and attritional forces. It is postulated that this protection is provided by the ERM network.

In 1961, Löe and Waerhaug [42] extracted and replanted fifty eight teeth in four monkeys and six dogs. They noted that in teeth where a vital periodontal membrane had been conserved, ankylosis was not observed, although almost all the teeth showed active or arrested root resorption. As normal periodontal membrane was only found in areas where ERM were present, these workers came to the conclusion that the ERM were responsible for maintenance of the periodontal space, thus limiting ankylosis and root resorption.

The protective function of ERM may be due to a protein secreted by the rests which is capable of inhibiting collagenalytic enzymes [138]. This protein (which was not given a name by the authors) was said to regulate collagenolysis, maintaining the

balance between synthesis and degradation during collagen turnover and could provide a defence against pathological destruction of tissue. Birek et al [50] and Brunette et al [75] have shown that porcine ERM secrete prostaglandin E when stimulated, which these authors propose is responsible for bone resorption. Nevertheless, the actions of prostaglandin E are numerous and just like those of other inflammatory mediators are dose dependent [64, 70, 71]. A low concentration of prostaglandin E produces a different action to a high dose. The protective function of ERM may be the result of the action of prostaglandin E on the invading blood vessels or due to some other as yet undetermined mediator.

Brice [46] and Brice et al [51] noted the presence of ERM in areas of repairing root resorption on the buccal surfaces of human premolars which had been used as anchor teeth during rapid maxillary expansion, but none within actively resorbing bays. They postulated that the ERM might be involved with the repair of orthodontic root resorption and reconstitution of the periodontium following orthodontic tooth movement. Leedham [43] also found ERM within repairing resorption areas and suggested that resorption repair occurs via ERM stimulation of reparative cementoblasts to form an initial layer of repaired cementum in the resorption lacunae.

The results of this current study were similar to those of Kittel [47] and Kittel and Sampson [74], although their study was conducted in human premolar teeth that had been anchor teeth in orthodontic patients who had undergone rapid maxillary expansion. They noted a larger number of PDL blood vessels around active resorption root surfaces. The number of blood vessels were directly related to resorption activity, that is, the more active the resorption, the greater the number of vessels. In active resorption bays, Kittel [47] and Kittel and Sampson [74] did find a number of blood vessels between the tooth surface and the ERM in areas where repair and active and resorption was present. In non-resorbed areas however, a network of ERM were noted near the cementum surface with no blood vessels found between the ERM and the root surface.

In this present study, no blood vessels were noted between any of the ERM and the root surfaces, even in resorption areas. This may be an indication of the protective function of the epithelial network against physiological root resorption. As stated before, although root resorption is commonly found in rat roots, it does not seem to be a rampant occurrence, which suggests the presence of a protective mechanism. It is most likely stimulated by occlusal trauma from attritional forces when the teeth come into occlusion.

In areas where resorption occurs, heavier traumatic forces may somehow overcome the protective mechanism of the ERM network. A break in the network occurs, and proliferation of blood vessels occurs across the width of the PDL. An inflammatory reaction may be produced with mediators released from surrounding cells which could stimulate periodontal clastic cells to commence root resorption (this is illustrated in Figure 45). However, it may also possible that the ERM, which are stimulated by the traumatic force or the resultant inflammatory reaction, in turn stimulate the proliferation of PDL vessels to commence repair of the resorbed areas on the root surface.

Thus, the distribution of blood vessels and ERM in the PDL at three, four and six weeks could possibly be influenced by the development and eruption of the root and its surrounding PDL, and possibly by inflammatory reactions produced by periodontal inflammation, tooth eruption, attrition and root resorption.

6.5 Methodology

The results obtained in this experiment only enable general observations to be made about the distribution of ERM and blood vessels of the PDL within each time period. Only four animals were sacrificed per time period, with counts from three, four and six week sections obtained from only two animals. Thus, results obtained from the maxillary sections could not be sufficiently statistically analysed to provide statistically significant results. Only means ($\bar{x}$) of ERM and blood vessel counts could be obtained. The standard deviations calculated for the ERM and blood vessel values were relatively high due to the fact that only two animals or four maxillae halves per time period were used in the experiment. This indicated a high variability between the animals which should be expected. Future experiments should be performed with a larger number of animals, perhaps only with rats at three, four and six weeks of age to obtain more statistically reliable results.

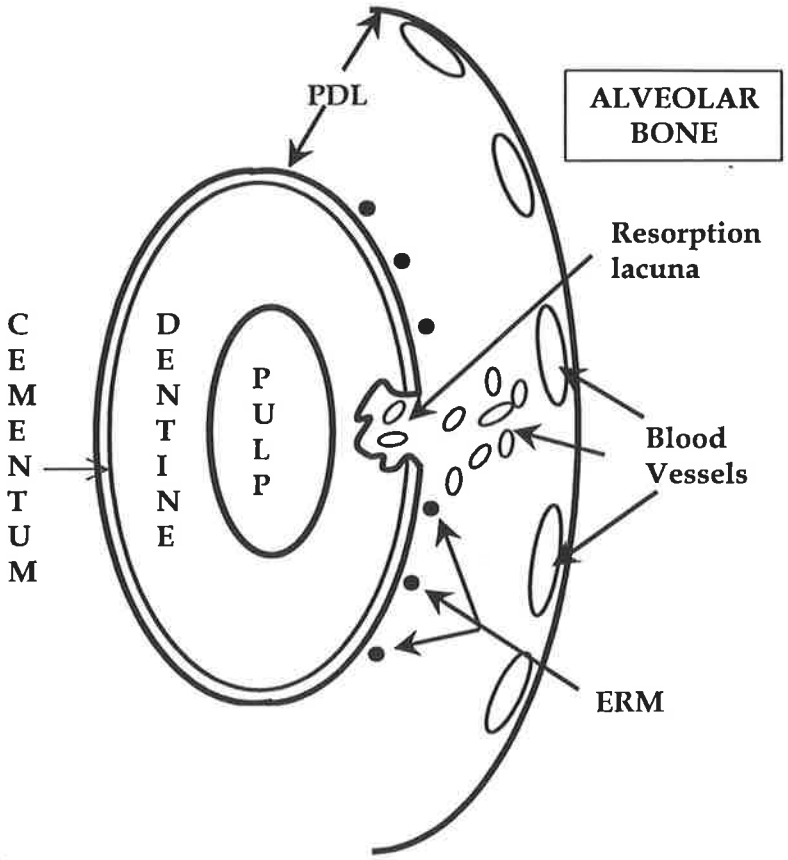

Figure 45

Summary of root resorption

This line diagram summarises the possible interactions which may occur during physiological root resorption during rat root development. It depicts a transverse root section with a network of ERM protecting the root surface. Occlusal trauma somehow induces a break in the network. Blood vessels proliferate and invade into the tooth third of the PDL playing a part in inducing root resorption and/or repair of the resorbed root surface.

6.5.1 *Immunohistochemical staining protocol*

The double immunohistochemical staining protocol developed during the course of this study proved relatively effective in simultaneously demonstrating both ERM and blood vessels in the same section. Nevertheless, some the stains produced were not completely identical for each and every section, as would have been expected.

AE1-AE3 (together with Vector SG™) which was used to demonstrate the ERM at a concentration of 1:2000 produced a clean dark blue stain in most sections. However, in some sections the blue stain produced was quite faint and difficult to detect under the light microscope. It is possible that in such sections, ERM counts may not have been as accurate as other sections as some ERM cells or clusters may have been missed if they were too faint.

The blood vessels were demonstrated with Factor VIII (together with DAB) at a concentration of 1:10 000. This concentration may appear to be very low. However, together with microwave and trypsin II antigen retrieval, this antibody produced a clean, clear brown stain with little background staining in most sections. Higher concentrations only resulted in a large amount of background staining. The use of antigen retrieval was essential to clearly demonstrate the vessels with this antibody. In sections which had not been microwaved, the blood vessels were not readily apparent, even at higher concentrations despite the use of trypsin antigen retrieval. However, very high and prolonged temperatures produced during the microwaving resulted in the loss of some decalcified tissue, especially those with larger areas, especially the four and six week longitudinally sectioned roots. Furthermore, despite the use of microwave antigen retrieval, not all blood vessels were effectively stained. The vessels of the pulp consistently stained a very dark brown. However, the PDL vessels were inconsistent which made the accuracy of vessel counts unreliable. Most of the vessels did demonstrate a clean, dark brown stain which was obvious under the light microscope, but there were others where the brown stain was quite faint. There were also some vessel-like structures in the PDL which did not appear to have picked up the antibody, that is, they did not stain at all. These were either not blood vessels or did not contain Weibel-Palade bodies in their endothelial cells to which the Factor VIII antibody binds to. The Weibel-Palade bodies have been described as being present in "virtually all vascular and lymphatic endothelial cells" [110]. However, this may apply only to human endothelial cells. It is possible that they are not present in all the endothelial cells of the rat PDL.

The sections which did not stain very well were not necessarily the same ones where both AE1-AE3 and Factor VIII did not stain well. In some sections, the blood vessels stained well, but the ERM were very faint and vice versa. They were also not necessarily from the same tissue. The difference in stain intensity may have been due to some discrepancy which occurred during the immunostaining process. This fact has been confirmed by True[77] who stated that "even in careful, experienced hands with defined reagents, there is often significant variability in immunostaining". He postulated that this was probably due to the large number of steps involved in immunostaining[77]. The difference in staining intensity in this particular study might also be due to the effects of decalcification on the tissue. There is some disagreement on the potential of decalcifying agents to deplete antigen sites in tissues. Some investigators believe that this is true[139] whilst others believe that it is still possible to obtain optimal immunostaining after decalcification[140].

Finally, the sections in this study were counter-stained with methyl green to better demonstrate both the blue and brown of the ERM and blood vessels respectively. However, the stain produced by methyl green was very light and did not exhibit the surrounding anatomy of the tooth and periodontium well, making descriptions of these structures difficult. In future studies, perhaps a different coloured chromogen could be utilised to enable the use of haematoxylin or some other dye which can produce a clearer counter-stain.

7 CONCLUSIONS

1. The double immunohistochemical staining protocol utilised in this study with AE1-AE3 and Factor VIII with the chromogens Vector SG and DAB respectively enabled the simultaneous visualisation of ERM blood vessels within a single section.

2. The ERM presented in two forms in transverse sections in this experiment – single cells (which appeared as strands of cells in longitudinal sections) which were equivalent to the "resting type" of ERM [39,44] and type II cells [6]; and as clusters of cells which were equivalent to the "proliferating type" [39, 44] of ERM or type I ERM [6].

3. All the ERM were noted in the tooth third of the PDL in cross-section.

4. Generally, counts in all thirds of the root increased with age, but not proportionally. Cell and cluster counts were most numerous in the cervical third of the root by the age of six weeks. This distribution may be related to the root development process when HERS breaks up to form the ERM which are carried occlusally with tooth eruption, or to gingival inflammation.

5. The highest number of ERM cells and clusters were noted on the distal surface in the cervical and middle third of the root. However, in the apical third, highest counts were noted on the mesial surface. This may be related to the distal direction of eruption of the maxillary molar into the oral cavity.

6. The greatest number of blood vessels were observed in the bone third of the PDL. Slightly less were noted in the middle third and very few were found in the tooth third. The tooth third vessels were only noted at four and six weeks with most of these related to resorption lacunae.

7. No blood vessels were detected between the ERM and tooth surface.

8. The highest number of vessels were noted in the cervical third. This may be related to gingival inflammation produced during root development or penetration of the crown into the oral cavity.

9. The highest proportion of blood vessels was noted on the distal surface in almost all the vertical root thirds and in all ages. The lowest was noted on the palatal surface. This distribution may be due to anatomical variation or may be related to inflammatory processes involved with root resorption, as blood vessel distribution appeared similar to distribution of resorption lacunae.

10. Root resorption lacunae were all found on the distal surfaces in four and six-week-old rats. Most of the lacunae were noted at the cervical and middle thirds of the root. This distribution may be due to trauma produced by occlusal and interproximal attrition [116, 117] or possibly to inflammation in the furcation area of the molar which corresponds to this area.

11. The distribution of the ERM and PDL blood vessels around root resorption lacunae together with results from previous investigations [43, 46, 47] points to a possible protective function of the ERM against root resorption.

12. It is possible that in areas where resorption has occurred, a traumatic force has somehow caused a break in the protective ERM network. This may have been induced by tooth eruptive forces or occlusal trauma after opposing teeth come into contact or possible by gingival inflammation. At the same time, adjacent and surrounding PDL vessels are stimulated to proliferate, perhaps to commence repair of the resorption lacunae

8 BIBLIOGRAPHY

1. Ten Cate A. Development of the tooth and its supporting structures. **In**: Ten Cate E, ed. Oral Histology: Development, Structure and Function. St Louis: C. V. Mosby Company, 1989. pp 57-79.
2. Spouge J. A new look at the Rests of Malassez. A review of their embryological origin, anatomy and possible role in periodontal health and disease. *Journal of Periodontology* 1980;51:437-444.
3. Freeman E. Periodontium. **In**: Ten Cate A, ed. Oral Histology: Development, Structure and Function. St Louis: C. V. Mosby, 1980. pp 244-276.
4. Schour I, Massler M. The teeth. **In**: Farris E, Griffith J, eds. The Rat in Laboratory Investigation. New York: Hafner Publishing Co, 1971. pp 104-165.
5. Alatli I, Lundmark M, Hammarstrom L. The localization of epithelial root sheath cells during cementum formation in rat molars. *Journal of Periodontal Research* 1996;31:433-440.
6. Gurling F, Sampson W. Epithelial root sheath changes during molar formation in the mouse. *Archives of Oral Biology* 1985;30:757-761.
7. Moxham B, Grant D. Development of the periodontal ligament. **In**: Berkovitz B, Moxham B, Newman H, eds. The Periodontal Ligament in Health and Disease. London: Mosby-Wolfe, 1995. pp 161-181.
8. Diamond M, Applebaum E. The epithelial sheath: Histogenesis and function. *Journal of Dental Research* 1942;21:331-411.
9. Hertwig O. Uber das zahnsystem de amphibien und sein bedeutung für die genese des skelets der munhole. *Arch Mikrosk Anat* 1874;11(suppl):55-56.
10. Paynter K, Pudy G. A study of the structure, chemical nature and development of cementum in rat. *Anatomy Record* 1958;131:233-251.
11. Davey A. A transmission electron microscopic and autoradiographic study of Hertwig's Root Sheath initiation. Masters Thesis. Department of Dentistry. Adelaide, South Australia: University of Adelaide, 1986.
12. Thomas H, Kollar E. Differentiation of odontoblasts in grafted recombinants of murine epithelial root sheath and dental mesencyme. *Archives of Oral Biology* 1989;34:27-34.

13. Lester K. The incorporation of epithelial cells by cementum. *Journal of Ultrastructure Research* 1969;27:63-87.
14. Owens P. Ultrastructure of Hertwig's epithelial root sheath during early root development in premolar teeth in dogs. *Archives of Oral Biology* 1978;23:91-104.
15. Lester K. The unusual nature of root formation in molar teeth of laboratory rats. *Journal of Ultrastructure Research* 1969;28:481-506.
16. MacNeil L, Thomas H. Development of the murine periodontium. I. Role of basement membrane in formation of mineralized tissue on the developing root dentin surface. *Journal of Periodontology* 1993;64:95-102.
17. Slavkin H, Bringas P, Jr., Bessem C, et al. Hertwig's epithelial root sheath differentiation and initial cementum and bone formation during long-term organ culture of mouse mandibular first molars using sreumless, chemically-defined medium. *Journal of Periodontal Research* 1988;23:28-40.
18. Owens P. A light and electron microscope study of the early stages of root surface formation in molar teeth in the rat. *Archives of Oral Biology* 1979;24:901-970.
19. Ten Cate A. The role of epithelium in the development, structure and function of the tissues of tooth support. *Oral Diseases* 1996;2:55-62.
20. Hammärstrom L, Alatl il, Fong C. Origins of cementum. *Oral Diseases* 1996;2:63-69.
21. Lindskog S. Formation of intermediate cementum I: Early mineralization of aprismatic enamel and intermediate cementum in monkey. *Journal of Craniofacial Genetics and Developmental Biology* 1982;2:147-160.
22. Lindskog S. Formation of intermediate cementum II: A scanning electron microscopic study of the epithelial root sheath of Hertwig in monkey. *Journal of Craniofacial Genetics and Developmental Biology* 1982;2:1671-169.
23. Lindskog S, Hammarstrom L. Formation of intermediate cementum III: ^{3}H-Tryptophan and ^{3}H-Proline uptake into the epithelial root sheath of Hertwig *in vitro*. *Journal of Craniofacial Genetics and Developmental Biology* 1982;2:171-177.
24. Harrison J, Roda R. Intermediate cementum. Development, structure, composition and potential functions. *Oral Surgery, Oral Medicine and Oral Pathology, Oral Radiology and Endodontics* 1995;79:624-633.
25. Owens P. Mineralisation in the roots of human deciduous teeth demonstrated by tetracycline labeling. *Archives of Oral Biology* 1973;18:889-897.
26. Arzate H, Robertson J, Mendoza M. Recombination of epithelial root sheath and dental papilla cells *in vitro*. *Archives of Medical Research* 1996;27:573-577.
27. Bosshardt D, Schroeder H. Cementogenesis reviewed: A comparison betwen human premolars and rodent molars. *The Anatomical Record* 1996;245:267-292.

28. Kaneko H, Hashimoto S, Enokiya Y, Ogiuchi H, Shimano M. Cell proliferation and death of Hertwig's eptithelial root sheath in the rat. *Cell and Tissue Research* 1999;298:95-103.

29. Gurling F. A transmission electron microscopic study of cementogenesis in the mouse molar. Masters Thesis. Department of Dental Health. Adelaide, South Australia: University of Adelaide, 1981.

30. McLean H. A transmission electron microscopic study of early and late root formation in the mouse mandibular molar. Masters Thesis. Department of Dentistry. Adelaide, South Australia: University of Adelaide, 1984.

31. Lester K, Boyde A. Scanning electron microscopy of developing roots of molar teeth of the laboratory rat. *Journal of Ultrastructure Research* 1970;33:80-94.

32. Diab M, Stallard R. A study of the relationship between epithelial root sheath and root development. *Periodontics* 1965;3:10-14.

33. Freeman E, Ten Cate A. Development of the periodontium. An electronmicroscopic study. *Journal of Periodontology* 1971;42:387-395.

34. Ten Cate A. The epithelial rests of Malassez and the genesis of the dental cyst. *Oral Surgery* 1972;34:956-964.

35. Mallasez M. Sur l'existence de masses épithéliales dans le ligament alvéolodentaires chez l'homme adulte et á l'état normal. *Comptes Rendus de la Société de Biologie* 1884;36:241-244.

36. Valderhaug J, Zander H. Relationship of epithelial rests of Malassez to other periodontal structures. *Periodontics* 1967;5:254-258.

37. Reitan K. Behaviour of Malassez' epithelial rests during orthodontic tooth movement. *Acta Odontologica Scandinavica* 1961;19:443-468.

38. Lambrichts I, Creemers J, Steenberghe D. Periodontal neural endings intimately relate to epithelial rests of Malassez in humans. A light and electron microscope study. *Journal of Anatomy* 1993;182:153-162.

39. Reeve C, Wentz F. The prevalence, morphology and distribution of epithelial rests in the human periodontal ligament. *Oral Surgery, Oral Medicine and Oral Pathology, Oral Radiology and Endodontics* 1962;15:785-793.

40. Hamamoto Y, Nakajima T, Ozawa H, Uchida T. Production of amelogenin be enamel epithelium of Hertwig's root sheath. *Oral Surgery, Oral Medicine and Oral Pathology, Oral Radiology and Endodontics* 1996;81:703-709.

41. Wesselink P, Beertsen W. The prevalence and distribution of rests of Malassez in the mouse molar and their possible role in repair and maintenance of the periodontal ligament. *Archives of Oral Biology* 1993;38:399-403.

42. Löe H, Waerhaug. Experimental replantation of teeth in dogs and monkeys. *Archives of Oral Biology* 1961;3:176-184.

43. Leedham M. An immunohistochemical study of epithelial rests of Malassez, incident to root resorption and repair. . Adelaide: University of Adelaide, 1990.

44. Wentz F, Weinmann J, Schour I. The prevalence, distribution and morphologic changes of the epithelial remnants in the molar region of the rat. *Journal of Dental Research* 1950;29:637-646.

45. Yamasaki A, Pinero G. An ultrastructural study of human epithelial rests of Malassez maintained in a differentiated state *in vitro*. *Archives of Oral Biology* 1989;34:443-451.

46. Brice G. The inter-relationship of epithelial rests of Malassez with orthodontic root resorption and repair in man. . Adelaide: University of Adelaide, 1988.

47. Kittel P. The relationship of epithelial rests of Malassez to orthodontic resorption lacunae. . Adelaide: University of Adelaide, 1990.

48. Yamashiro T, Fujiyama K, Fukunaga T, Wang Y, Takano-Yamamoto T. Epithelial Rests of Malassez express imuunireactivity of TrkA and its distribution is regulated by sensory nerve innervation. *the Journal of Histochemistry and Cytochemistry* 2000;48:979-984.

49. MacNeil R, Sommerman M. Molecular factors regulating development and regeneration of cementum. *Journal of Periodontal Research* 1993;28:550-559.

50. Birek C, Heersche D, Jez D, Brunette D. Secretion of a bone resorbing factor by epithelial cells cultured from porcine rests of Malassez. *Journal of Periodontal Research* 1983;18:75-81.

51. Brice G, Sampson W, Sims M. An ultrastructural evaluation of the relationship between epithelial rests of Malassez and orthodontic root resorption and repair in man. *Australian Orthodontic Journal* 1991;12:90-93.

52. Li T-J, Browne R, Matthews J. Expression of epidermal growth factor receptors by odontogenic jaw cysts. *Virchows Archiv A Pathological Anatomy and Histopathology* 1993;423:137-144.

53. Gilhuus-Möe O, Kvam E. Behaviour of epithelial remnants of Malassez following experimental movement of rat molars. *Acta Odontologica Scandinavica* 1972;30:139-149.

54. Sims M. The morphology of the vasculature of the periodontal ligament. **In**: Berkovitz B, Moxham B, Newman H, eds. The Periodontal Ligament In Health And Disease. London: Mosby-Wolfe, 1995. pp

55. Edwall L, Aars H. The physiology of the vasculature of the periodontal ligament. **In**: Berkovitz B, Moxham B, Newman H, eds. The Periodontal Ligament In Health And Disease. London: Mosby-Wolfe, 1995. pp 121-131.

56. Sims M. A model of the anisotropic distribution of microvascular volume im the periodontal ligament of the mouse mandibular molar. *Australian Orthodontic Journal* 1987;10:21-24.

57. Douvartizidis I. A morphometric examination of the periodontal ligament vasculature of the marmoset molar. Orthodontic. Adelaide: University of Adelaide, 1984.

58. Blaushild N, Michaeli Y, Steigman S. Histomorphometric study of the periodontal vasculature of the rat incisor. *Journal of Dental Research* 1992;71:1908-1912.

59. Foong K. A transmission electron microscope stereological analysis of the blood vessels and nerves in the human mandibular premolar periodontal ligament. Department of Dentistry. Adelaide, South Australia: University of Adelaide, 1994.

60. Freezer S. A study of periodontal ligament mesial to the mouse mandibular first molar. Department of Dentistry. Adelaide, South Australia: University of Adelaide, 1984.

61. Kumar V, Cotran R, Robbins S. Acute and chronic inflammation. **In**: Kumar V, Cotran R, Robbins S, eds. Basic Pathology. Philadelphia: W. B. Saunders, 1992. pp 25-46.

62. Ten Cate A. Repair and regeneration of dental tissue. **In**: Ten Cate A, ed. Oral Histology: Development, Structure and Function. St Louis: C. V. Mosby Company, 1989. pp 395-408.

63. Kumar V, Cotran R, Robbins S. Repair: Cell growth, regeneration and wound healing. **In**: Kumar V, Cotran R, Robbins S, eds. Basic Pathology. Philadelphia: W. B. Saunders, 1992. pp 47-60.

64. Cockerill G, Gamble J, Vadas M. Angiogenesis: models and modulators. *International Review of Cytology* 1995;159:113-156.

65. Guyton A. Local control of blood flow by the tissues, and humoral regulation. **In**: Guyton A, ed. Textbook of Medical Physiology. Philadelphia: W. B. Saunders Company, 1991. pp 185-193.

66. Polverini P. The pathophysiology of angiogenesis. *Critical Reviews in Oral Biology and Medicine* 1995;6:230-247.

67. Bosari S, Lee A, DeLellis R, Wiley B, Heatley G, Silverman M. Microvessel quantitation and prognosis in invasive breast carcinoma. *Human Pathology* 1992;23:755-761.

68. Weidner N, Semple J, Welch W, Folkman J. Tumour angiogenesis and metatasis - correlation in invasive breast carcinoma. *The New England Journal of Medicine* 1991;324:3-8.

69. Weidner N, Folkman J, Pozza F, et al. Tumour angiogenesis: a new significant and independent prognostic indicator in early-stage breast carcinoma. *Journal of the National Cancer Institute* 1992;84:1875-1887.

70. Sunderkötter C, Steinbrink K, Goebeler M, Bhardwaj R, Sorg C. Macrophages and angiogenesis. *Journal of Leucocyte Biology* 1994;55:410-419.

71. Norrby K. Interleukin-8 and de novo mammalian angiogenesis. *Cell Proliferation* 1996;29:315-323.

72. Hu D, Hori Y, Fan T-P. Interleukin-8 stimulates angiogenesis in rats. *Inflammation* 1993;17:135-143.

73. Cohen T, Nahari D, Cerem L, Neufeld G, Levi B-Z. Interleukin-6 induces the expression of vascular endothelial growth factor. *Journal of Biological Chemistry* 1996;271:736-741.

74. Kittel P, Sampson W. RME-induced root resorption and repair: a computerised 3D reconstruction. *Australian Orthodontic Journal* 1994:444-451.

75. Brunette D, Heersche J, Purdon A, Sodek J, Moe H, Assuras J. In vitro cultural parameters and protein and prostaglandin secretion of epithelial cells derived from porcine rests of Malassez. *Archives of Oral Biology* 1979;24:199-203.

76. Mighell A, Hume W, Robinson P. An overview of the complexities and subtleties of immunohistochemistry. *Oral Diseases* 1998;4:217-223.

77. True L. Principles of Immunohistochemistry. **In**: True L, ed. Atlas of Diagnostic Immunohistopathology. Philadelphia: J. B. Lippincott Company, 1990. pp 1.1-1.34.

78. Leong A-Y. Immunohistochemistry - theoretical and practical aspects. **In**: Leong A-Y, ed. Applied Immunohistochemistry for the Surgical Pathologist. London: Edward Arnold, 1993. pp 1-22.

79. Hsu S, Raine L, Fanger H. Use of avidin-biotin-peroxidase complex (ABC) in immunoperoxidase techniques: A comparison between ABC and unlabelled antibody (PAP) procedures. *Journal of Histochemistry and Cytochemistry* 1981;29:577-580.

80. Shi S-R, Key M, Kalra K. Antigen retrieval in formalin-fixed, paraffin-embedded tissues: an enhancement method for immunohistochemical staining based on microwave oven heating of tissue sections. *The Journal of Histochemistry and Cytochemistry* 1991;39:741-748.

81. Shi S-R, Imam S, Young L, Cote R, Taylor C. Antigen retrival immunohistochemistry under the influence of pH using monoclonal antibodies. *The Journal of Histochemistry and Cytochemistry* 1995;43:193-201.

82. Evers P, Uyling H. Microwave-stimulated antigen retrival is pH and temperature dependent. *The Journal of Histochemistry and Cytochemistry* 1994;42:1555-1563.

83. Cuevas E, Bateman A, Wilkins B, et al. Microwave antigen retrieval in immunocytochemistry: a study of 80 antibodies. *Journal of Clinical Pathology* 1994;47:448-452.

84. Norton A, Jordan Y, Yeoman P. Brief, high-temperature denaturation (pressure cooking): a simple and effective method of antigen retrival for routinely processed tissues. *Journal of Pathology* 1994;173.

85. von Wasielewski R, Werner M, Nolte M, wilkens L, Georgii A. Effects of antigen retrival by microwave heating in formalin-fixed sections on a broad panel of antibodies. *Histochemistry* 1994;102:165-172.

86. Battifora H. Assessment of antigen damage in immunohistochemistry. *American Journal of Clinical Pathology* 1991;96:669-671.

87. Hautzer N, Wittkuhn J, WTE M. Trypsin digestion in immunoperoxidase staining. *The Journal of Histochemistry and Cytochemistry* 1980;28:52-53.

88. Battifora H, Kopinski M. The influence of protease digestion and duration of fixation on immunostaining of keratins. *The Journal of Histochmistry and Cytochemistry* 1986;34:1095-1100.

89. Division of Tissue Pathology IoMaVS. Avidin-biotin peroxidase technique for paraffin sections. Immunocytochemistry Manual. Adelaide, 1998. pp

90. Scopsi L, Larsson L. Increased sensitivity in peroxidase immunocytochemistry. A comparitive study of a number of peroxidase visualisation methods employing a model system. *Histochemistry* 1986;84:221-230.

91. Gao Z, Mackenzie I, Williams D, Cruncley A, Leigh I, Lane E. Patterns of keratin-expression in rests of Malassez and periapical lesions. *Journal of Oral Pathology* 1988;17:178-185.

92. Peters B, Peters J, Kuhn C, Zoller J, Franke W. Maintenance of cell-type-specific cytoskeletal character in epithelial cells out of epithelial context: Cytokeratins and other cytoskeletal proteins in the rests of Malassez of the periodontal ligament. *Differentiation* 1995;59:113-126.

93. Berkovitz B, Whatling R, Barret A, Omar S. The structure of bovine periodontal ligament with special reference to the epithelial cell rests. *Journal of Periodontology* 1997;68:905-913.

94. Tatemoto Y, Okada Y, Mori M. Squamous odontogenic tumour: Immunohistochemical identification of keratins. *Oral Surgery Oral Medicine and Oral Pathology* 1989;67:63-67.

95. Sun T-T, Eichner R, Nelson W, et al. Keratin classes: molecular markers for different types of epithelial differentiation. *The Journal of Investigative Dermatology* 1983;81:109s-115s.

96. Woodcock-Mitchell J, Eichner R, Nelson W, Sun T-T. Immunolocalisation of keratin polypeptides in human epidermis using monoclonal antibodies. *The Journal of Cell Biology* 1982;95:580-598.

97. Barwick K. Intermediate filaments and keratin. **In**: True L, ed. Atlas of Diagnostic immunohistopathology. Philadelphia: J.B. Lippincott, 1990. pp 3.1-3.18.

98. Franke W, Weber K, Osborn M, Scmid E, Freudenstein C. Antibody to prekeratin: decoration of tonofilament-like arrys in various cells oc epithelial character. *Experimental Cell Research* 1978;116:429-445.

99. Sun T, Tseng S, Huang A-W. Monoclonal antibody studies of mammalian eptihelial keratins: A review. *Annals of the New York Academy of Science* 1985;455:307-329.

100. Oda D, Bigler L, Lee P, Blanton R. HPV immortalization of human oral epithelial cells: a model for carcinogenesis. *Experimental Cell Research* 1996;226:164-169.

101. Matthews J, Mason G, Browne R. Epithelial cell markers and proliferating cells in odontogenic naw cysts. *Journal of Pathology* 1988;156:283-290.

102. Smith A, Wilson C, Matthews J. An immunocytochemical study of keratin reactivity during rat odontogenesis. *Histochemistry* 1990;94:329-335.

103. Fajardo L. The complexity of endothelial cells. A review. *American Journal of Clinical Pathology* 1989;92:241-250.

104. Hollingsworth H, Kohn E, Steinberg S, Rothenberg M, Merino M. Tumour angiogenesis in advanced stage ovarian carcinoma. *American Journal of Pathology* 1995;147:33-41.

105. Traweek S, Kandaleft P, Mehta P, Battifora H. The human hematopoietic progenitor cell antigen (CD34) in vascular neoplasia. *American Journal of Clinical Pathology* 1991;96:25-31.

106. Poblet E, Gonlalez-Palacious F, Jimenez F. Different immunoreactivity of endothelial markers in well and porly differentiatied areas of angiosarcomas. *Virchows Archiv A Pathological Anatomy and Histopathology* 1996;428:217-221.

107. Siitonen S, Haapsalo H, Rantala I, Helin H, Isola J. Comparison of different immunohistochemical methods in the assessment of angiogenesis: Lack of

prognostic value in a group of 77 selected node-negative breast carcinomas. *Modern Pathology* 1996;8:745-752.

108. True L. Vascular antigens. **In**: True L, ed. Atlas of Diagnostic Immunohistopathology. Philadelphia: J. B. Lippincott Company, 1990. pp 9.1-9.19.

109. Duijvestijn A, van Goor H, Klatter F, Majoor G, van Bussel E, van Breda Vriesman P. Antibodies defining rat endothelial cells: RECA -1, a pan-endothelial cell-specific monoclonal antibody. *Laboratory Investigation* 1992;66:459-166.

110. Ewenstein B, Handin R. Von Willebrand's Disease. **In**: Handin R, Lux S, Stossel T, eds. Blood. Principles and practice of hematology. Philadelphia: JB Lippincott Company, 1995. pp 1069-1094.

111. Hobson M, Brown R, Green C, Terenghi G. Inter-relationships between angiogenesis and nerve regeneration: A histochemical study. *British Journal of Plastic Surgery* 1997;50:125-131.

112. Imperato-Kalmar E, McKinney R, Schnell L, Rubin B, Schwab M. Local changes in vascular architecture following partial spinal cord lesion in the rat. *Experimental Neurology* 1997;145:322-328.

113. Doerr-Schott J, Lichte C. A double-immunostaining procedure using colloidal gold, ferritin and peroxidase as markers for simultaneous detection of ywo hypophysial hormones with the electron microscope. *The Journal of Histochemistry and Cytochemistry* 1984;32:1159-1166.

114. Mori M, Kurane I, Janus J, Ennis F. Cytokine porduction by dengue virus antigen-responsive human T-lymphocytes in vitro examined using a double immunocytochemical technique. *Journal of Leucocyte Biology* 1997;61:338-345.

115. Zhou M, Grofova I. The use of peroxidase substrate Vector VIP in electron microscopic single and double antigen localization. *Journal of Neuroscience Methods* 1995;62:149-158.

116. Belting C, Schour I. Age changes in the periodontal tissues of the the rat molar. *Journal of Dental Research* 1953;12:332-353.

117. Weinmann J, Schour I. Experimental studies in calcification. 1: The effect of rachitogenic diet in the tissues of the white rat. *American Journal of Pathology* 1945;21:821.

118. Hamamoto Y, Suzuki I, Nakajima T, Ozawa H. Immunocytochemical localization of laminin in the epithelial rests of Malassez of immature rat molars. *Archives of Oral Biology* 1991;36:623-626.

119. Cutress T, Crigger M. The cell rests of the sheep periodontium. *New Zealand Dental Journal* 1974;70:39.

120. Shibata R, Stern I. Hertwig's sheath in the rat incisors I. Histologic study. *Journal of Periodontal Research* 1967;2:227-237.

121. Everts V, Delaisse J-M, Korper W, Beertsen W. Involvement of matrix metalloproteinases and cycteine proteinases in degration of bone matrix. The Biological Mechanisms of Tooth Eruption, Resorption and Replacement by Implants., 1994. pp 85-97.

122. Orban B. The epithalial network in the periodontal membrane. *Journal of the American Dental Association* 1952;44:632-635.

123. Valderhaug J. A histologic study of experimentally induced radicular cysts. *International Journal of Oral Surgery* 1972;1:137-147.

124. Kerr J, Wyllie A, currie A. Cepaptosis: A basic biological phenomenon with wide ranging implacations in tissue kinetics. *British Journal of Cancer* 1972;26:239-257.

125. Dreyer C. A Histologic and Radioautographic study of migration patterns in the mandibular molars of normal and lathyritic mice. Department of Dental Health. Adelaide: University of Adelaide, 1980.

126. Weekes W, Sims M. The vasculature of the rat molar periodontal ligament. *Journal of Periodontal Research* 1986;21:186-194.

127. Bernick S. Vascular supply to the developing teeth of rats. *Anatomy Records* 1960;137:141-151.

128. Nakamura H, Kiyomura H, Nakamura T, Hanai H. Scanning electron microscopy of vascular system of rat molar periodontium. *Journal of Dental Research* 1983;62:651.

129. Götze W. Quantitative Untersuchungen zur Verteilung der Blutgelafässe in Demodont. *Dtsh Zahnärztl A* 1976;31:428-430.

130. Kindlova M. Development of vessels in the marginal periodontium of rats. *Journal of Dental Research* 1968;47:507.

131. Birn H. The vascular supply of the periodontal membrane. *Journal of Periodontal Research* 1966;1:51-68.

132. Parlange L, MR S. A TEM stereological analysis of blood vessels and nerves in marmoset periodontal ligament following endodontics and magnetic incisor extrusion. *European Journal of Orthodontics* 1993;15:33-44.

133. Kishi Y, Takahishi K. A scanning electron microscope study of the vascular architecture of the periodontal membrane. *Japanese Journal of Oral Biology* 1977;28:247-252.

134. Ten Cate A. The histochemical demonstration of specific oxidative enzymes and glycogen in the epithelial rests of Malassez. *Archives of Oral Biology* 1965;10:207-213.

135. Grant D, Bernick S. A possible continuity between epithelial rests and epithelial attachment in miniature swine. *Journal of Periodontology* 1969;40:87-95.

136. Johansen J. Incorporation of tritiated thymidine by epithelial rests of malassez after attempted extraction of rat molars. *Acta Odontologica Scandinavica* 1970;28:463-470.

137. Harris M, Toller P. The pathogenesis of dental cysts. *British Medical Bulletin* 1975;31:159-163.

138. Pettigrew D, Sodek J, Wang H, Brunette D. Inhibitors of collagenolytic enzymes synthesized by fibroblasts and epithelial cells from porcine and macaque periodontal ligament. *Archives of Oral Biology* 1980;25:269-274.

139. Massoth D, Dale B. immunohistochemical study of structural proteins in developing junctional epithelium. *Journal of Periodontology* 1986;57:756-763.

140. Matthews J, Mason G. Influence of decalcifying agents on immunoreactivity of formalin-fixed, paraffin-embedded tissue. *Histochemical Journal* 1984;16:771-787.

APPENDIX 1

10% Neutral buffered formalin (pH 7)

900mL distilled water
6.5g anhydrous sodium phosphate dibasic
3.5g anhydrous sodium phosphate monobasic
100mL of 40% formaldehyde solution

Mix all of the above together to obtain 4% buffered neutral formalin.

Paraffin Embedding

Soak tissues in :

1. 70% alcohol	2 hours
2. 80% alcohol	2 hours
3. 90% alcohol	2 hours
4. 100% alcohol	2 hours
5. 100% alcohol	2 hours
6. 100% alcohol	2 hours
7. Clearene (Surgipath)	2 hours
8. Clearene	2 hours
9. Clearene	1 hour
10. Paraffin	2 hours
11. Paraffin	3 hours

Then embed tissues in paraffin blocks.
Freeze to set paraffin before sectioning tissue.

APPENDIX 2

EDTA in Phosphate Buffered Saline (pH 7)

Phosphate Buffered Saline (PBS) (pH 7)

Solution A	31.2g $NaH_2PO_4.H_2O$ in 1L distilled water
Solution B	28.3g Na_2HPO_4 in 1L distilled water

Then:

Add 169mL of solution A to 840mL of solution B. Dilute to 2L (with distilled water) to make PBS at pH7

EDTA

Add 80g EDTA to 2L of PBS

APPENDIX 3

2% APT (3-amino propyltriethoxysilane) (Sigma)

(All procedures must be carried out in a fume extracted environment)

1. Load slides into racks and soak in detergent overnight.
2. Wash slides in several changes of running water. Drain but do not dry.
3. Rinse (for 30 seconds) in two consecutive containers of ABSOLUTE ALCHOHOL.
4. Dip for 10 seconds in 2% APT (2mL of APT dissolved in 98mL of absolute alcohol).
5. Rinse (for 10 seconds) in absolute alcohol.
6. Rinse in distilled water.
7. Dry slides in 37°C oven overnight.
8. Store slides ready for use.

APPENDIX 4

10mM Sodium Citrate (pH 6.3)

Mix 25mL of 5N NaOH and 10.5g of citric acid in 5L of distilled water

To make 5N of NaOH: Add 20g of NaOH to 100mL of distilled water

APPENDIX 5

Example of the spreadsheet used to tabulate ERM cells and clusters, blood vessel counts and presence of root resorption lacunae along and around the mesiobuccal root of the rat first molar.

Rat age:

		ERM cells												ERM clusters												Total
		Buccal			Mesial			Palatal			Distal			Buccal			Mesial			Palatal			Distal			
		T 1/3	M 1/3	B 1/3	T 1/3	M 1/3	B 1/3	T 1/3	M 1/3	B 1/3	T 1/3	M 1/3	B 1/3	T 1/3	M 1/3	B 1/3	T 1/3	M 1/3	B 1/3	T 1/3	M 1/3	B 1/3	T 1/3	M 1/3	B 1/3	
Cerv	1																									
	2																									
	3																									
Mid	4																									
	5																									
	6																									
Ap	7																									
	8																									
	9																									
Total																										

		Blood vessels												Total
		Buccal			Mesial			Palatal			Distal			
		T 1/3	M 1/3	B 1/3	T 1/3	M 1/3	B 1/3	T 1/3	M 1/3	B 1/3	T 1/3	M 1/3	B 1/3	
Cerv	1													
	2													
	3													
Mid	4													
	5													
	6													
Ap	7													
	8													
	9													
Total														

Resorption lacunae				
Buc	Mes	Pal	Dis	Total